Latest Cretaceous-Tertiary Stratigraphy on the LaHave Platform, Offshore Nova Scotia, Canada

Stephan Denis Bigg

Undergraduate Honours Thesis
Department of Earth Sciences
Dalhousie University

Submitted in partial fulfilment of the requirements for the degree of Bachelor of Science (Honours) at Dalhousie University (May 10, 2002).

DALHOUSIE University

Department of Earth Sciences
Halifax, Nova Scotia
Canada B3H 3I5
(902) 494-2358
FAX (902) 494-6889

DATE May 10, 2002

AUTHOR Stephan Denis Bigg

TITLE Latest Cretaceous-Tertiary Stratigraphy on the LaHave Platform, Offshore Nova Scotia, Canada

Degree BSc Convocation Spring Year 2002

Contents

Table of Figures

Table of Tables

Abstract

The LaHave Platform is a relatively stable segment of the continental margin of Nova Scotia, developed along the flank of the Scotian Basin. The latest Cretaceous through Tertiary part of the succession, designated the Wyandot and Banquereau formations, is the subject of this study. At least three mappable seismic 'packages' that approximate seismic sequences are identifiable in the study interval. The packages and their bounding surfaces were mapped using industry seismic reflection profiles acquired in the 1970s and 1980s. Faults were relatively uncommon in the study area/interval, except near the shelf edge, where the horizons begin to be offset by minor normal faults. Here also, canyons have been incised that continue to the southeast onto the slope.

Ties between the seismic and eight wells show that the seismic packages correspond to at least two successive transgressive-regressive cycles that deposited alternating units of mudstone (during transgression) and sandstone (during regression) from the early Campanian to Miocene. The Wyandot Formation represents the maximum transgression near the base of the interval, during the Santonian to early Campanian. The Wyandot is followed by regression during the Campanian to Paleocene portion of the Banquereau Formation. The regression is characterized in the well logs as mudstone grading to sandstone, and in the seismic by progradational seismic horizons of seismic package 1 and most of package 2. The maximum regression occurred during the Maastrichtian-Paleocene, and is represented by sandstones up to 225 m thick at the Alma K-85 well. Another transgressional episode and subsequent regression during the Eocene-Oligocene and Miocene are represented as mainly mudstone and sandstone, respectively, and further progradational seismic packages (the remainder of seismic package 2 and package 3). Erosion on top of the Wyandot was also observed, possibly representing an additional regressive event before the beginning of the Banquereau Formation deposition.

The geometry of the seismic packages and canyons in the study area indicate the location of the main depocentres and sediment transport directions. The thickest accumulation of Campanian-Paleocene mudstones and sandstones (450 m) was deposited near the centre of the study interval, in the area between the Ojibwa, Oneida, and Demascota wells. If transported over the paleoshelf edge, significant accumulations of sandstone-dominated units may be expected on the slope adjacent to this depocentre. The depocentre of the Eocene-Miocene sandstones (up to 275 m) was slightly seaward of the Oneida well. The thickest accumulation of later Tertiary (Oligocene-Miocene) sandstones should therefore occur on the slope beyond Oneida. Furthermore, canyons in the southwest portion of the study area were infilled during the Oligocene-Miocene, implying that coeval prograding sandstones may have been intermittently transported through the canyons and onto the slope. Future oil and gas exploration efforts should concentrate on these areas as sites of potentially significant hydrocarbon reservoirs, especially in the interval of the Maastrichtian-Paleocene and Oligocene-Miocene sands.

Abbreviations and Symbols Used

AI .....acoustic impedance
API .....American Petroleum Institute
CanStrat.....Canadian Stratigraphic Service Ltd.
CDP.....common depth point
cm.....centimetres
CMP .....common midpoint
CNSOPB .....Canada-Nova Scotia Offshore Petroleum Board
EPS.....Encapsulated PostScript File
GMT.....Generic Mapping Tools
GSC (Atlantic) .....Geological Survey of Canada (Atlantic)
Hz.....hertz
in .....inches
KB.....Kelly Bushing
km .....kilometres
NMO .....normal moveout
ms.....milliseconds
QC Data .....QC Data International Inc.
R_A.....Reflection A
R_B.....Reflection B
R_C.....Reflection C
RC .....reflection coefficient
R_D.....Reflection D
R_W .....Wyandot Reflection
R_{W-1} .....Wyandot-1 Reflection
S_1.....Seismic package 1
S_2.....Seismic package 2
S_3.....Seismic package 3
S/N .....signal-to-noise
s.....seconds
sec .....seconds
SEG.....Society of Exploration Geophysicists
SH .....shale
SP .....shotpoint
SS .....sandstone
TVF.....time-variant filter
TWT.....two-way time
$TWT_{top\ log}$ .....TWT to top of well log (from sea level)
V_{rock}.....velocity of rock
V_{water}.....velocity of water
µs.....microseconds

Acknowledgements

This project could not have been completed without the help and support of a number of individuals. First and foremost, my infinite thanks go out to my supervisor Dr. Andrew MacRae at the GSC (Atlantic), who never failed to express an exciting outlook on the project and its potential. His help preparing and refining my dataset, and patience while I struggled with the many foreign concepts and software packages, was unremitting. Additionally, I would especially like to thank Andrew for writing the 'makefile' GMT program that digitally plotted my seismic picks data, saving me countless hours of plotting by hand. Most of all, thank you for never giving up hope, even when things seemed their darkest.

Also at the GSC, I would like to extend thanks to John Shimeld for his help and suggestions for interpreting and manipulating the seismic data, and to Chris Jauer for his help producing the synthetic seismograms and performing the well/seismic ties. I also owe thanks to Arthur Jackson for his continued workstation and PC support, and Nelly Koziel for helping me enter what seemed like an endless amount of measured seismic picks. I would also like to extend a general thank you to everyone at the GSC for letting me invade their space to work on this project, and to the CNSOPB for giving me some data to work with.

At Dalhousie University, I wish to thank Dr. Patrick Ryall for his continued support and guidance towards not only this Thesis, but through the rest of my Earth Sciences degree as well. Thank you, and everyone else in the Department of Earth Sciences, for a truly enjoyable four years.

1. Introduction

1.1 Overview

This study assesses the depositional history and sediment distribution within the Wyandot and Banquereau formations on the LaHave Platform, offshore Nova Scotia. The LaHave Platform is a relatively stable basement platform on the northwest flank of the Scotian Basin along the passive continental margin of Nova Scotia, Canada (Figure 1.1). The platform is covered with a seaward-thickening series of sandstone, shale, limestone, and chalk units that accumulated following the opening of the Atlantic Ocean in the Late Triassic (Wade and MacLean, 1990). This study focuses on the latest Cretaceous through Tertiary part of the succession (Figure 1.2). The base of the study interval is defined by the Wyandot Formation (Jansa and Wade, 1975), a distinctive chalk unit deposited in the Late Cretaceous. Underlying the Wyandot Formation is the Late Cretaceous Dawson Canyon Formation (McIver, 1972). These lower two units have been previously interpreted as part of an overall transgressive sequence, and are comprised mainly of marine shales and chalky limestones (Wade and MacLean, 1990). The lower and/or upper contacts of the Wyandot Formation act as distinct regional markers, due to the persistence of the unit and their strong acoustic contrast. The overlying latest Cretaceous-Tertiary sediments are designated the Banquereau Formation (McIver, 1972), a series of mostly mudstones and sandstones. The most recent (Pleistocene-Holocene) sediments are referred to as the Laurentian Formation (Jansa and Wade, 1975).

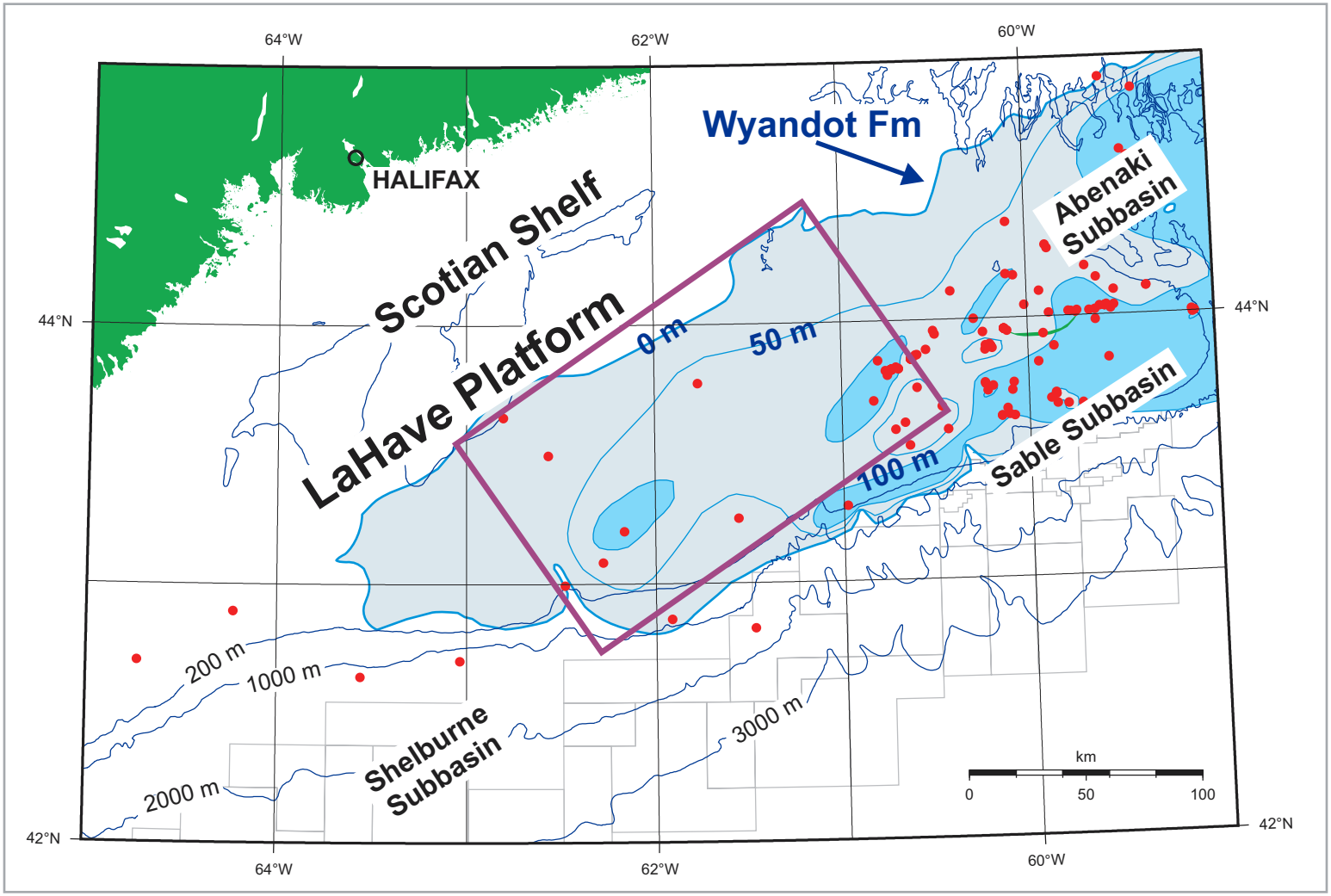

Figure 1.1 Project Area (outlined in purple) illustrating wells (red points; from BASIN, courtesy of the CNSOPB, 2002), Wyandot Formation isopach (blue contours and fill; after Wade and MacLean, 1991), bathymetry (dark blue contours; courtesy of the Atlantic Geoscience Centre, 1991), and active exploration licences (grey boxes; courtesy of the CNSOPB).

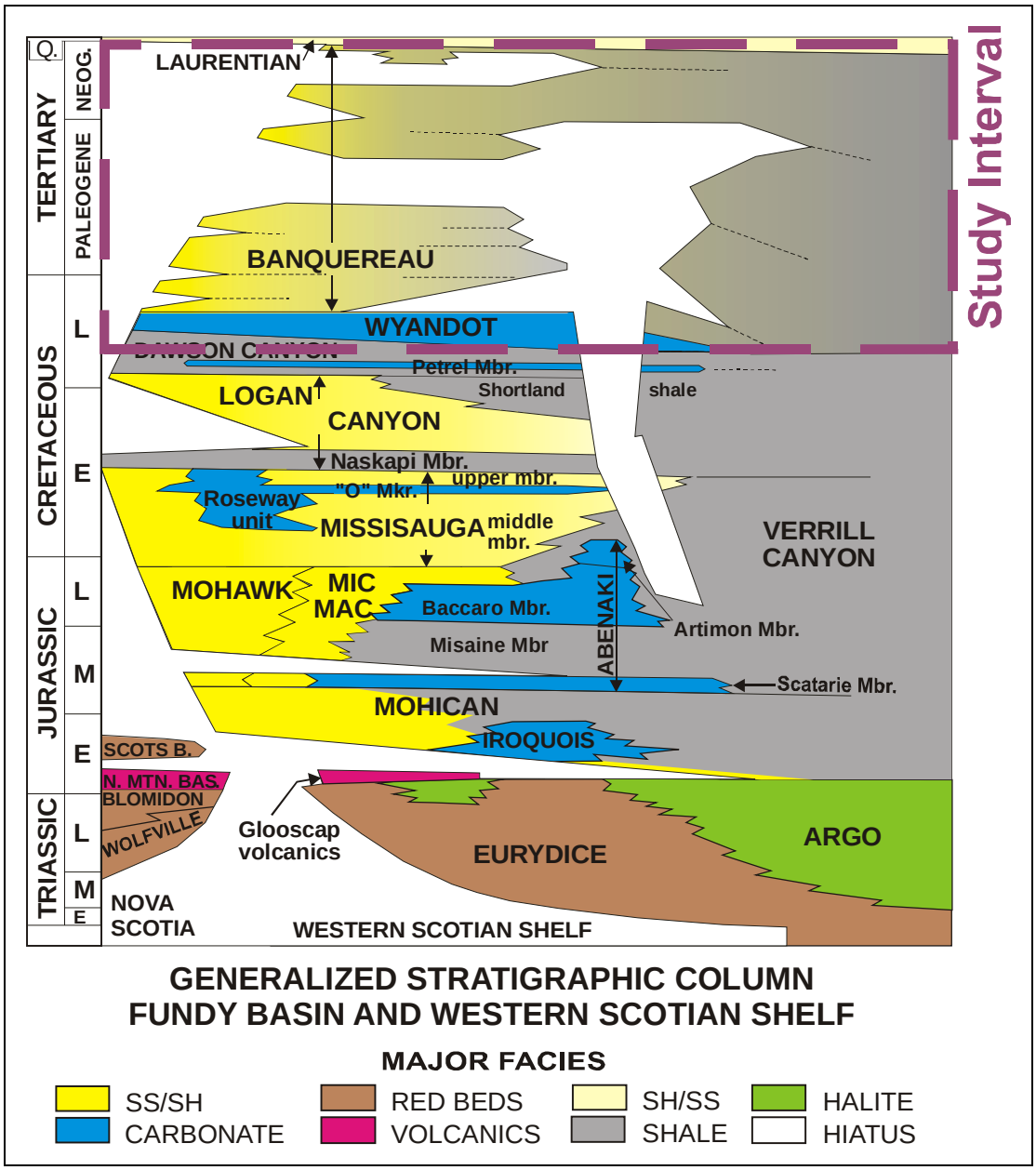

Figure 1.2 Generalized western Scotian Shelf stratigraphy (after Wade and MacLean, 1990). The study interval is outlined by the purple box.

No significant reservoirs of oil and/or gas were discovered in wells drilled on the LaHave Platform by the petroleum industry in the late 1970's through the 1980's (Wade and MacLean, 1990). The lack of even a single economic deposit has resulted in few further studies. This relative lack of knowledge is especially evident when compared with the extensive progress (and production) in the area of the nearby Sable Island fields to the northeast (note the significant difference in the number of exploration wells between the two regions in Figure 1.1). Information within the study area thus relies primarily on exploration data acquired by industry. In particular, the hardcopies of seismic sections acquired during the 1970s and 1980s that have since been made publicly available, and the log data recorded from the wells. Shallow, single-channel seismic data acquired by the Geological Survey of Canada (Atlantic) is also available in the study area, but was not studied in this project.

1.2 Objectives

This project will address the following questions relating to the latest Cretaceous-Tertiary stratigraphy in the project area:

- What is the lithofacies distribution and timing?
- When and where are the main sediment depocentres in time and space?
- Where are canyon incisions present, and what is their timing?

The interpretation of shelf sedimentation will allow a model of sediment supply to be created, and an assessment made of potential reservoir sand distribution further out on the Scotian Slope where natural gas may be present and industry has made substantial exploration commitments. Thus, this project will be of interest from both an academic and industry perspective.

1.3 Organization

Chapter Two presents a general background of the project area, including historical studies and the geologic history of the Scotian Basin, as well as a background to the concepts and data used, including seismic and sequence stratigraphy and other interpretation techniques. Chapter Three specifies the data and methods used to complete the project. Both seismic and well-log data are presented, including an account of data sources. Chapter Four includes the results of the seismic and well-log analysis, how the two complement each other, and the final interpretation of the geology of the study area. Chapter Five presents a summary of the results, and provides answers to the questions posed at the beginning of the project. The report concludes with recommendations for future work in the study area.

2. Background

2.1 Location and Historical Studies of the Scotian Basin

In general, the Scotian Basin extends from the coast of Nova Scotia out to the continental rise, and from the southern edge of Nova Scotia to the southern edge of Newfoundland (Figure 2.1). More specifically, the Scotian Basin extends from the edge of the sediments off the coast of Nova Scotia, out to the continental rise, and from the eastern part of Georges Bank to the central Grand Banks, approximately 300,000 square kilometres in total (Wade and MacLean, 1990). This encompasses the eastern portion of the Scotian Shelf, the southwestern Grand Banks, the Laurentian Channel, and the continental slopes and rises of these areas (Jansa and Wade, 1975).

Several major studies have established the stratigraphic nomenclature of the Scotian Basin. McIver completed one of the first major studies for Shell Canada Limited in 1972, entitled "Cenozoic and Mesozoic Stratigraphy of the Nova Scotia Shelf". This was a broad stratigraphic interpretation, based on approximately 20 offshore wells, plus an extensive grid of industry seismic data. McIver subdivided the stratigraphy of the shelf into 3 groups, 12 formations, and 4 members (Table 2.1). Most of his designations are still used today, although modified. Studies prior to McIver included test and exploration well data, as well as analyses of various dredged and collected bottom samples used to classify the stratigraphy of the Quaternary shelf sediments. For example: Stephenson (1936) described fossils in a bottom sample from the Banquereau Bank; Marlow and Bartlett (1967) described samples from the Gully; and King (1970) systemized the stratigraphy of the Quaternary shelf sediments (McIver, 1972).

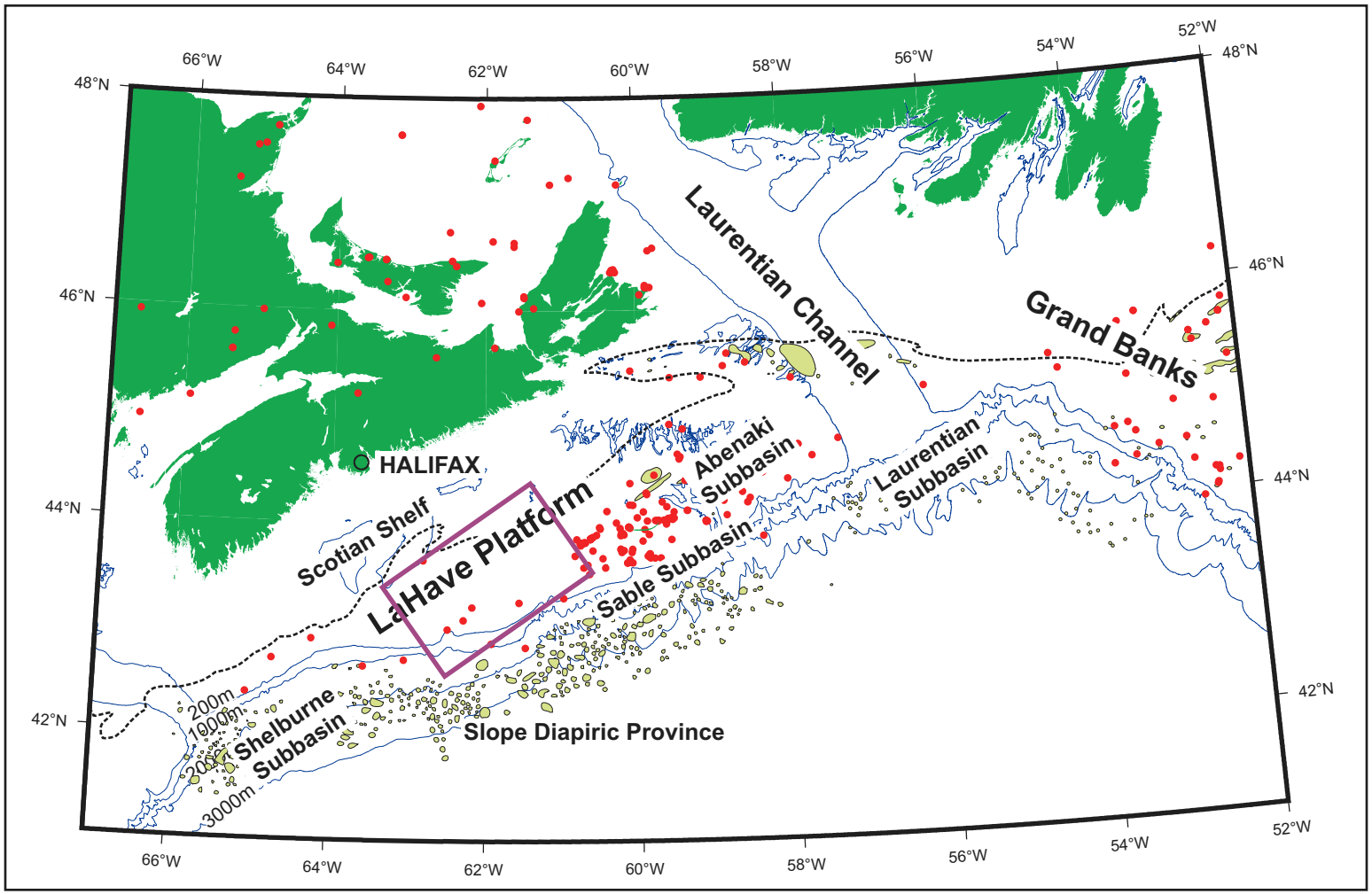

Figure 2.1 Regional map of the Scotian Basin, illustrating study area (outlined in purple), approximate extent of basin (dashed black line, representing the 2 km depth to basement contour; after Williams and Grant, 1988), wells (red points; from BASIN, courtesy of the CNSOPB, 2002), Triassic/Jurassic salt (green structures; after Wade, 1991), and bathymetry (dark blue contours; courtesy of the Atlantic Geoscience Centre, 1991).

Group	Formation	Member	Dominant Lithology	Maximum Thickness (feet)
Quaternary	Sable Island		sand & gravel	
	La Have		clay	
	Sambro		sand	
	Emerald		silt	
	Scotian Shelf		glacial drift	
The Gully Group	Banquereau		mudstone	4000'
	Wyandot		chalk	750'
	Dawson Canyon		shale	3000'
Nova Scotia Group	Logan Canyon	Marmora	sandstone & shale	800'
		Sable	shale	500'
		Cree	sandstone & shale	2000'
		Naskapi	shale	750'
	Missisauga		sandstone	3700'
Western Bank Group	Mic Mac		calcareous shale, sandstone	4000'
	Verrill Canyon		shale	> 2000'
	Abenaki	Baccaro	limestone	2500'
		Misaine	calcareous shale	300'
		Scatarie	limestone	400'
	Mohawk		sandstone & shale	3500'
	Iroquois		dolomite	650'
	Argo		salt	> 3000'

Table 2.1 Scotian Shelf stratigraphy, as designated by McIver (1972). For current nomenclature refer to Figure 1.2.

A second major study was published by Jansa and Wade in 1975, entitled "Geology of the Continental Margin off Nova Scotia and Newfoundland". This study further refined the stratigraphy of the basin, and developed the geologic history in greater detail. Their interpretation was also based on marine reflection seismic profiles and well-log data (46 exploratory wells and 25 core holes). The larger quantity of data available to Jansa and Wade enabled a more detailed study to be completed, although most of McIver's designations were retained. These two studies established the majority of the nomenclature of the units within the Scotian Basin.

Wade and MacLean (1990) summarized the pre-existing literature on the Scotian Basin, and revised many of the concepts within, in their paper "Aspects of the Geology of the Scotian Basin from Recent Seismic and Well Data". This publication has been

recognized as the definitive work on the stratigraphy of the Scotian Basin to date, and includes a detailed description of the geologic history.

MacLean and Wade also completed the 'Seismic Markers and Stratigraphic Picks in the Scotian Basin Wells' portion of the East Coast Basin Atlas Series (MacLean and Wade, 1993), which includes well picks for all wells in the Scotian Basin available at the time of publishing. The East Coast Basin Atlas Series acts as an overview of the sedimentary basins of offshore Eastern Canada using seismic reflection and refraction data, as well as surficial, geotechnical, magnetic, gravity, biostratigraphic, and well log data. The Scotian Shelf Area portion of the East Coast Basin Atlas Series (Atlantic Geoscience Centre, 1991) includes maps and a generalized write-up for each of the formations and other documented areas on the shelf. These maps, in combination with the various illustrations, charts, plots, and descriptive text provided, attempt to define the surficial geology, stratigraphy, structure, and sedimentology of each study area. These volumes serve as excellent references to the regional geology of the entire Scotian Shelf.

2.2 Geology of the Scotian Basin

The Scotian Basin is a series of Mesozoic-Cenozoic depocentres deposited during the development of the North Atlantic ocean basin. Deposition began in the Middle Triassic, with salt and redbed deposition in a rift setting. Regional depositional units were lens-shaped in cross-section, with the thickest sediments accumulating in the outer shelf/upper slope environments and building outwards over time (Figure 2.2; Wade and MacLean, 1990).

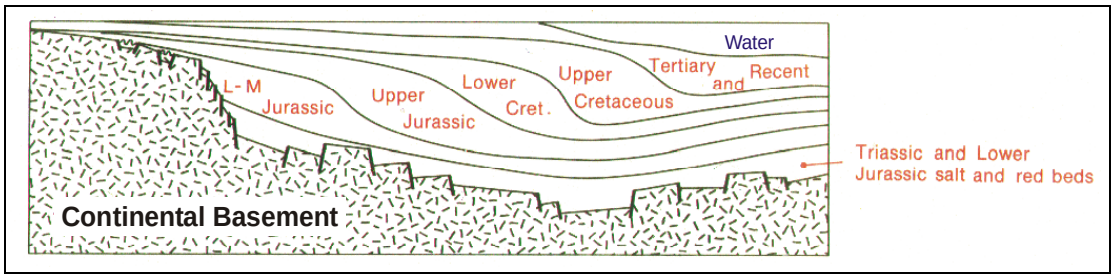

Figure 2.2 Generalized depositional units in the Scotian Basin (after Wade and MacLean, 1990).

The basement of the Scotian Basin is a seaward-dipping surface broken up into a complex of horsts and grabens by numerous northeast trending normal faults (ibid.). Within the basin, movements as young as the Tertiary can be recognized on some normal faults (Figure 2.3), including some involving the basement.

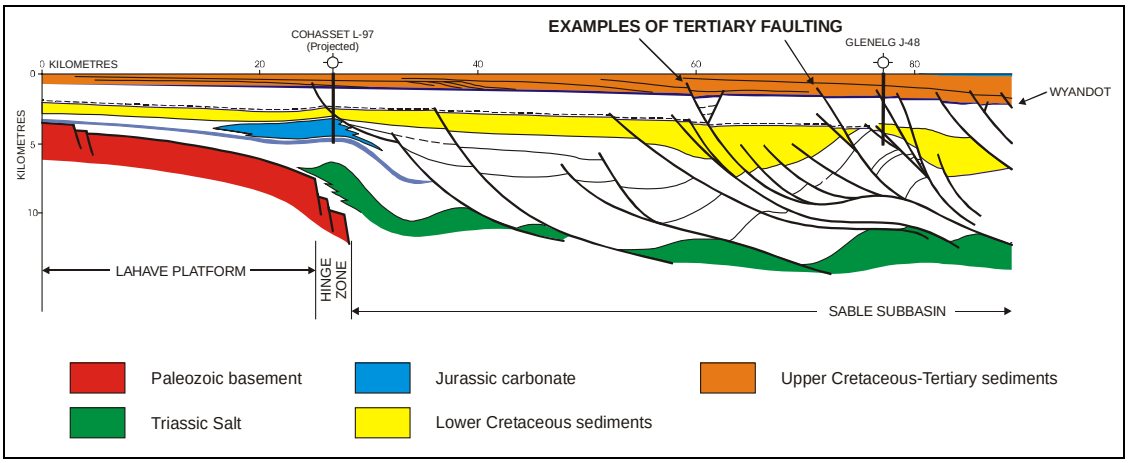

Figure 2.3 Cross-section illustrating deposition and faulting (after Wade and MacLean, 1990).

The LaHave Platform is a regionally stable area on the southwestern part of the Scotian Shelf (Figure 2.1). The relative tectonic stability of the platform has resulted in the deposition of a thin (approximately 4 km) sedimentary sequence compared to nearby basins. In those subbasins, prolonged subsidence has resulted in the accumulation of more than 12 km of strata, and maximum thickness may approach 18 km (ibid.; also see Figure 2.4).

The subbasins of the Scotian Basin include Shelburne, Sable, Abenaki, and Laurentian (Figure 2.1 and Figure 2.4). The subbasins are interconnected areas of thick sediments that were, initially, the loci of evaporite deposition, with each subbasin accumulating thick sequences of redbeds and evaporites which thinned across the intervening highs (Wade and MacLean, 1990). Two other areas with thick pre-breakup sediment fill in the basin are the Mohican Graben (in the LaHave Platform area, Figure 2.4) and the Orpheus Graben (east of Canso). A significant rift-related basin is also present on the basement of the LaHave Platform, the Naskapi Graben Complex (Figure 2.4). The Scotian Basin is also characterized by a major zone of diapiric structures trending from eastern Georges Bank to the western Grand Banks, referred to as the 'Slope Diapiric Province' (Figure 2.1).

2.2.1 Basement

Based on well penetrations, the basement on most of the Scotian Shelf consists of Paleozoic metasedimentary rocks, with several granitic intrusions (Wade and MacLean, 1990). These rocks can be correlated with the Cambro-Ordovician Meguma Group on mainland Nova Scotia, which also harbours granitic intrusions, such as the South Mountain Batholith (ibid.). During the Triassic, the rifting involved with the continental breakup of Pangea resulted in the formation of a series of northeast-trending normal faults, forming a large number of horsts and grabens on the margin of the Scotian Basin (Figure 2.2). Within these grabens, locally very thick accumulations of redbeds and evaporites were deposited.

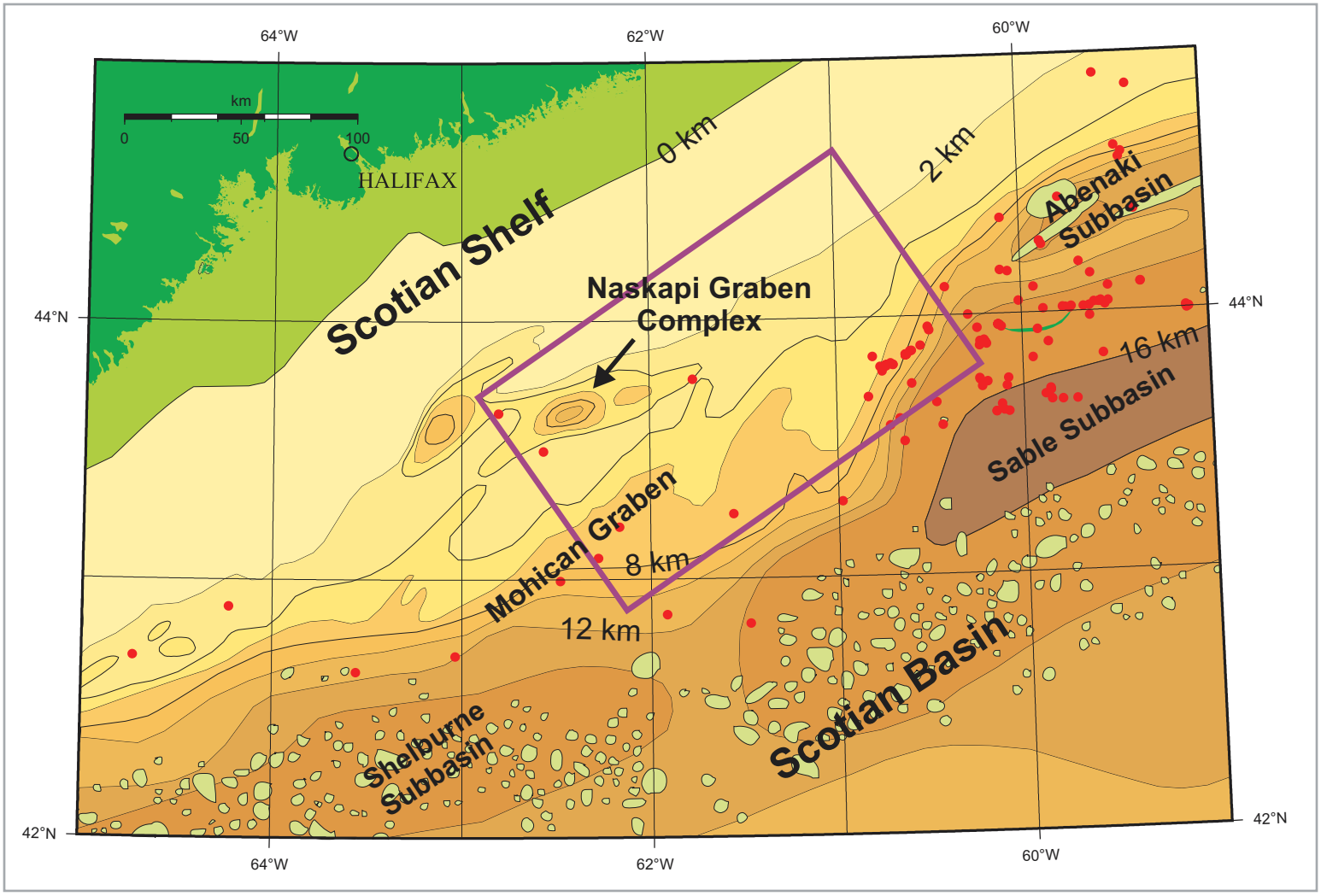

Figure 2.4 Depth to basement map (after Williams and Grant, 1998). The study interval is outlined by the purple box. The green structures represent Triassic/Jurassic salt (compiled by Wade, 1991).

2.2.2 Basin Stratigraphy Below Study Interval (after Wade and MacLean, 1990)

During the passive margin phase following the rifting phase of basin formation, salt deposition ceased in the Early Jurassic and was succeeded by continental clastics of the Mohican Formation and carbonates of the Iroquois Formation. During the Middle and Late Jurassic, clastic and carbonate facies developed along the margin of the basin, including the clastic Mic Mac and Verrill Canyon formations (primarily in the Sable Subbasin), and carbonate Mohawk and Abenaki formations (primarily on the LaHave Platform). Thick fluvial-deltaic Missisauga and Logan Canyon formations characterized the Early Cretaceous of the Sable Island area.

2.3 Stratigraphy of the Study Interval (after Wade and MacLean, 1990)

The Late Cretaceous-Tertiary sediments on the LaHave Platform include the Dawson Canyon, Wyandot, and Banquereau formations of the Gully Group (McIver, 1972). Within the shales and limestones of the Dawson Canyon Formation, a persistent series of thin (generally less than 30 metres) limestone beds, designated the Petrel Member (Jansa and Wade, 1975), forms a regional seismic marker. The thickness of the Dawson Canyon Formation varies from more than 500 m in the South Whale Subbasin and on the LaHave Platform, to just over 100 m in the outer part of the Sable Subbasin. The upper (as well as lower) contact of the overlying Wyandot Formation chalk also acts as a distinct regional marker, and serves as the base of the study interval for this project. The thickness of the Wyandot Formation increases eastward from an average of about 50 m on the LaHave Platform, to nearly 400 m beneath the eastern end of the Scotian Shelf. The overlying Banquereau Formation consists predominantly of mudstone that grades upward into increasing amounts of sandstone and conglomerate. The thickness of the

Banquereau Formation ranges from a zero edge along the middle part of the shelf to more than 1500 m in some wells in the Sable Subbasin. Hardy (1974) subdivided the Banquereau into four informal units, based on wells available at the time, the "Maskonomet beds" (mudstone-dominated), "Nashwauk beds" (sandstone-dominated), "Manhasset beds" (mudstone-dominated), and the "Esperanto beds" (sandstone-dominated). Wade and MacLean have noted the difficulty in correlating these units with the seismic data, and the nomenclature has not been widely adopted or subsequently formalized. The regional stratigraphy of the study interval is summarized in Figure 1.2 (after Wade and MacLean, 1990).

2.4 Stratigraphic Concepts

In the study of sediment distribution on the LaHave Platform, or in any other depositional setting, an understanding of stratigraphy and stratigraphic concepts is necessary. Stratigraphy is defined as the "distribution of layered rocks through time and space", and asks the following questions (Prothero and Schwab, 1997): How do these rocks correlate with others? How can their age be established? What is the pattern of transgressions and regressions of the coastline? How completely do sediments represent the geologic record? What environments do they represent, and how do they vary? These questions can be addressed by using the concepts of sequence and seismic stratigraphy.

2.4.1 Seismic Stratigraphy

Although preceded by earlier, related studies, seismic stratigraphy mainly grew out of investigations performed by the Exxon Production Research Company, summarized initially by Vail and Mitchum (1977). This publication explains many of the

fundamentals of large-scale stratigraphic analysis (both seismic and otherwise) and is a good starting point for anyone attempting this kind of work.

Seismic stratigraphy is "basically a geologic approach to the stratigraphic interpretation of seismic data" (Vail and Mitchum, 1977), or "the study of seismic data for the purpose of extracting stratigraphic information" (Boggs, 1987). Seismic sequence analysis is based on the identification of stratigraphic units composed of a "relatively conformable succession of genetically-related strata bounded by unconformities and their correlative surfaces", termed depositional sequences (Vail and Mitchum, 1977. Depositional sequence boundaries are recognized on seismic data by identifying the geometry of reflections caused by lateral terminations of strata, termed onlap, downlap, toplap, and truncation (see Section 2.4.12, including Figure 2.8). The analysis of seismic facies is the description and interpretation of reflection geometry, continuity, amplitude, frequency, and interval velocity, as well as the external form and associations of seismic facies units within the framework of depositional sequences (ibid.). Where the seismic facies are described and mapped, an interpretation of the sedimentary processes and environmental settings allows the interpreter to predict the lithology of the seismic facies (ibid.), and test these hypotheses with well data.

2.4.1.1 Depositional Sequences

A depositional sequence is a stratigraphic unit composed of relatively conformable succession of genetically related strata bounded at its top and base by unconformities or their correlative conformities (Mitchum et al., 1977). Sequences of different magnitudes may be recognized on seismic sections, well-log sections, and

surface outcrops. The basic concepts of a depositional sequence are illustrated in Figure 2.5.

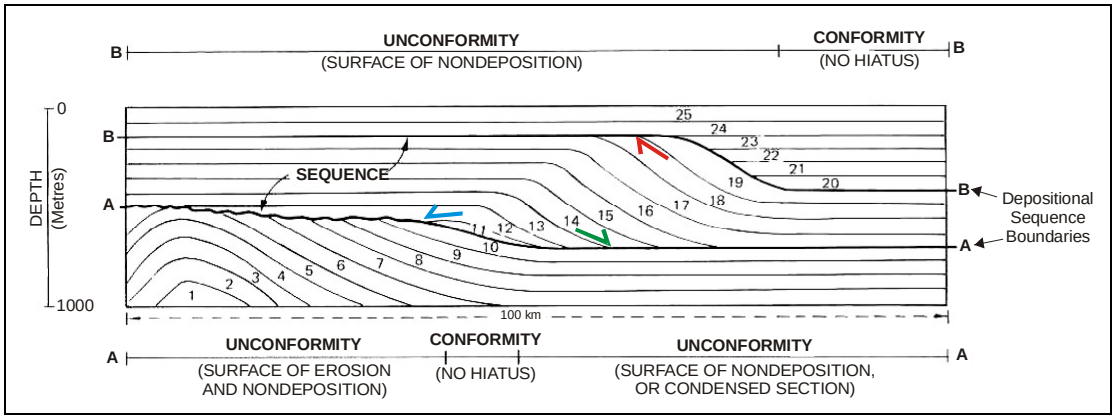

Figure 2.5 Generalized vertical section of a sequence (after Mitchum et al., 1977). Arrows represent geometrical relationships of strata to depositional sequence boundaries (Section 2.4.1.2).

In this generalized depiction of a sequence, boundaries, defined by surfaces A and B, pass laterally from unconformities to their correlative conformities. Individual units of strata, 1 through 25, are traced by following stratification surfaces, and assumed conformable where successive strata are present. Where units of strata are missing, hiatuses are evident. Figure 2.6 illustrates these relationships as a chronostratigraphic section.

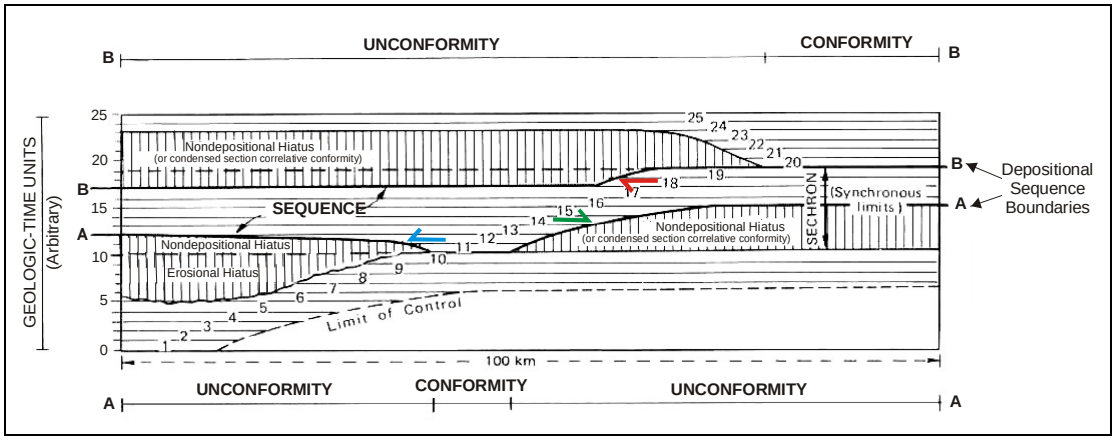

Figure 2.6 Generalized chronostratigraphic section of a sequence (after Mitchum et al., 1977). Arrows represent geometrical relationships of strata to depositional sequence boundaries (Section 2.4.1.2).

Here, the geologic time range of the sequence between A and B varies, but the variation is confined within the parts of the sequence's boundaries that are conformable. Unconformities that bound depositional sequences are observable discordances in a given stratigraphic section that show evidence of erosion or nondeposition with obvious stratal terminations.

2.4.1.2 Depositional Sequence Boundaries

To define and correlate a depositional sequence correctly, the sequence boundaries must first be defined and traced. As a particular sequence boundary is traced laterally, the strata may become concordant, but enough of a hiatus may still be evident to continue the designation of an unconformity (a paraconformity). If the boundary is traced to where there is no evidence of a hiatus, the unconformity has been traced to its laterally equivalent, correlative conformable surface (its correlative conformity).

An unconformity is a surface of erosion or nondeposition that separates younger strata from older rocks and represents a significant hiatus. A conformity is a surface that separates younger strata from older rocks, but along which there is no evidence of erosion or nondeposition, and no significant hiatus is indicated. A hiatus is the total interval of geologic time that is not represented by strata at a specific position along a stratigraphic surface. If the hiatus encompasses a significant interval of geologic time, the stratigraphic surface is an unconformity.

Figure 2.7 illustrates the concordant and discordant relations of strata to boundaries of depositional sequences. These relationships are based on the parallelism (concordance), or lack of it, between the strata and the boundary surface itself. If the strata both above and below a surface are concordant, then there is no geometrical

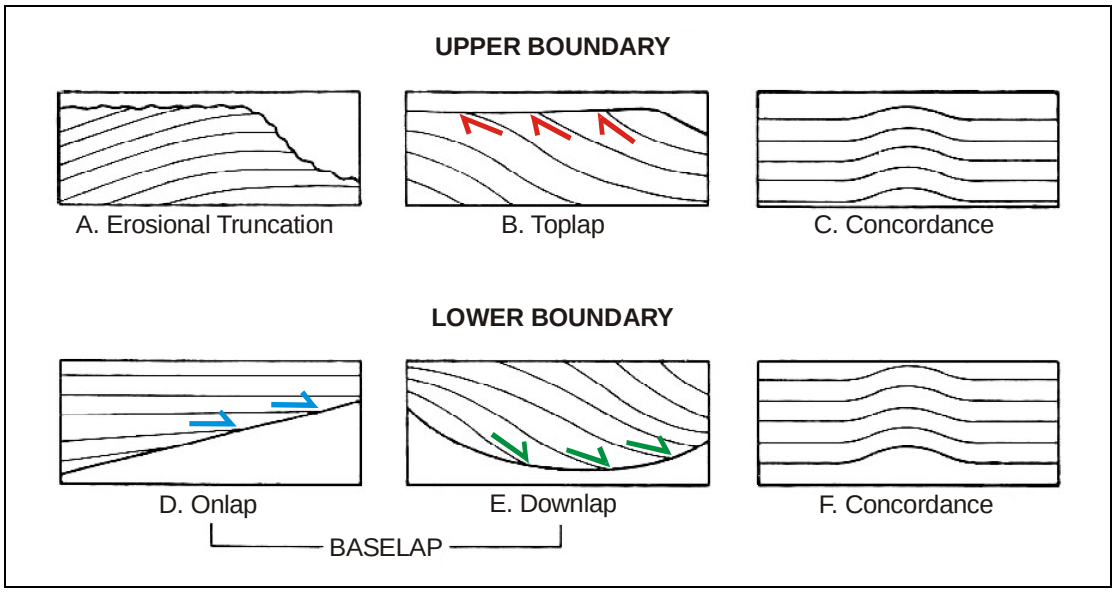

Figure 2.7 Various geometrical relationships of strata to depositional sequence boundaries (after Mitchum et al., 1977). Arrows represent the geometrical relationships of strata to the depositional sequence boundaries.

the strata above or the strata below a surface are discordant, then there is evidence of an unconformity. Unconformities without significant discordance at seismic resolution can be recognized by other means, such as biostratigraphy, or detailed outcrop or core-scale observations demonstrating a smaller-scale discordant relationship.

2.4.1.3 Baselap

Baselap is lapout at the lower boundary of a depositional sequence. Two important types of baselap are recognized: onlap and downlap. Onlap is baselap in which an initially horizontal stratum laps out against an initially inclined surface, or in which an initially inclined stratum laps out updip against a surface of greater initial inclination (Figure 2.7-D). Downlap is baselap in which an initially inclined stratum terminates downdip against an initially horizontal or inclined surface (Figure 2.7-E). Onlap and downlap are usually indicators of nondepositional hiatuses, rather than erosional hiatuses (Mitchum et al., 1977).

2.4.1.4 Condensed Sections

Condensed sections are formed as the result of very slow but continuous deposition, and often represent the correlative conformity (or concordance in Figure 2.7-C,F) of a depositional sequence (Walker, 1992). Condensed sections are usually recognized from outcrop rather than seismic data, due to the limited resolution of most seismic information. Because the beds are too thin to resolve seismically, when viewed at seismic resolution the section may appear to represent an unconformity, even though deposition was continuous and no unconformity exists. Condensed sections are thus often inferred in seismic sections in areas of downlap, where the thickness of the units are thinning below seismic resolution.

2.4.1.5 Toplap

Toplap is lapout at the upper boundary of a depositional sequence, and is evidence of a nondepositional hiatus (Figure 2.7-B). During the development of toplap, sedimentary bypassing and some minor erosion occurs above base level (often sea level; see discussion in Section 2.4.2), while prograding strata are deposited laterally below base level. The distinction between toplap and erosional truncation (the lateral termination of a stratum by erosion) may be difficult, but in the latter relation the strata tend to maintain parallelism as they terminate abruptly against the upper boundary rather than taper to it (Mitchum et al., 1977).

2.4.1.6 Seismic Sequence Analysis

Seismic sequence analysis involves identification of major reflection packages that can be delineated by recognizing horizons of discontinuity. The external form or geometry of seismic units and their areal associations can be used to identify seismic

facies, which can provide information on sediment source and geologic setting; in other words, a hypothetical depositional history of the units (Boggs, 1987). Seismic sequence and facies analysis thus proceeds as follows: once the major depositional units, such as marine onlap-offlap systems, are identified, these sequences provide a first-order stratigraphic framework within which more detailed seismic facies studies can be carried out. Seismic facies within the sequences are then distinguished on the seismic section on the basis of either the dominant type of reflection configuration, reflection continuity, bounding relationships, reflection amplitude and frequency, and/or other seismic attributes (Boggs, 1987). The concepts used in seismic stratigraphy are thus closely parallel to those developed in sequence stratigraphy, although generally on a larger scale and limited by seismic resolution.

Following the investigations performed by Mitchum et al. (1977), the correlation between seismic stratigraphic concepts and geology were described by authors such as Wilgus et al. (1988), culminating in the concept of sequence stratigraphy, detailed below.

2.4.2 Sequence Stratigraphy

Sequence stratigraphy is essentially seismic stratigraphy at a smaller, more detailed scale, using rock rather than seismic data. In sequence stratigraphy, the unconformity-bound depositional sequences (identifiable at seismic resolution) are further subdivided into systems tracts, which represent stratal wedges produced during various episodes of high or low relative sea level and/or sediment supply, and include highstand, lowstand, and transgressive system tracts. An idealized continental margin profile, often referred to as the ‘sea slug’ model, is commonly used to illustrate the

different components, and relationships between those components, in sequence stratigraphy (Figure 2.8).

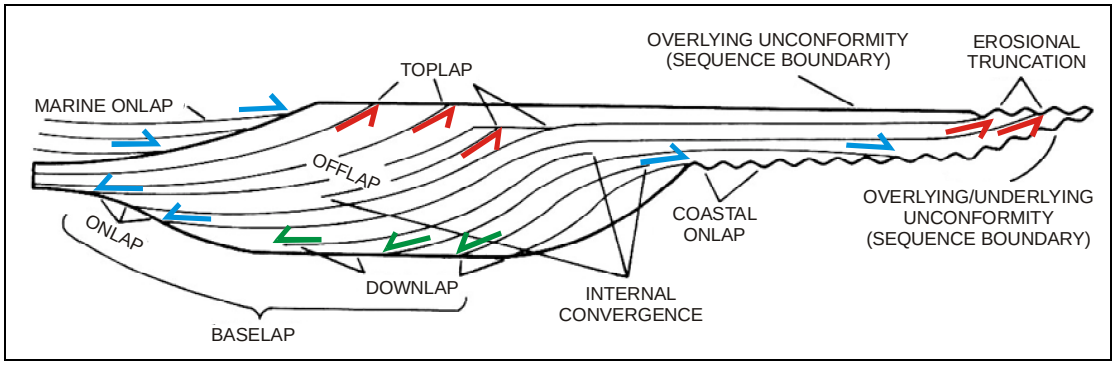

Figure 2.8 Idealized sea slug sequence stratigraphic model. Onlap is represented by blue arrows, downlap by green arrows, and toplap and erosional truncation by red arrows (after Mitchum et al., 1977).

The model is composed of numerous system tracts that are stacked on top of and adjacent to one another. The analysis of the stratigraphic features of modern analogs has allowed the establishment of the typical relationships between rock units, which can be used to infer the geologic history of the rocks with a particular relationship. Although much of the literature on sequence stratigraphy is based upon the concept of eustatic (i.e. global) sea level change as the major controlling factor, and global sea level charts have been developed (Haq et al., 1987), it is important to understand that sequences are controlled by the interplay of sediment supply, tectonism, and sea level change, and that they can be recognized and described independent of global sea level.

2.5 Seismic Data

2.5.1 Data Acquisition

The acquisition of seismic data begins with a bang, or shot, generated by an airgun (during offshore acquisition) that sends a short, sharp pulse of sound into the water (called the source wavelet; Figure 2.9-A).

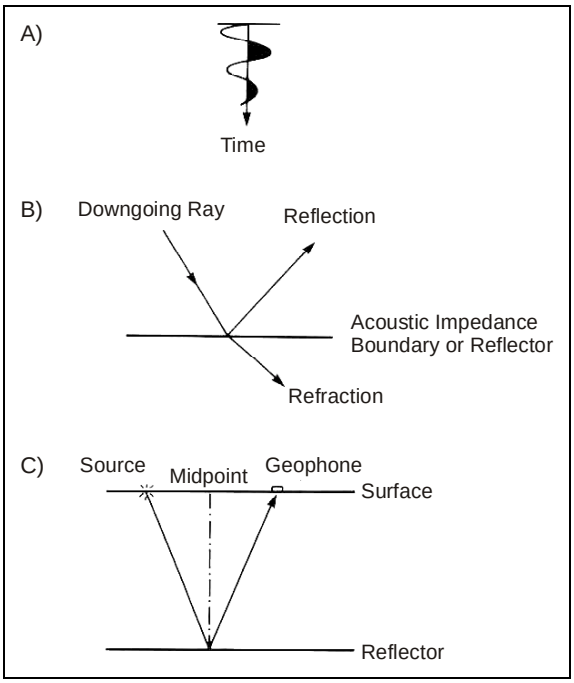

Figure 2.9 Basic elements of seismic-reflection data acquisition. A) Diagrammatic source wavelet; B) Reflection and refraction at an acoustic impedance boundary; C) Reflection geometry for a horizontal reflector (after Badley, 1985).

This sound wave passes down through the rock until it encounters a new rock layer of different hardness, or acoustic impedance (AI = density*velocity), than the rock in which it is travelling. The reflection coefficient (RC) between two layers is defined by the acoustic impedance contrast:

$$RC = (AI_2-AI_1)/(AI_2+AI_1)$$

where AI_2 is the acoustic impedance of the upper layer, and AI_1 is the acoustic impedance of the lower layer. If the overlying layer is softer (i.e. has a lower acoustic impedance), the reflection coefficient is positive. If the overlying layer has a higher acoustic impedance, the reflection coefficient is negative. The higher the acoustic impedance contrast, the higher the reflection coefficient.

A portion of the energy of the downward-travelling wavelet echoes back to the surface, while the original, and now weaker, pulse continues downward through the rock, producing reflections as it passes through additional acoustic impedance boundaries

(Figure 2.9-B). The seismic echoes are then recorded by hydrophones as they return to the surface. Because the sound waves travel down to a reflector and back up to the surface again (Figure 2.9-C), the time recorded is two-way time (TWT). Further details of the trace are recognized in terms of: amplitude - a measure of reflection strength; frequency (measured in Hz) - the number of oscillations per second; bandwidth - the range of frequencies present; and phase - which describes the relative shape and time position of a reflection. To increase the signal-to-noise (S/N) ratio, reflections are recorded from the same subsurface point with different source-to-hydrophone offset, a procedure known as common depth point (CDP) or common midpoint (CMP) shooting.

2.5.2 Processing

The processing of seismic field data begins by editing and reordering the data so that the series of samples corresponding to each hydrophone are brought together, resulting in a separate trace for each hydrophone. This process is called demultiplexing. Next, the data undergoes deconvolution, which is a mathematical procedure for unscrambling the overlapping effects of waveshape convolution to reveal only those reflections that are the result of real reflectors.

The traces are then grouped together by common midpoints, and are then known as CMP or CDP gathers. Velocity analysis is then performed on the CMP gathers, which provides the normal moveout (NMO) velocities. Because of the continually increasing travel paths during CMP data acquisition, the same reflection on each CMP trace will have been recorded at progressively greater times for increasing offsets. Applying the appropriate NMO velocity to a reflector brings the reflection to the same time for all traces in the CMP gather.

Next, all the values corresponding to a particular reflection time on each trace are added together, through a process known as stacking. Stacking serves two major purposes: it enhances the reflections from true reflectors, and reduces noise levels, improving the signal-to-noise ratio. Commonly, a second deconvolution operation is applied after stacking, followed by the application of a time-variant filter (TVF). This filter removes unwanted frequencies by using a filter whose bandpass becomes a lower frequency as depth increases. This removal of frequencies above the estimated maximum frequency not only improves the cosmetics of the line, but also further improves the signal-to-noise ratio.

Finally, because a basic assumption of the CMP method is that the reflections originate from the midpoint between the source and hydrophone, if the reflector is inclined the assumption is no longer valid. To restore the reflections to their correct subsurface positions, the data is migrated. Even when migration is performed there can still be inaccurate assumptions in the processing methodology. For example, some reflection energy could be from out of the plane of the seismic section. Possible artefacts and limitations of seismic data must be understood for proper interpretation.

For additional information relating to the acquisition and nature of seismic data, refer to “Practical Seismic Interpretation” by M.E. Badley (1985). For a more detailed introduction and background to the acquisition and processing of seismic data, refer to “Seismic Data Processing” by Ö. Yilmaz (1987).

3. Data and Methods

3.1 Seismic Data

The seismic data used for this project includes multi-channel exploration data acquired by industry during the 1970s and 1980s that has since been made publicly available. The main dataset used for this project was acquired during a Petro-Canada 2D reflection seismic survey in 1982, survey number 8624-P028-049E. This survey was made available on mylar from the Canada-Nova Scotia Offshore Petroleum Board (CNSOPB), as was the navigation data for the lines. The survey was borrowed and paper copies of the lines were made. To tie together the ends of some of the lines, selected lines from a PAREX/Soquip 2D survey shot in 1983, survey number 8620-S014-006E, were also used. Copies of these lines were also available from the CNSOPB, and paper copies were made for this study. Three seismic lines from a Shell 2D survey (survey number 8624-S006-005E,6E, 1970), were also used to fill in gaps in the seismic grid. Additional lines from each of the two secondary surveys were also used to help identify canyons. The Shell survey was only available as microfiche, therefore the lines had to be reformatted to be easily used. This was accomplished by scanning the individual microfiche pieces at 1200 dots per inch and splicing them together using Adobe Photoshop to recreate the complete line (A. MacRae, pers. comm., 2002). Although the resolution obtained from such a process was not ideal, the now-digital nature of the data allowed the lines to be manipulated further (as discussed in Section 3.1.1). These lines were then plotted onto paper at a suitable scale to tie with the paper copies of the lines from the other two surveys. Interpretation of all seismic lines was completed exclusively by hand on the paper copies. Figure 3.1 is a map of the surveys and seismic lines used

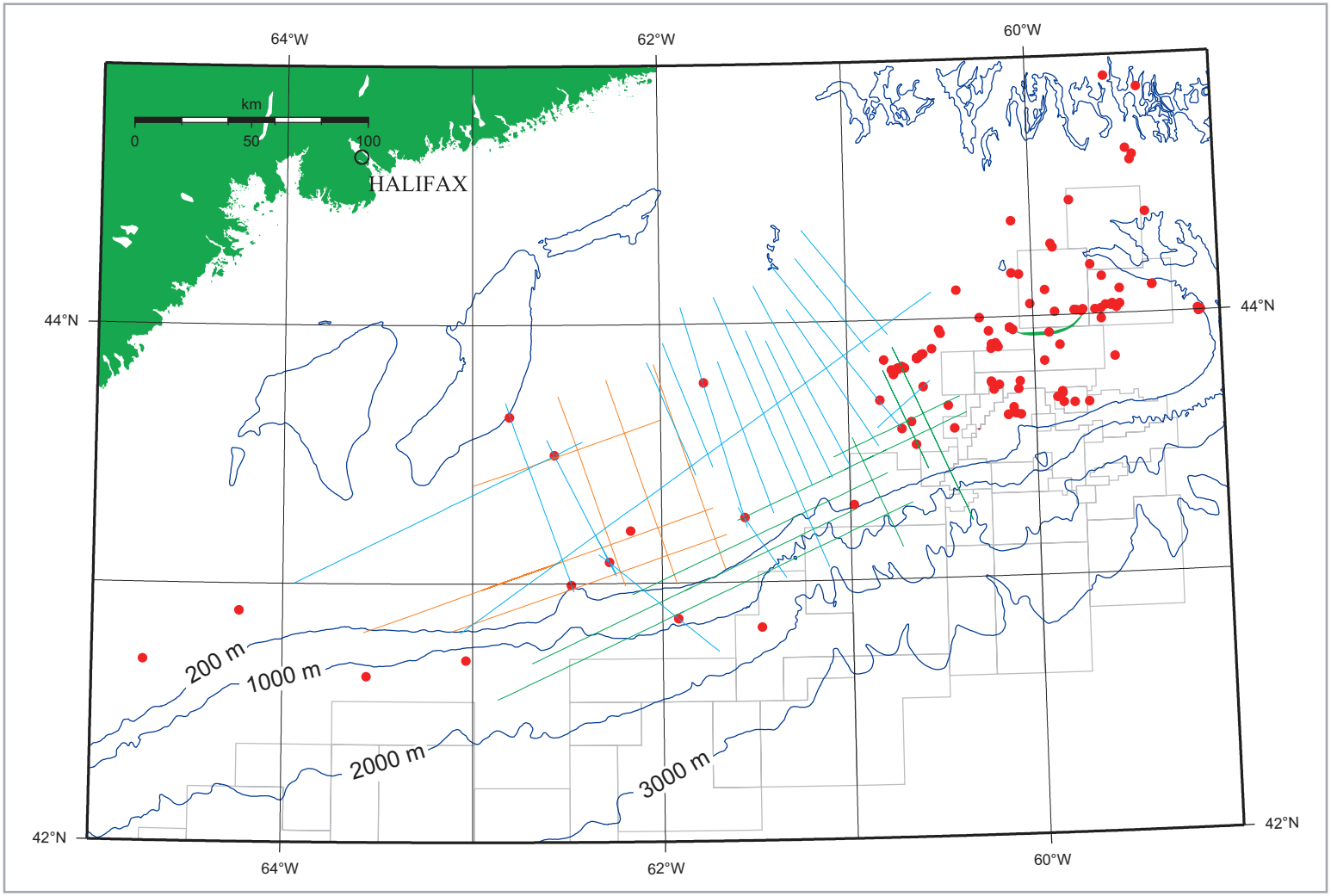

Figure 3.1 Seismic lines used for this project (navigation from the BASIN database, 2002, 2002). Light blue lines represent the Petro-Canada survey, green lines represent the selected lines of the PAREX/Soquip survey, and orange lines represent the selected lines of the Shell survey (see text). The study area is outlined by the purple box. For other data sources refer to Figure 1.1.

for this project. The survey details and line numbers used are provided in Appendix A.

3.1.1 Seismic Interpretation Techniques

First, the vertical scales for the PAREX/Soquip and Shell seismic profiles were rescaled to 2.5 inches per second (2.5 in/sec) to correspond with the Petro-Canada survey. Before the lines were resized, the scales were manually checked to insure that their quoted scales were correct. The scaling on all lines was satisfactory. The resizing of the 5.0 cm/sec PAREX/Soquip survey was accomplished by photocopying the lines with an enlargement of 127%. Although photocopying can introduce some minor distortion, this simple method produced a good tie between the two surveys (Figure 3.2). This suggests that the surveys were recorded using a similar source wavelet (Section 3.2.3), and underwent comparable processing, although it is apparent from the figure that data scaling and water bottom processing were somewhat different.

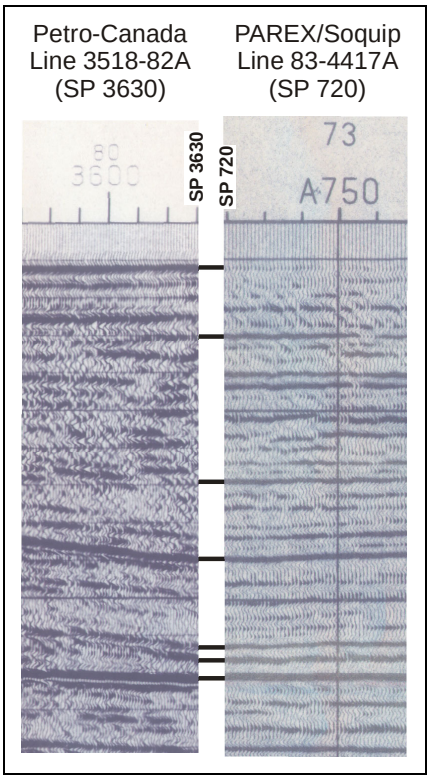

Figure 3.2 Sample tie between Petro-Canada (line 3516-82B) and PAREX/Soquip (line 83-4417A) seismic data (data courtesy of the CNSOPB, 2002).

For the Shell survey, the lines were rescaled digitally and plotted. Because of the size limitations of the digital image, the Shell lines were horizontally compressed, so that each line could be plotted at a practical length (on 36-inch wide plotting paper). Although this reduced the horizontal resolution of the lines (such as the precision of shotpoint positions), having the lines plotted in this manner did enhance subtle angular relationships, and allowed the entire line to be examined at once.

With all data now at a consistent vertical scale, onlap, downlap, and toplap surfaces were identified. Potential unconformity surfaces were then identified by recognizing a series of similar relationships (for example, if a number of minor reflections onlapped onto the same reflection). Such reflections (recognized on individual lines) were then tied to adjacent lines, to observe if the relationship persisted. The most consistent reflections were then mapped, where present, over the entire dataset (see Section 4.1 for details). Reflections were picked on the strongest positive reflection (the shaded peak) for practical reasons: on paper sections the shaded peak is easier to follow around than either the trough or zero-crossing of the trace, and it illustrates relationships between other reflections more easily. Because the main objective of this study was to identify mappable seismic packages, initially recognizing and applying the source wavelet was not necessary, and selecting the peak was considered acceptable.

After the reflection surfaces were mapped over the study area, their two-way time (TWT) was measured. The measurements were made using a scale constructed out of clear plastic, with a 2.5 in/sec scale printed on the sheet (Figure 3.3). This scale allowed the TWT to be estimated to the nearest thousandth of a second, with a degree of measurement uncertainty estimated at approximately ± 5 milliseconds (or ± 0.005

seconds). Because of stretching of the paper during reproduction and folding, the total uncertainty is probably slightly higher.

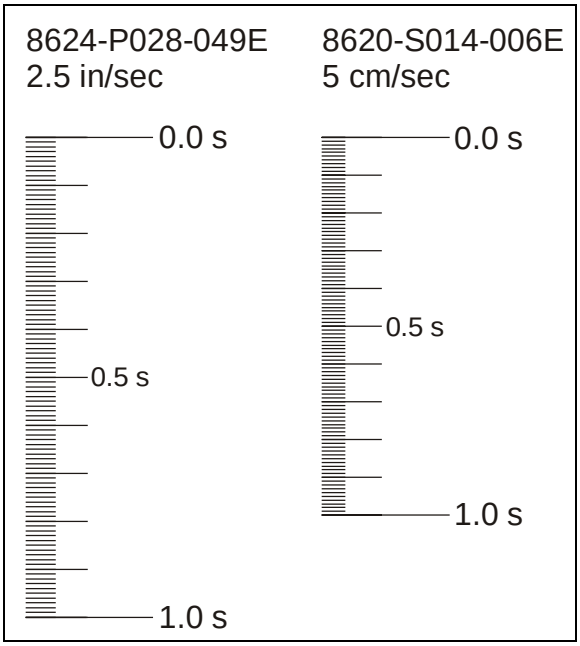

Figure 3.3 Sample of scale used to measure TWT on seismic profiles (not to scale).

3.1.1.1 Canyon and Fault Picks

Canyon locations were recorded by measuring the shotpoints of the centre, maximum curvature, and outer onlap edges of the canyons (Appendix G). Fault locations were recorded by measuring the shotpoints of the footwall and hanging wall termination points of a particular reflection against the fault (Appendix H). The offset of the fault (if perceptible) was also recorded at each reflection.

3.1.2 Digital Cartography

The seismic picks were plotted digitally using a program written by A. MacRae (GSC (Atlantic)) using the Generic Mapping Tools (GMT), version 3.4.1. GMT is a collection of approximately 60 UNIX tools that allow users to manipulate (x,y) and (x,y,z) data sets to produce Encapsulated PostScript File (EPS) illustrations. GMT was

developed and is maintained by P. Wessel and W.H.F. Smith, and is supported by the National Science Foundation (Wessel and Smith, 1998).

Once the seismic picks were tabulated, the GMT program cross-correlated the values with the navigation data for the surveys (from the BASIN database), using the unique seismic project number, line number, and shot point number for each pick to identify where the value should be plotted. Because BASIN did not contain the navigation data for some of the lines, their co-ordinates had to be retrieved by hand-digitizing the original shotpoint map (which was available at the GSC). Once the navigation for the picks had been established, the program then plotted the values along the seismic lines on the shotpoint map.

Once the data were plotted, TWT contours were plotted by hand (rather than digitally) to avoid encountering problems that can often arise when using digital contouring routines and algorithms (Badley, 1995). These contours were digitized using a digitizing tablet and "digit.exe", a FORTRAN program written by A. Jackson (GSC (Atlantic)). The final maps, including the digitized contours and the seismic picks values, were then produced using GMT. The Postscript files were modified further using CorelDraw 10 to add legends and annotations.

3.1.3 Data Coverage and Challenges

As previously mentioned, the main seismic program used for this project was a Petro-Canada 2D reflection seismic survey shot in 1982, survey number 8624-P028-049E. The seismic lines used from this survey can be seen in Figure 3.1. Although the lines do not create a tight grid (compared with more recent and extensive 2D surveys, or modern 3D surveys), the quantity of data was sufficient for this project. Seismic line

number 3526-82A of this survey was not available from the CNSOPB. Due to the dominance of lines in the eastern portion of the survey area, this project focused on that region. Most of the lines in this part of the survey are dip lines (seismic lines that run in the direction of the dip of the geology), as opposed to strike lines (seismic lines that run approximately parallel to the strike of the geology). Thus, the study area primarily consists of a series of dip lines connected by a single continuous strike line, with no complete grid on the north or south side upon which to test the continuity of the reflections. An important part of any seismic interpretation exercise is the ability to 'tie to a grid' (or loop-tying), as it allows the reflections to 'test themselves' as they are being interpreted, to assure that the same reflection is being selected as it is mapped. To create seismic grids so that ties could be performed, lines from other seismic programs were merged with the Petro-Canada survey (discussed in Section 3.1.1; see Appendix A for seismic survey details). Although the other seismic programs were of a different vintage, and were recorded and processed separately, the data complimented each other well, and the seismic data were successfully incorporated (see Section 3.1.1 for discussion on how the surveys were integrated with one another).

3.2 Well Data

3.2.1 BASIN Database

BASIN (http://agcwww.bio.ns.ca/BASIN/) is a digital database maintained by the GSC (Atlantic) that contains various geological, geophysical, and engineering information acquired during petroleum exploration from the offshore of eastern Canada (Moir, 1999). BASIN contains both raw data as well as interpreted information for most of the exploration wells drilled offshore, and for a large number of the seismic surveys

conducted in the area. Much of the information within BASIN is available elsewhere in hardcopy, dispersed through technical documents and publications (Moir, 1999). The database was developed out of the need to better archive and simplify access to the large quantity of geological, geophysical, and engineering information available. Much of these data can be accessed via the Internet for clients of the GSC and GSC staff. A demonstration session of the database is also available publicly on the web. Client Access is available to clients of the GSC who have purchased the BASIN database for private use. For this project I was granted GSC Internal Access to the database, which is intended for employees and collaborators of the GSC, and allows complete access to the database.

3.2.2 Wells Used

The wells used for this project are summarized in Figure 3.4 and Table 3.1, and Figure 3.5 is a sample of the BASIN well log data. Data was plotted with a program, "lithoplot3.perl" written by A. MacRae (GSC (Atlantic)). The BASIN database software was used to generate and plot these data, using wireline logs available from QC Data International Inc. (QC Data) of Calgary, Alberta, and lithostratigraphy data courtesy of Canadian Stratigraphic Service Ltd. (CanStrat), also of Calgary, Alberta. A more detailed summary of each well is included in Appendix B. Note that all well depth measurements are measured relative to kelly bushing datum. All wells in the study area were plugged and abandoned.

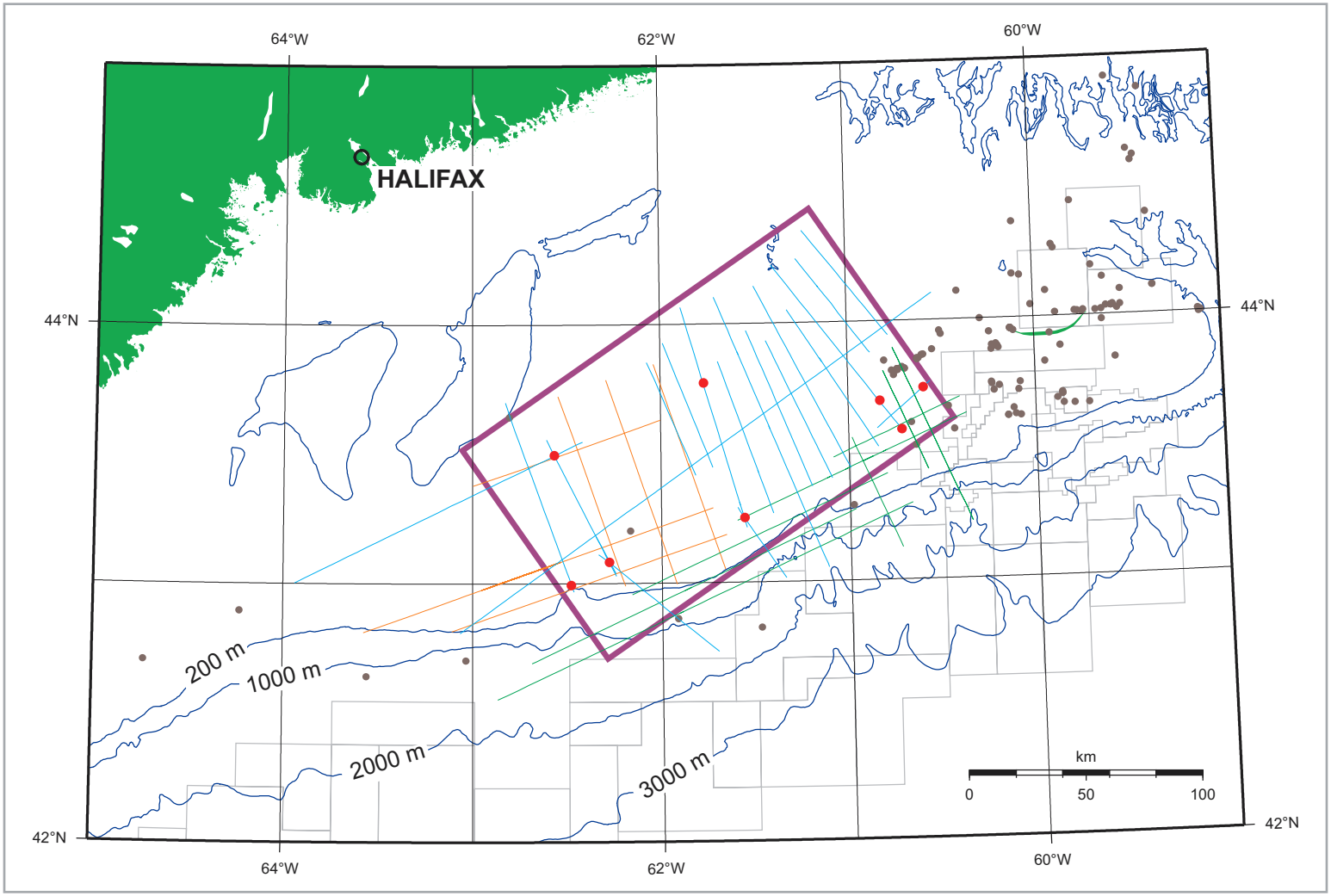

Figure 3.4 Wells used for this project (red points; data from BASIN and the CNSOPB, 2002). Brown dots represent wells not used for this project. For other data sources refer to Figure 1.1.

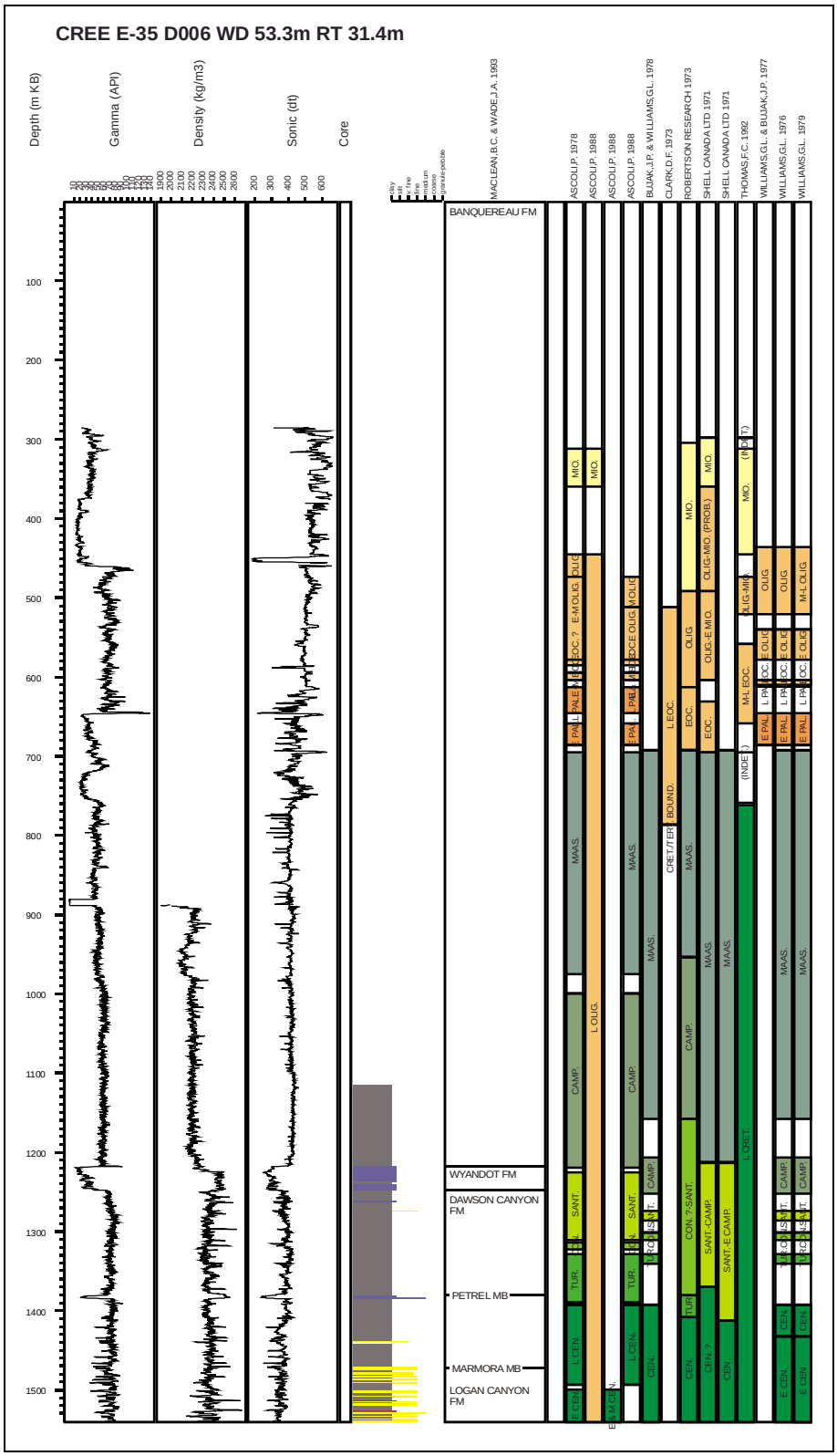

Figure 3.5 Well log data for Cree E-35 well (obtained from BASIN, 2002; wireline data courtesy of QC Data Inc.; lithostratigraphy courtesy of CanStrat Ltd.; biostratigraphy courtesy of individual authors, obtained from BASIN). For remainder of wells, refer to Appendix D.

Well Name	Year Drilled	Company	Total Depth (m KB)	Water Depth (m)	Kelly Bushing (m)
Alma K-85	1985	Shell/Petro-Canada/others	3602.0	65.3	24.0
Cree E-35	1970	Shell	3983.7	53.3	31.4
Demascota G-32	1974	Shell	4672.3	54.3	29.9
Moheida P-15	1976	Petro-Canada/Shell	4297.7	111.9	29.9
Mohican I-100	1971	Shell	4393.4	153.3	29.9
Naskapi N-30	1970	Husky/Bow Valley/others	2205.2	95.1	25.9
Ojibwa E-07	1974	Union/Shell/others	2329.6	75.6	29.9
Oneida O-25	1969	Shell	4109.9	82.3	25.9

Table 3.1 Wells used for this project (data from BASIN and the CNSOPB, 2002).

3.2.3 Well Ties

Synthetic seismograms for each of the wells were produced using GeoSyn version 4.8.1.5 (2001), a Windows-based synthetic and modelling software package created by IHS AccuMap Limited of Calgary, Alberta. Figure 3.6 is a sample of the synthetic seismic produced by GeoSyn. Seismograms for all wells used in this study are available in Appendix E. Synthetic seismograms are simulated seismic traces produced from the well log data using the sonic and density logs (from which reflectivity coefficients are calculated for the well). The reflectivity coefficients were then convolved with a suitable wavelet with a frequency response and band intended to be similar to the seismic sections. Because all of the wells in the study area were positioned over lines from the Petro-Canada survey, and because the source wavelet used was not indicated on the section labels, a conventional 22 Hz Ricker wavelet was used, as well as a similar 10/15-30/45 bandpass wavelet (22.5 Hz peak).

The synthetic seismic traces were used to tie the seismic data to the well log data. Because the reference point (or zero two-way time (TWT)) of the synthetic seismogram is initially placed at the start of the well log, which is usually hundreds of metres below sea level, the TWT from kelly bushing to the start of the log had to be approximated. This was calculated by estimating the TWT of both the water column and overlying rock

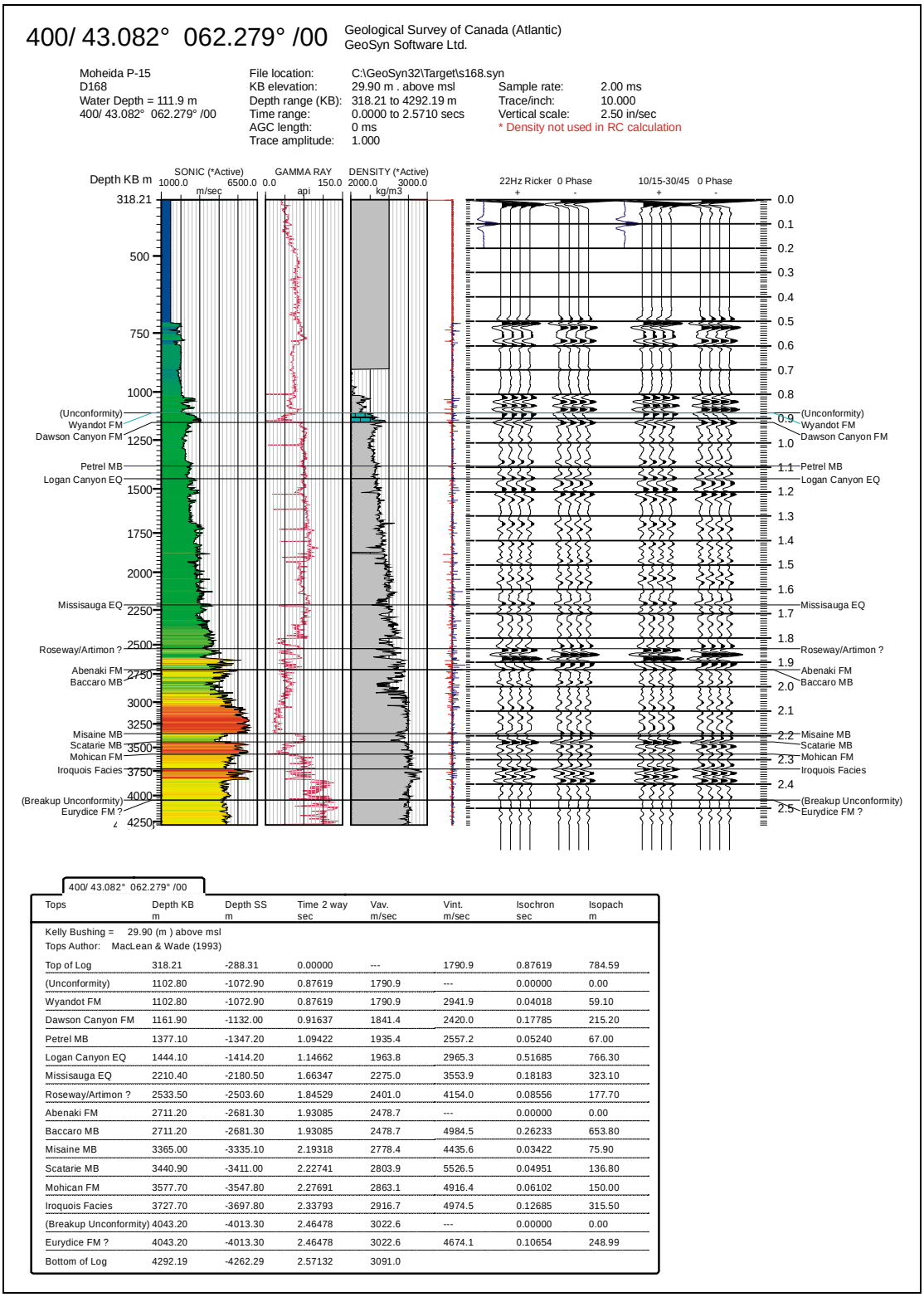

400/ 43.082° 062.279° /00

Tops	Depth KB m	Depth SS m	Time 2 way sec	Vav. m/sec	Vint. m/sec	Isochron sec	Isopach m
Kelly Bushing = 29.90 (m) above msl							
Tops Author: MacLean & Wade (1993)							
Top of Log	318.21	-288.31	0.00000	---	1790.9	0.87619	784.59
(Unconformity)	1102.80	-1072.90	0.87619	1790.9	---	0.00000	0.00
Wyandot FM	1102.80	-1072.90	0.87619	1790.9	2941.9	0.04018	59.10
Dawson Canyon FM	1161.90	-1132.00	0.91637	1841.4	2420.0	0.17785	215.20
Petrel MB	1377.10	-1347.20	1.09422	1935.4	2557.2	0.05240	67.00
Logan Canyon EQ	1444.10	-1414.20	1.14662	1963.8	2965.3	0.51685	766.30
Missisauga EQ	2210.40	-2180.50	1.66347	2275.0	3553.9	0.18183	323.10
Roseway/Artimon ?	2533.50	-2503.60	1.84529	2401.0	4154.0	0.08556	177.70
Abenaki FM	2711.20	-2681.30	1.93085	2478.7	---	0.00000	0.00
Baccaro MB	2711.20	-2681.30	1.93085	2478.7	4984.5	0.26233	653.80
Misaine MB	3365.00	-3335.10	2.19318	2778.4	4435.6	0.03422	75.90
Scatarie MB	3440.90	-3411.00	2.22741	2803.9	5526.5	0.04951	136.80
Mohican FM	3577.70	-3547.80	2.27691	2863.1	4916.4	0.06102	150.00
Iroquois Facies	3727.70	-3697.80	2.33793	2916.7	4974.5	0.12685	315.50
(Breakup Unconformity)	4043.20	-4013.30	2.46478	3022.6	---	0.00000	0.00
Eurydice FM ?	4043.20	-4013.30	2.46478	3022.6	4674.1	0.10654	248.99
Bottom of Log	4292.19	-4262.29	2.57132	3091.0			

Figure 3.6 Synthetic seismogram for Moheida P-15 well (prepared using GeoSyn version 4.8.1.5). For remainder of wells, refer to Appendix E.

using standard approximate velocities for each medium. The velocity of water (V_{water}) used was 1470 m/s (Badley, 1985), and the velocity within the overlying rock (V_{rock}) used was 1700 m/s (C. Jauer, pers. comm., 2002). These velocities were then converted to TWT and summed, and the top of the log was referenced to that datum. Note that the effect of having several metres of air (equal to the kelly bushing elevation) calculated as part of the water column was assumed to be negligible, and thus not included in the calculation. The distinctive character of (and confidence in) the Wyandot reflection was used to confirm the offset of the synthetic seismogram. Table 3.2 includes the estimated TWT to the top of the log ($TWT_{top\ log}$) for each of the wells used.

Well Name	Water Depth (m)	TWT_{water} (ms)	Overlying Rock Thickness (m)	TWT_{rock}	$TWT_{top\ log}$
Alma K-85	65.3	89	477	561	650
Cree E-35	53.3	73	232	273	346
Demascota G-32	54.3	74	210	247	321
Moheida P-15	111.9	152	206	242	358
Mohican I-100	153.3	209	210	247	456
Naskapi N-30	95.1	129	236	278	407
Ojibwa E-07	75.6	103	223	262	365
Oneida O-25	82.3	112	139	164	276

Table 3.2 Estimated TWT to the top of well logs (from BASIN, courtesy of the CNSOPB, 2002).

When correlated with the synthetic seismogram produced using the 22 Hz normal, zero-phase Ricker wavelet, the relationship between the peaks was acceptable in the shallow part of the section (Figure 3.7). With the uppermost reflections matched, however, the deeper record (below the study interval) does not tie precisely. This is most likely due the fact that because the line was (probably) processed with emphasis placed on the deeper record, the resulting plot of the data was not scaled consistently over the entire interval. Even so, this deeper mistie was considered satisfactory due to the relatively shallow study interval of this project. Note that the negative acoustic impedance contrast at the limestone boundary at the top of the Wyandot Formation produces a peak where a

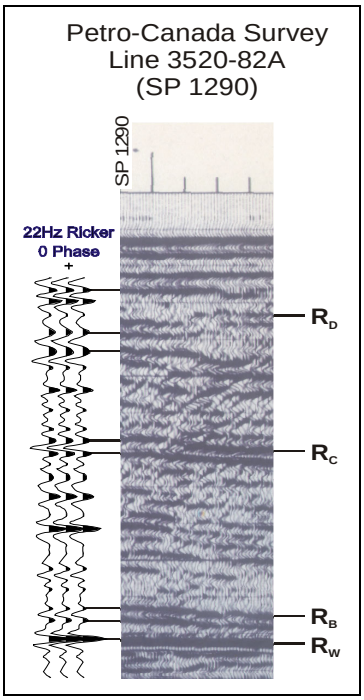

Figure 3.7 Synthetic seismogram/seismic data tie for Oneida O-25 well. R_W represents Wyandot Reflection, R_B = Reflection B, R_C = Reflection C, and R_D = Reflection D (see Section 4.1 for details).

trough should result if a normal polarity source wavelet is used (Badley, 1985). Because the three surveys are assumed to have been plotted using a similar wavelet (based on the success of the ties between them, Section 3.1.1), this suggests that the source wavelets for all three surveys used were reverse-polarity. Because the usual SEG plotting convention is to plot the data using a normal-polarity wavelet, it is surprising (and unlikely) that each of the three surveys used were plotted using reverse wavelets. Although it is possible that the reflection coefficient at the Wyandot boundary is positive, and that the response is being represented accordingly, the occurrence of mudstone overlying limestone should be expected to yield a negative acoustic impedance contrast. Since, for the purposes of this project, recognizing the polarity of the source wavelet was unnecessary (recall that the peak of the wavelet was chosen simply for practical purposes, Section 3.1.1), and

extraction of the data was not possible without digital data, the cause of the discrepancy was not resolved.

With the relationship between the well and seismic data established, the lithologies of the seismic packages could be approximated, based on the well/seismic ties. To facilitate the well/seismic ties, the synthetic seismograms were plotted at the same scale as the seismic profiles: 2.5 in/sec. Appendix E contains the synthetic seismograms produced for each well in the study area.

GeoSyn was also used to produce a time/depth curve for each well using the well log data. Although the checkshot correction for this time/depth correlation was not applied, for this shallow interval of interest the time/depth relationship recorded by the wireline log should be adequate (in fact, checkshot corrections may have not even been recorded at these relatively shallow depths). The time/depth curves were used to convert the well log scales and lithologies from depth to two-way time, which facilitated more detailed correlation of the wells with the seismic lines (see Appendix C).

3.2.4 Biostratigraphy and Ages

Geologic ages quoted in this report are based on biostratigraphic ages obtained from reports available in BASIN. These represent published industry reports (available courtesy of the CNSOPB) and published and unpublished internal reports from researchers at the GSC (Atlantic). The biostratigraphic reports used for this study varied for each well, because only the most consistent and precise age picks were used. Highly discrepant ages between studies were considered less reliable. Biostratigraphic ages were generally based on reports from Cree, Demascota, Naskapi, and Oneida, as these wells contained the most consistent biostratigraphic picks. In particular, the most recent

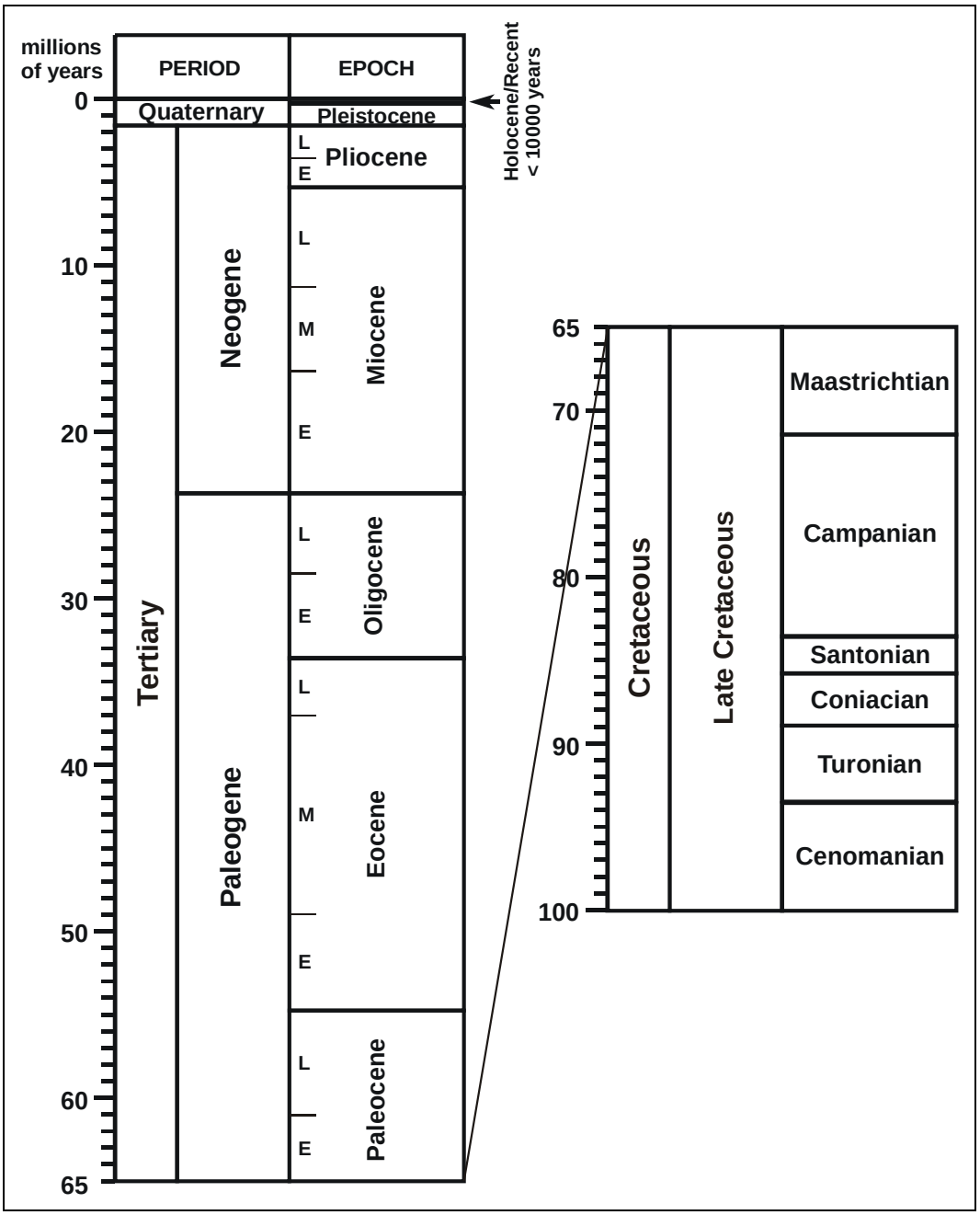

Figure 3.8 Geologic timescale used for this study (after Gradstein et al., 1995, and Berggren et al., 1995). L = Late, M = Middle, and E = Early.

biostratigraphic reports by Ascoli (1988), Fensome (pers comm., 2002), Robertson Research (1973), and Williams (1979) were considered the most reliable, and were most often used to approximate geologic ages. In general, ages are reported to stage (or epoch) precision (i.e. Campanian, Maastrichtian, etc.).

The geologic timescales used for this project were the Mesozoic timescale of Gradstein et al. (1995), and Cenozoic timescale of Berggren et al. (1995). The Late Cretaceous and Cenozoic portions of their timescales are summarized in Figure 3.8.

3.2.5 Data Coverage and Challenges

Although the number of wells in the area was limited, all wells used had seismic lines that passed over them which allowed well/seismic ties to be produced using the synthetic seismograms.

4. Results and Interpretations

4.1 Seismic Analysis

The latest Cretaceous-Tertiary interval on the LaHave Platform consists of at least 3 mappable seismic packages (Figure 4.1). Each package represents a group of seismic facies bounded by what are interpreted to be regional unconformities, identified by seismic horizons with a distinctive relationship to overlying and underlying reflections. In total, 6 seismic reflections (horizons) were identified and mapped, including (from oldest to most recent): Wyandot (R_W), Wyandot-1 (R_{W-1}), Reflection A (R_A), Reflection B (R_B), Reflection C (R_C), and Reflection D (R_D). The Wyandot reflection represents the base of the study interval and the base of seismic package 1 (S_1). Wyandot-1 is an upward branch of the Wyandot reflection that merges with R_W basinward, and can be traced over the western portion of the study area. Reflection B (R_B) represents the upper boundary of seismic package 1 (S_1), which onlaps onto R_W landward and downlaps onto R_W seaward. Seismic package 1 encompasses Reflection A (R_A), which has a relationship parallel to R_B. Seismic package 2 is bounded at its base by R_B and at its upper boundary by R_C. The reflections within seismic package 3 (S_3) toplap into Reflection D (which represents the upper boundary of the package), and downlap onto Reflection C (the base of the package).

In general, the reflections on the LaHave Platform dip seaward, as would be expected for sediments deposited off the coast on the continental shelf of a passive margin (Figure 2.2).

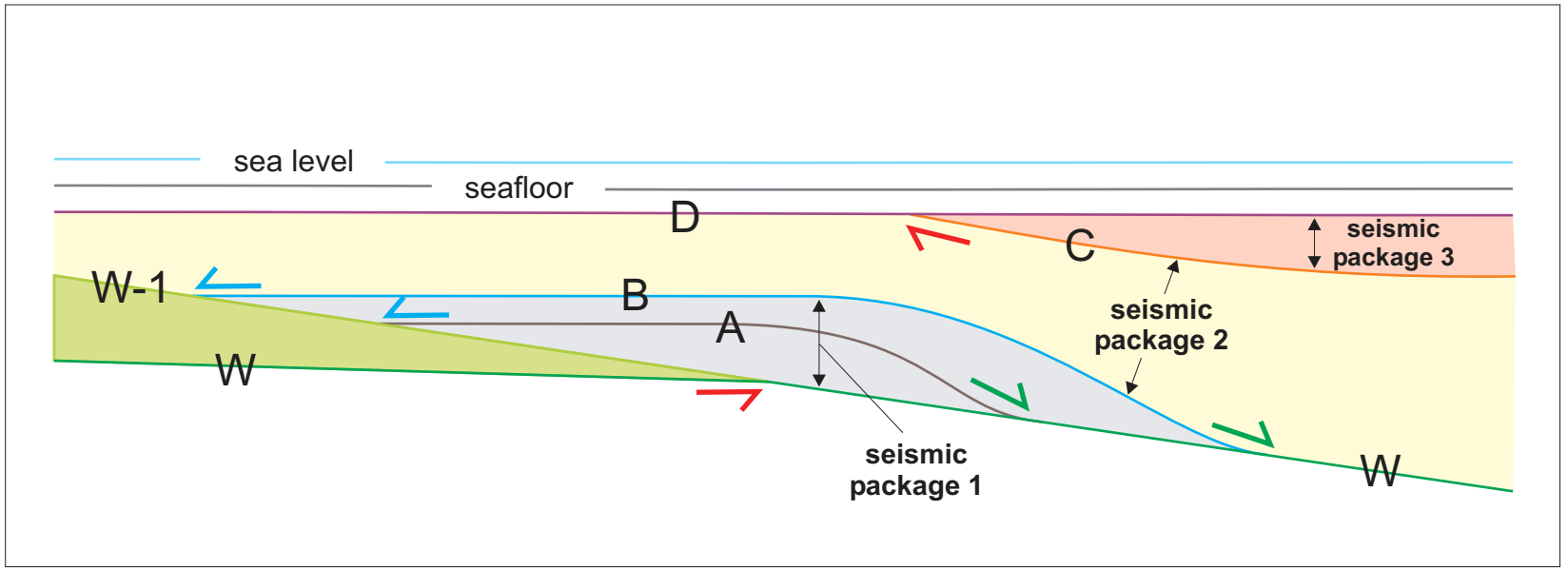

Figure 4.1 Composite of all reflections and seismic packages interpreted for this study.

4.2 Seismic Stratigraphy

4.2.1 Wyandot Reflection (R_W)

The Wyandot reflection is a strong regional reflection that is the base of the study interval (Figure 4.1). R_W is characterized by strong amplitude and the discordant onlap and downlap relationships produced by overlying reflections. The reflection extends beyond the boundaries of seismic lines in the study area.

R_W is interpreted to represent the approximate top of the Wyandot Formation chalk, a well-recognized regional seismic marker that has been referred to as "…perhaps the most distinctive and widely recognized lithologic unit on the shelf…" (McIver, 1972). Although considered to represent the top of the Wyandot in most of the study area, refer to the next Section (Section 4.2.2, Wyandot-1 Reflection) for an exception. The strong nature of the reflection is due to the high acoustic impedance contrast between the chalk and the overlying mudstone. This large negative contrast would typically be expected to produce a trough on the seismic trace (if the section follows SEG plotting conventions), but recall from Section 3.2.3 that in this dataset the boundary produces a peak. It is not known what produces this discrepancy.

The interpretation and mapping of the Wyandot completed in this project is similar to those made by previous authors (e.g. Wade and MacLean, 1990), including its discontinuous nature, discussed in Section 4.2.2. Wade and MacLean (1990, p. 224) also recognized a broad area where erosion has "…cut into but not through the Wyandot…". This is visible on the seismic time-structure map of the Wyandot (Figure 4.2) as a north-trending 'trough' approximately 35 km wide where the erosion has resulted in the top of the Wyandot appearing at a slightly greater two-way time.

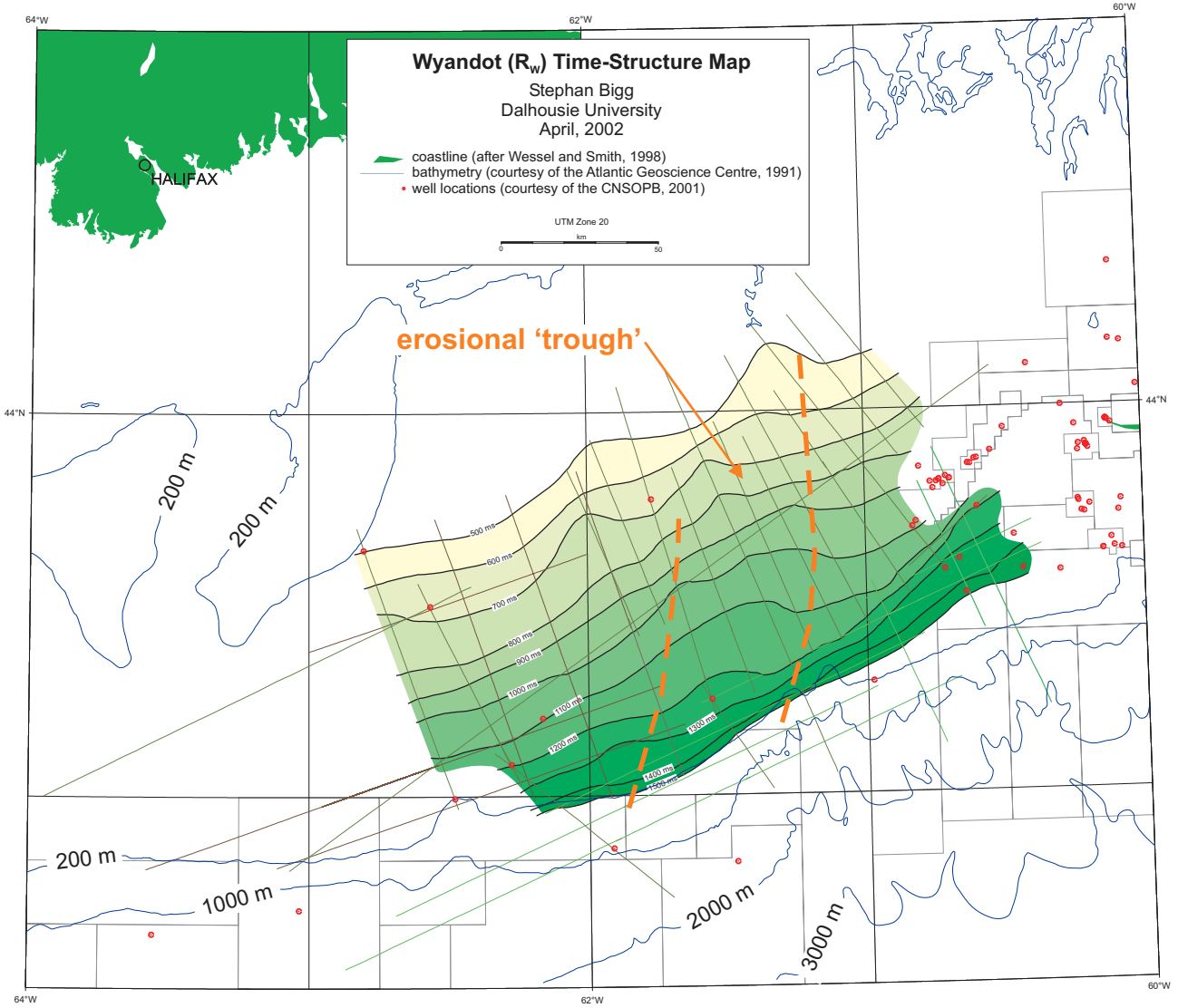

Figure 4.2 Time-structure map of the Wyandot Reflection (R_w). See also Mapsheet 1.

4.2.2 Wyandot-1 Reflection (R_{W-1})

The Wyandot-1 Reflection is a strong reflection present in the western portion of the study area. R_{W-1} is characterized by the erosional truncation of the Wyandot Reflection (R_W) into its base (Figure 4.1 and Figure 4.3). This termination occurs near the centre of the study area, and diverges to the west beyond the extent of seismic lines. Due to a lack of tie lines, R_{W-1} cannot be interpreted east of line 3516-82A (Figure 4.3).

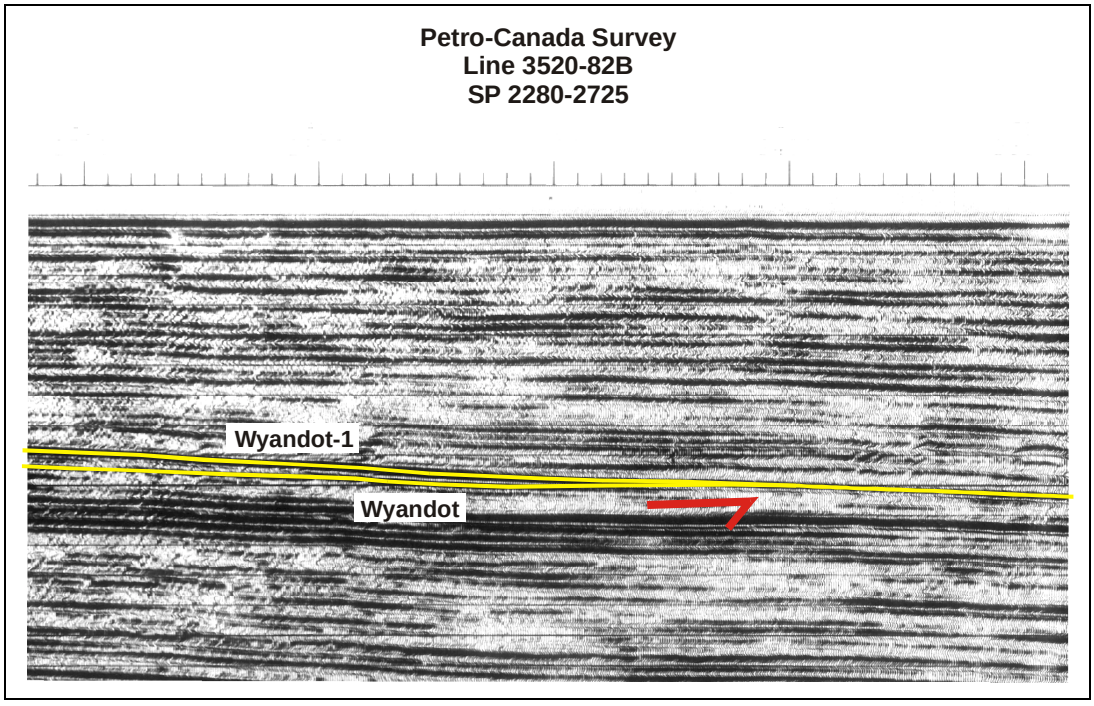

Figure 4.3 Relationship between R_{W-1} and R_W, illustrating the erosional truncation of R_W into the base of R_{W-1}.

W_{R-1} is interpreted as a 'divergence' of the Wyandot Reflection as it separates into two distinct chalk units. For example, at the Ojibwa E-07 and Moheida P-15 wells, two chalk bodies are clearly evident (Section 4.3.1.1). Also, at the Naskapi N-30 well, although the lower unit is not recorded as limestone in the cuttings log, the chalky lithofacies is evident from the wireline logs (most notably in the sonic and gamma ray logs; see Figure 4.9). As noted by Wade and MacLean (1990), "although the Wyandot typically produces a single strong and clean reflection, it also appears on some seismic

profiles as several strong events". Thus, where Wyandot-1 is present, it should be considered the top of the Wyandot. Figure 4.4 is an isochron map of the 'wedge' created by the diverging chalk units.

4.2.3 Seismic Package 1 (S_1)

Seismic package 1 is defined by the Wyandot Reflection (or R_{W-1} where present, as discussed in Section 4.2.2) at its base, and by Reflection B at its upper boundary (Figure 4.1). S_1 forms a continuous, lobate body, and consists of low- to high-amplitude, discontinuous, southeast-dipping reflections which downlap onto the basal boundary (R_W) seaward, and onlap onto R_W landward. Figure 4.5 illustrates as an isochron (with the Wyandot Reflections (R_W or R_{W-1}) acting the base of the isochron) the package's thick centre and thinning edges. Note that the erosion on the Wyandot recognized by Wade and MacLean is also apparent as a thickening of the package on the isochron map of S_1 in the same area (Figure 4.5). This is expected, as deposition of S_1 sediments over that depression would have likely been greater, due to the greater accommodation space made available by the erosion of some of the Wyandot.

Seismic package 1 includes Reflection A within it, which is essentially parallel to, but lower than, Reflection B, and shares the same downlap and onlap relationships onto the R_W horizon (Figure 4.1).

4.2.4 Seismic Package 2 (S_2)

Seismic Package 2 is defined by Reflection B (or R_W where R_B is locally absent) at its base, and by Reflection C (or Reflection D where R_C is absent; see Section 4.2.5 for discussion) at its upper boundary (Figure 4.1). S_2 forms a discontinuous, sheet-like body, and consists of a low- to high-amplitude, discontinuous to continuous series of southeast-

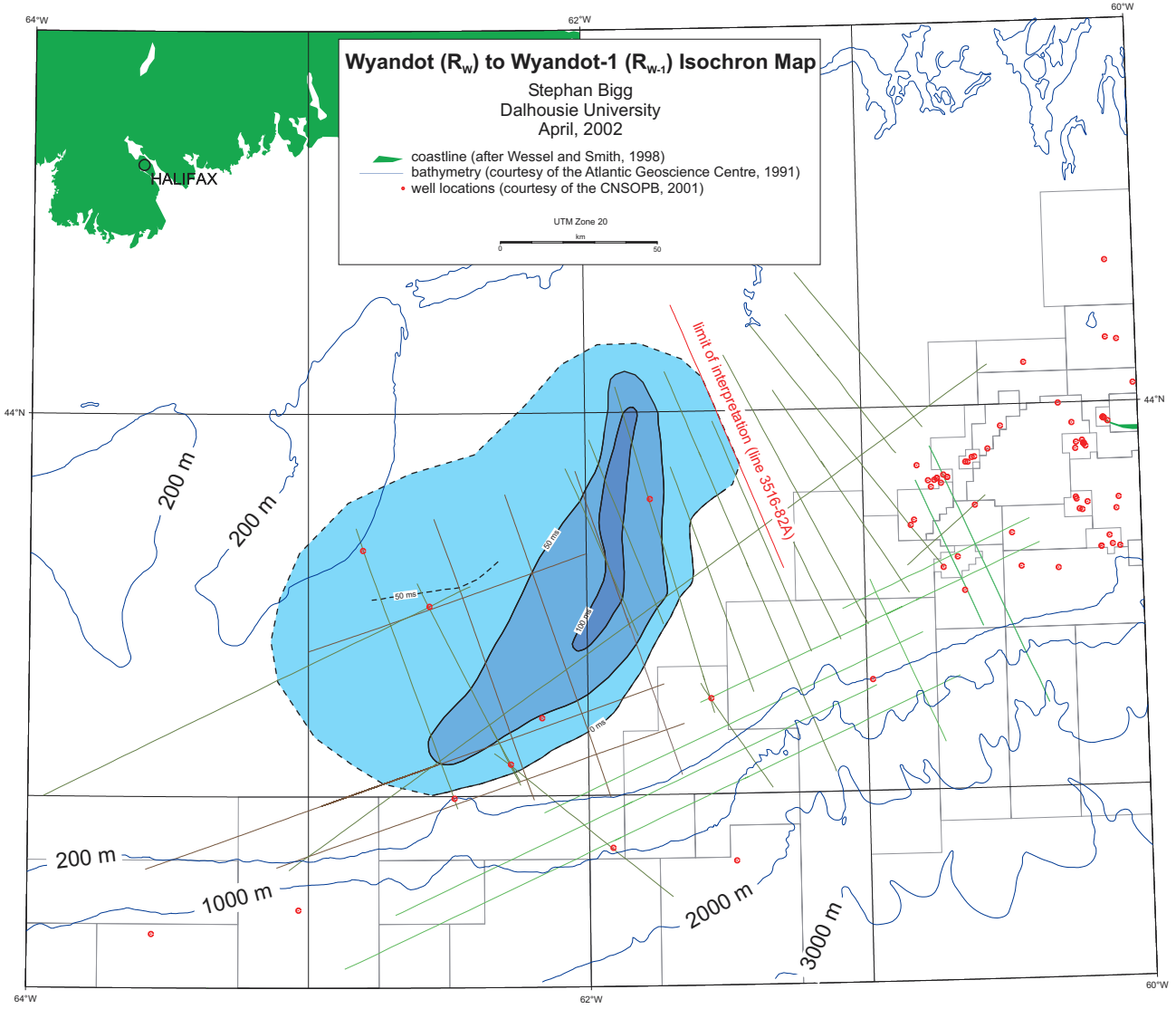

Figure 4.4 Isochron map of the wedge formed between R_W and R_{W-1}. See also Mapsheet 2.

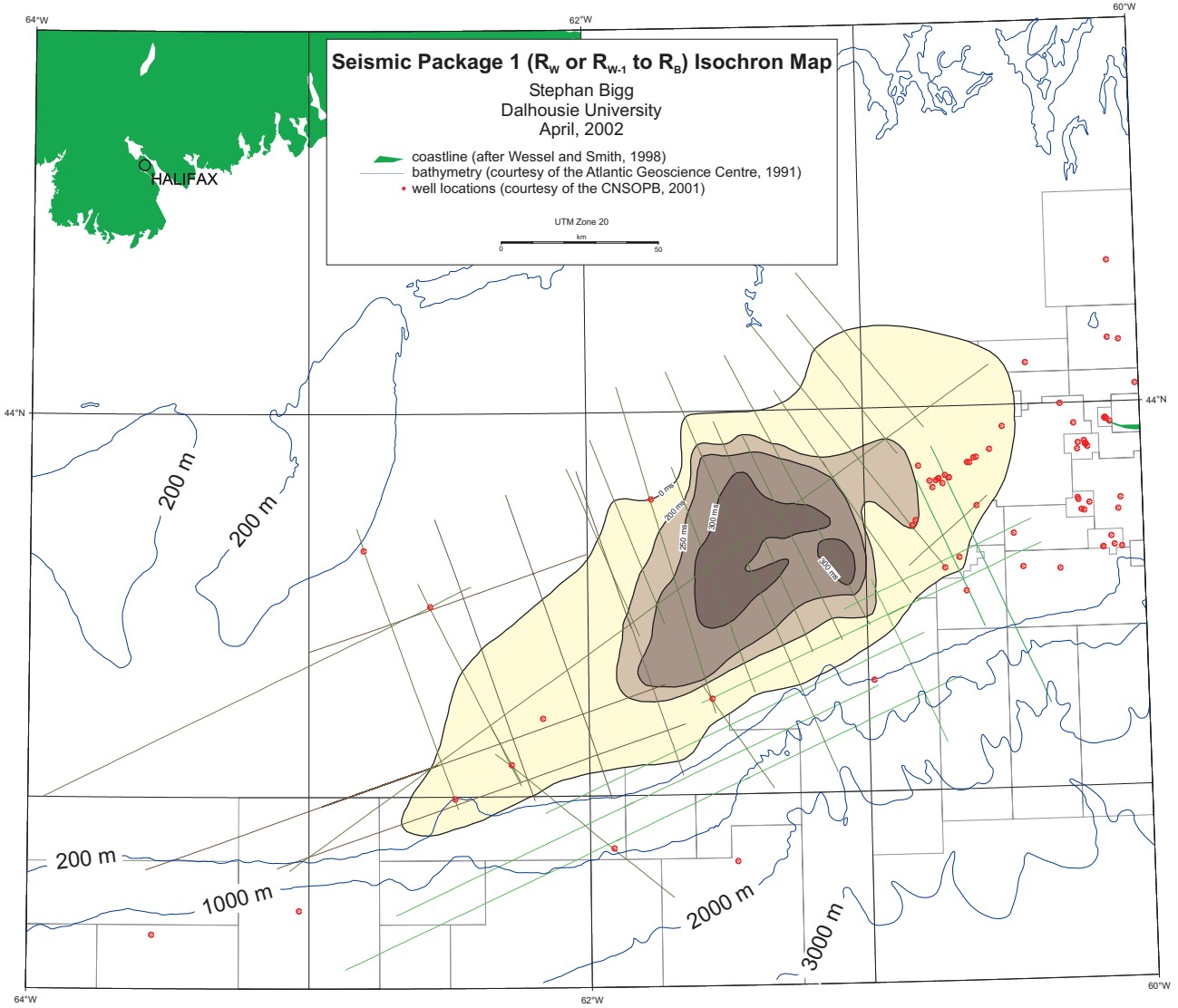

Figure 4.5 Isochron map of seismic package 1 (R_W or R_{W-1} to R_B). See also Mapsheet 3.

dipping reflections which downlap onto the basal boundary (R_B) seaward, and onlap onto R_B (or R_W) landward. At the upper boundary of the package, these reflections toplap (or are truncated) into R_C (or R_D). Figure 4.6 illustrates the time thickness of seismic package 2. Note the thickening in the southwest and northeast corners of the study area (especially in the northeast).

4.2.5 Seismic Package 3 (S_3)

Seismic package 3 is defined by Reflection C at its base, and by Reflection D at its upper boundary (Figure 4.1). S_3 forms a wedge-shaped body that pinches out landward, and consists of very discontinuous moderate- to high-amplitude reflections which onlap onto the basal boundary (R_C) landward and downlap onto R_C seaward, and either toplap (or are truncated) into R_D at the top of the package, although some of this appearance may be an artifact of truncation by water-bottom multiples. Figure 4.7 illustrates seaward-thickening nature of the package and its landward extent.

4.2.6 Interpretation Limitations

As discussed in Section 4.2.2, the thin upper Wyandot chalk reflection, R_{W-1}, could not confidently be interpreted to the east of seismic line 3516-82P (and 3516-82A), due to the absence of a strike line upon which to correlate the reflection to the next line. An additional strike like would have allowed the reflection to be accurately traced. R_{W-1} could have been predicted on the next line (3514-82P), based on its character and expected downlap position, but without the presence of a tie line, this interpretation would have been fundamentally speculative.

4.2.7 Canyon Development

Few canyons are present in the study area, except near the shelf edge, where the

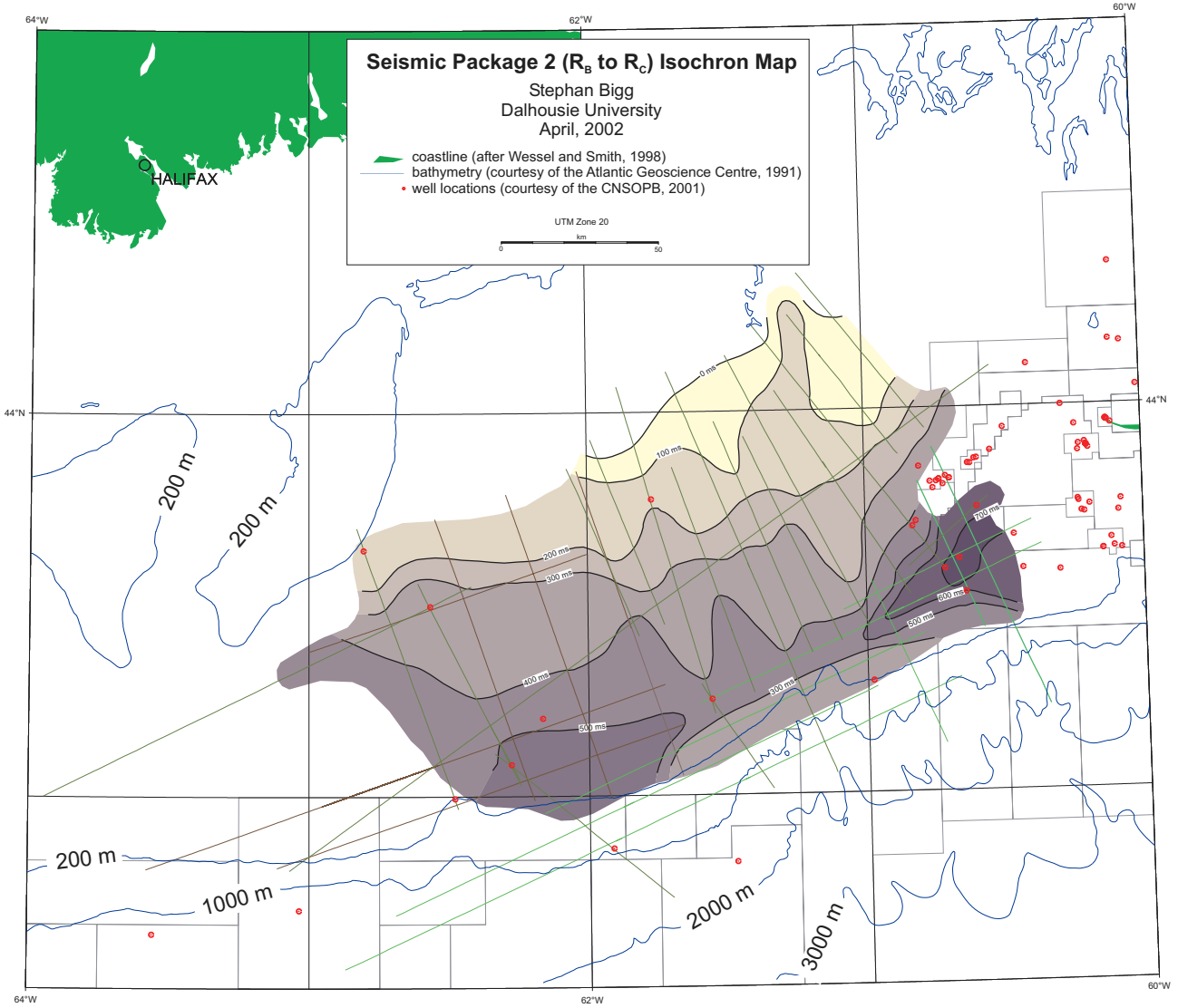

Figure 4.6 Isochron map of seismic package 2 (R_B to R_C). See also Mapsheet 4.

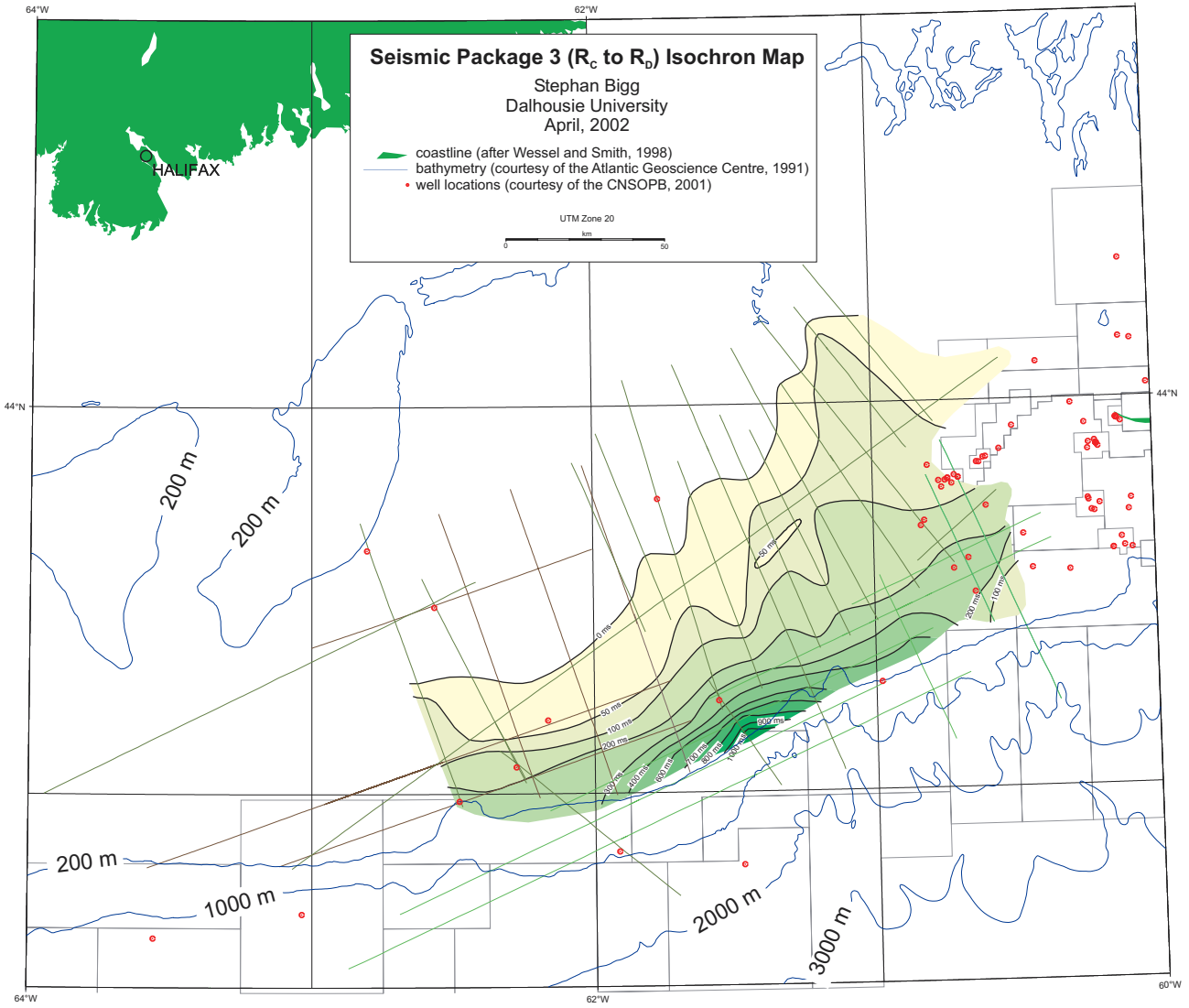

Figure 4.7 Isochron map of seismic package 3 (R_C to R_D). See also Mapsheet 5.

canyons cut into the shelf and continue onto the slope. Figure 4.8 illustrates the location and direction of the canyons in map view. The canyons display the typical pattern of several canyon tributaries merging together 'downstream' to form a single major conduit as the canyon advances down the slope. The orientation of the canyons in the study interval indicates that sediment was being deposited mainly to the southeast. Appendix F lists the shotpoint locations of the interpreted canyons.

4.2.8 Faults

Faults are also relatively sparse in the study area. Most faults occur near the shelf edge, where the horizons (especially R_W) begin to be broken by faults as they continue onto the slope. Two large faults are also present around Ojibwa E-07 and Naskapi N-30, and form the boundaries of deeper half-graben structures developed in the acoustic basement. Figure 4.9 illustrates the location and (approximate) extent of the faults in the Ojibwa and Naskapi areas in map view. Although interpreted as separate faults, the two may represent a single large fault, as their offsets are similar in size and character. Because of the large number of faults in the eastern portion of the study area (at the shelf edge) and the relatively few seismic lines used for this project in the area, only the fault intersections were mapped, and not interpolated. Where faults are present, all are normal faults with offsets of generally less than 50 milliseconds (TWT). Appendix G lists the shotpoints and estimated offsets of the interpreted faults.

4.3 Well Stratigraphy

4.3.1 Well Logs

The lithostratigraphy of the survey area was established from a synthesis of the available well log data from the region. Eight exploration wells were used, with all wells

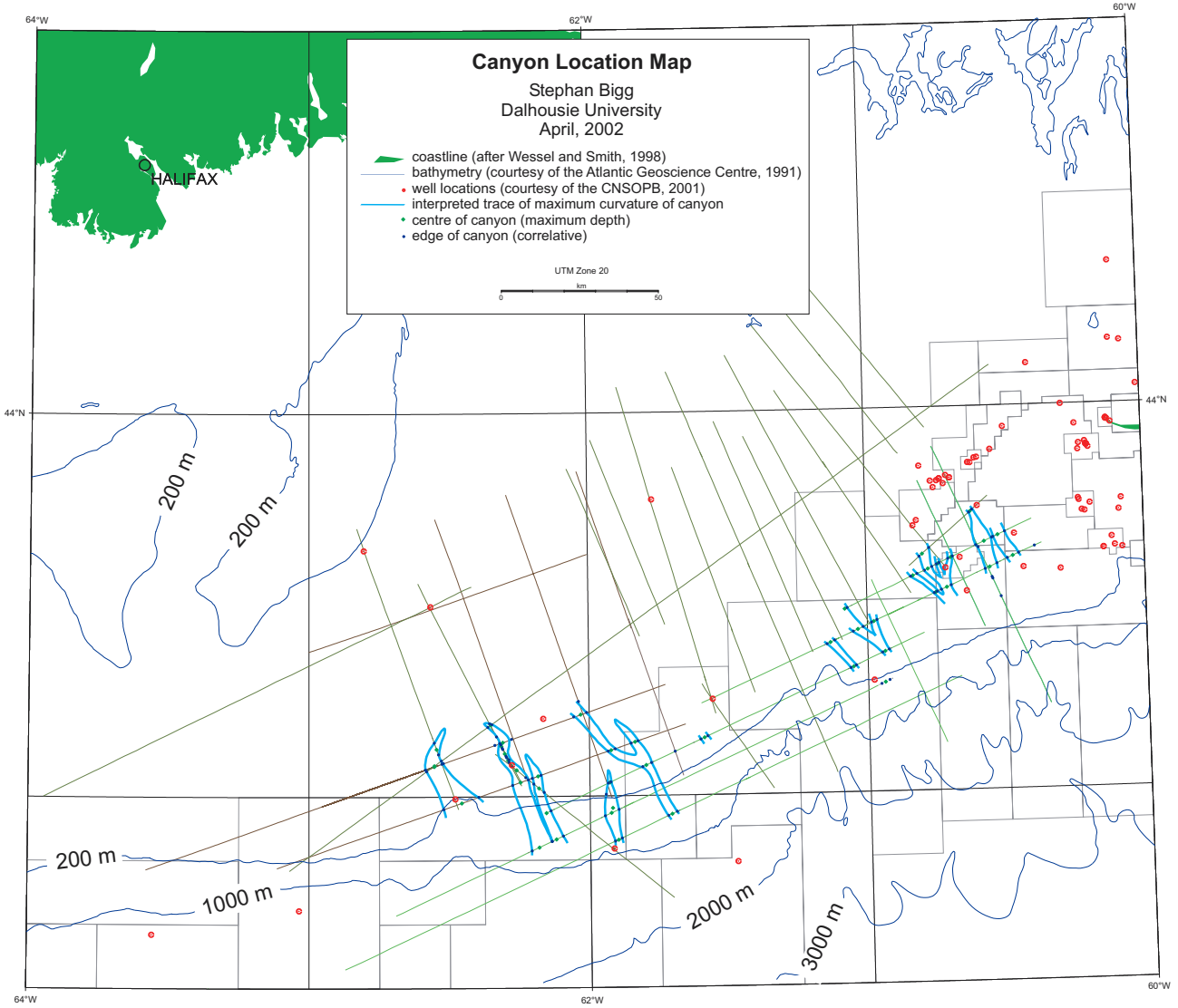

Figure 4.8 Canyon development in the study area. The outlines show the interpreted extent of the canyons at their point of maximum curvature. See also Mapsheet 6.

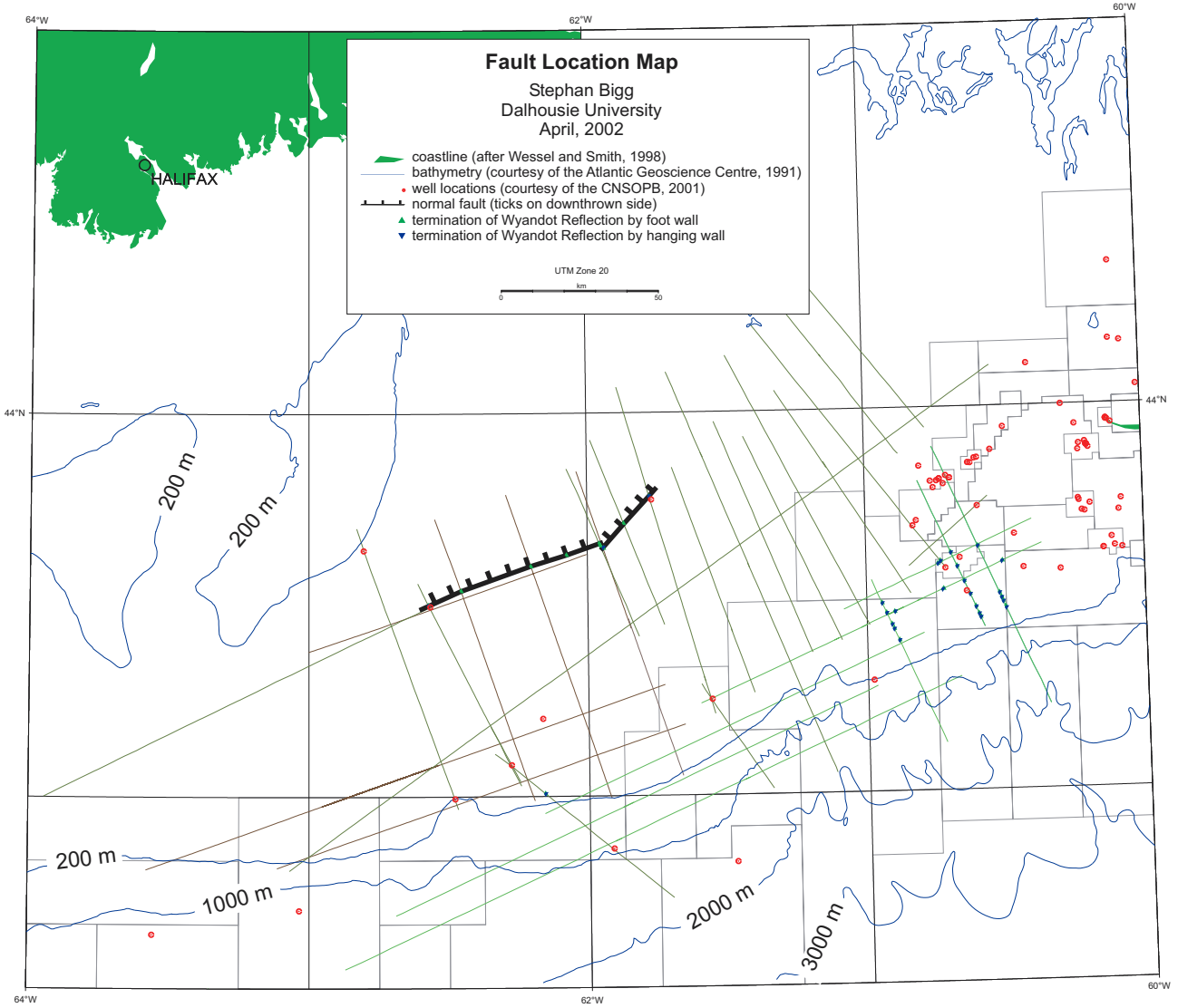

Figure 4.9 Faults in the study area. See also Mapsheet 7.

(with the exception of Mohican I-100) including at least part of the latest Cretaceous-Tertiary section. The wells logs used are included in Appendix C.

4.3.1.1 Wyandot Formation

The chalk of the Wyandot Formation appears as a decrease in the gamma ray log with a high velocity recorded in the sonic log, which is typical of limestone (Prothero and Schwab, 1997). The Wyandot is generally observed to occur from the Santonian to the base of the Campanian (based on biostratigraphic reports by Ascoli, Fensome, Robertson Research, and Williams; see Section 3.2.4). In some of the wells (Moheida, Naskapi, and Ojibwa), another low gamma, high velocity unit is present below MacLean and Wade's interpreted tops. The similar wireline log character of this unit suggests that it is another chalk unit, an interpretation consistent with the cuttings logs for Moheida and Ojibwa (Figure 4.10).

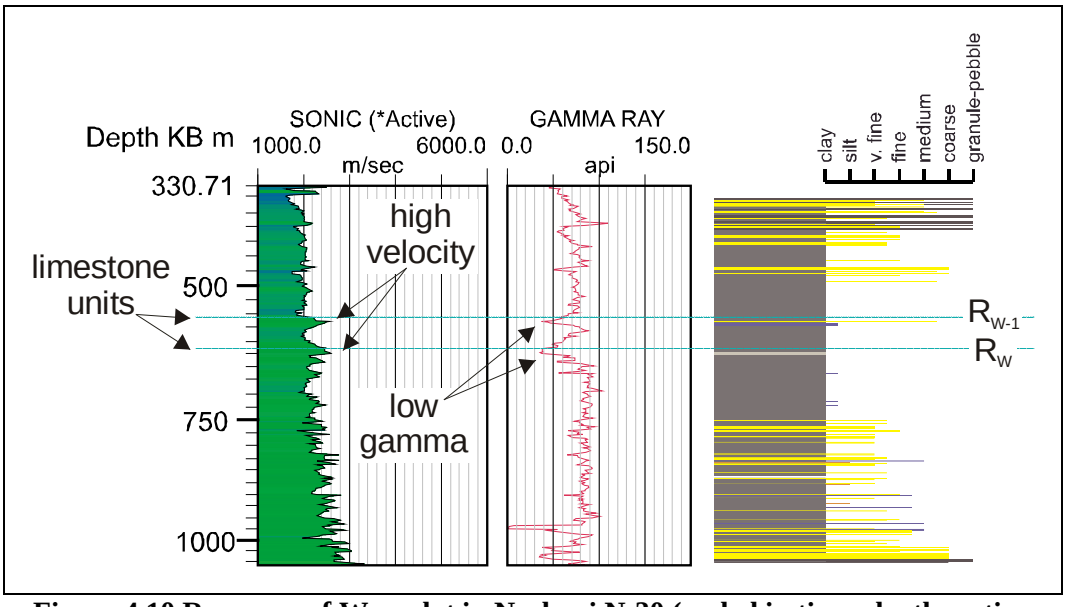

Figure 4.10 Response of Wyandot in Naskapi N-30 (scaled in time, depth section available in Appendix D). Note the two distinct limestone units interpreted to correspond to the R_W (lower) and R_{W-1} (upper) reflections (from BASIN, courtesy of the CNSOPB, 2002).

Above the Wyandot Formation, most wells chronicle an alternating series of mudstone and sandstone units — the Banquereau Formation.

4.3.1.2 Unit I

Unit I overlies the Wyandot, and maintains relatively constant gamma (≈ 60-70 API) and sonic (≈ 2600 m/s) logs (Figure 4.11). This character (combined with the cuttings logs) suggests that the unit is comprised predominately of mudstone. Where present in the wells, the unit is typically 300-400 metres thick, but ranges from 80-450 metres in the study area. The sonic log becomes increasingly variable near the top of the unit, with several low-velocity peaks present, which suggest interbedded layers of sandstone.

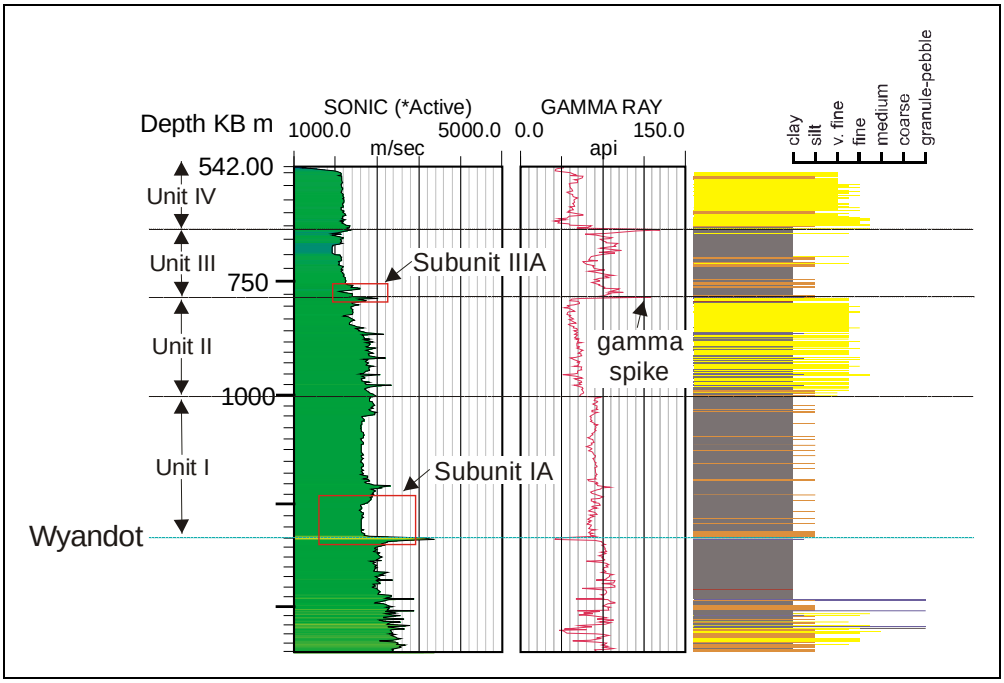

Figure 4.11 Response of well log units in Alma K-85 (scaled in time, depth section available in Appendix D). From BASIN, courtesy of the CNSOPB (2002).

Unit I was deposited within the Campanian to Maastrichtian (based on biostratigraphic reports by Ascoli, Fensome, Robertson Research, and Williams; see Section 3.2.4). Unit I is observed in all wells in the study area, with the exception of Mohican I-100, which

consists (at the study interval) of Neogene and Quaternary channel fill deposited within the Mohican Channel.

In a number of wells (Alma, Cree, Demascota, and Oneida), a lower velocity, predominantly mudstone unit (≈ 75-100 m) capped by a thin (≈ 25 m) sandstone unit is present at the base of Unit I (overlying the Wyandot Formation). It is designated 'Subunit IA'.

4.3.1.3 Unit II

Overlying Unit I is a lower gamma (≈ 50-60 API) and decreasing velocity (from ≈ 2750-2400 m/s) unit, referred to as Unit II (Figure 4.11). Where observed in the wells, the unit is typically 100-150 metres thick, but ranges from 85-225 metres in the study area. Unit II is interpreted as predominately sandstone, and occurs (in general) within the Maastrichtian to Paleocene (based on biostratigraphic reports by Ascoli, Fensome, Robertson Research, and Williams; see Section 3.2.4). Unit II is observed in all the wells (again with the exception of Mohican I-100). A very distinct peak (up to 160 API) in the gamma ray log is present at or near the upper boundary of Unit II on most of the well logs studied (Figure 4.12). The spike is also observed in several other wells to the west and southwest of Sable Island (A. MacRae, pers. comm., 2002). Although the source of the anomaly is unknown, in other areas of the Scotian Shelf the 'gamma spike' is associated with high concentrations of glauconite (A. MacRae, pers. comm. 2002). The 'gamma spike' occurs just above the Cretaceous-Tertiary boundary, within the Paleocene.

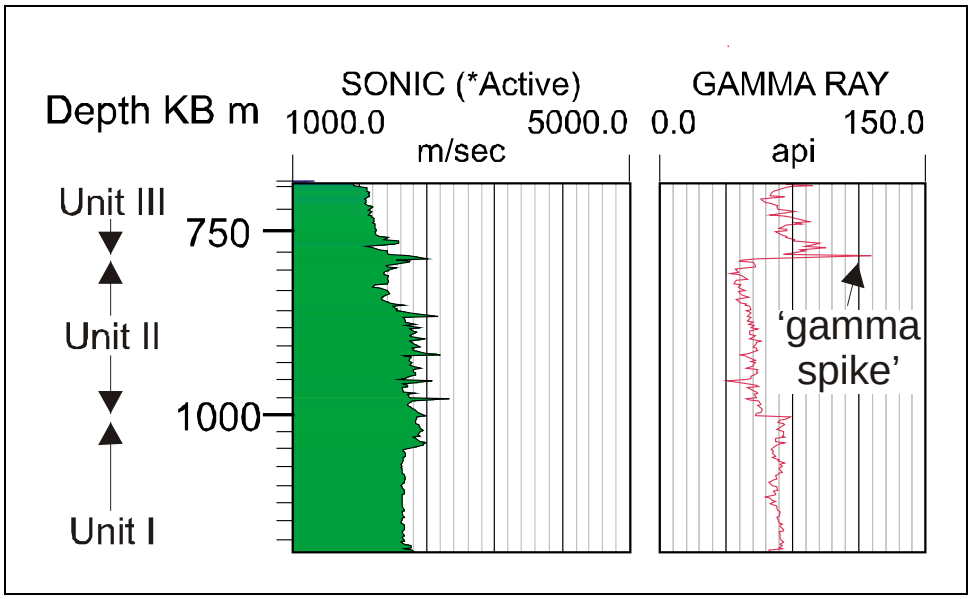

Figure 4.12 Detail of Unit II in Alma K-85 illustrating the 'gamma spike' at the upper boundary of the unit (from BASIN, courtesy of the CNSOPB, 2002).

4.3.1.4 Unit III

Unit III maintains a relatively constant, higher gamma reading (≈ 60-80 API), along with a consistently decreasing (but without significant variability within) velocity up the log (≈ 2400-2000 m/s; Figure 4.11). Similar to Unit I, the sonic log becomes increasingly variable near the top of the unit, with low-velocity peaks present, which suggest interbedded layers of sandstone. Again, the wireline log character and cuttings log suggests that the unit is comprised predominately of mudstone. Where present in the wells, the unit is typically 100-180 metres thick, but ranges from 60-215 metres in the study area. Unit III is generally observed to occur within the Eocene-Oligocene (based on biostratigraphic reports by Ascoli, Fensome, Robertson Research, and Williams; see Section 3.2.4), and is visible in all of the wells with sufficiently shallow logs.

In two of the wells (Alma K-85 and Demascota G-32), there appears to be a small low velocity, high gamma unit at the base of Unit III (overlying the 'gamma spike';

Figure 4.11), representing a thin, lower velocity, predominantly mudstone unit capped by sandstone, designated Subunit IIIA (similar to Subunit IA discussed in Section 4.3.1.2).

4.3.1.5 Unit IV

Unit IV is another low gamma, low velocity unit, similar to Unit II (Figure 4.11). The similar wireline log character and cuttings log suggests that the unit is also comprised predominantly of sandstone. The portion of the unit observed in the wells is typically 150-200 metres thick, but ranges from 100-274 metres in the study area. Although in most wells this unit appears almost entirely of relatively homogeneous sandstone, in Oneida O-25 the unit presents several alternating layers of (most likely) mudstone and sandstone, due to the more variable gamma and sonic curves. Unit IV was deposited within the Miocene (based on biostratigraphic reports by Ascoli, Fensome, Robertson Research, and Williams; see Section 3.2.4). No well logs are present above this unit (with the exception of the Mohican I-100 and Moheida P-15 wells, which consists of Miocene-Quaternary fill within the canyons; see Section 4.4.1).

4.3.1.6 Summary of Well Stratigraphy

The wells indicate that there were, overall, two successive transgression-regression periods in the study interval (Figure 4.13). The Wyandot Formation represents an initial maximum transgression in the study interval. The 'branching' observed at the upper boundary of the Wyandot may represent erosion, perhaps due to an additional regressive event before subsequent major regression. The coarsening-up succession of mudstone grading to interbedded sandstone (units I and III) represent progradation of the system, or regression, while the sandstone units (units II and IV) represent the maximum regression and probably the initial stages of the subsequent transgression. The upper

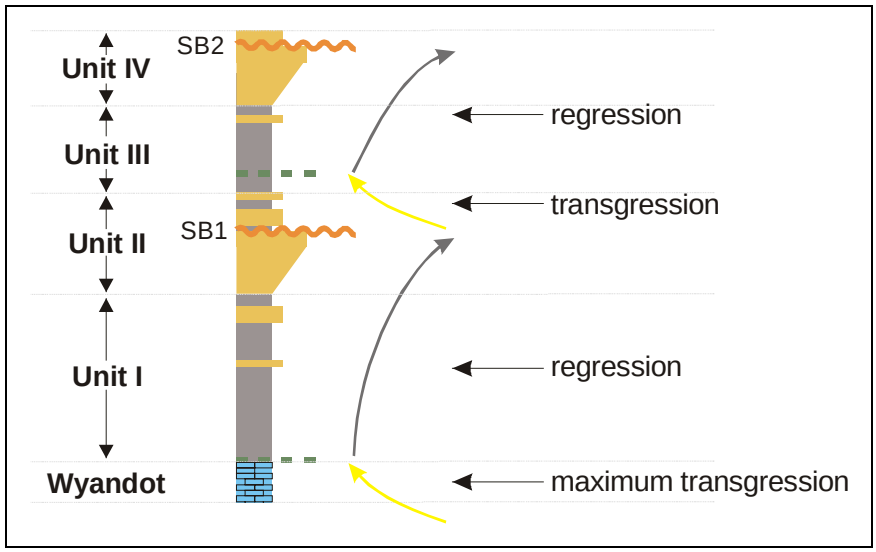

Figure 4.13 Summary of well log stratigraphy. Orange units represent sandstone, grey units represent mudstone, the blue unit represents limestone, and SB1 and SB2 represent the interpreted sequence boundaries at the maximum regression.

sequence boundary of each major regressive-transgressive episode is interpreted to lie somewhere within the sandstone units, where erosion would have occurred in the most proximal locations. The small, lower-velocity mudstone Unit 1A at the base of Unit I probably represents a smaller episode of regression (and subsequent transgression) within the overall regressional trend of the unit.

4.4 Well/Seismic Ties

Figure 3.7 illustrates the well to seismic tie between the Oneida synthetic seismogram and seismic line 3520-82A (from the Petro-Canada survey), which passes over the well. Figure 4.14 also illustrates the tie between the Ojibwa and Oneida synthetic seismograms and seismic line 0-101-70/1 (from the Shell survey). The interpreted reflections on the section correspond well with the synthetic seismogram reflections. This helps to confirm that the chosen reflections are authentic. The synthesis of the interpreted well log and seismic data (Figures 4.14 and 4.15) demonstrate that Reflection B correlates with the top of Subunit IA (the small unit of mudstone capped by

sand described at the base of Unit I), which may represent a brief regressional period and a smaller-scale sequence (Section 4.3.1.2). The acoustic impedance contrast observed in the seismic data is produced at the boundary between the relatively low-velocity sand and the underlying, higher-velocity, mud. The base of seismic package 2 then lies somewhere within Unit I, which is comprised of several similar series of alternating mud and sand layers, with the total amount of coarse-grained sand increasing up the section. Conceivably then, these smaller alternations also correspond to brief episodes of regression, possibly smaller-scale depositional sequences, while the entire succession is associated with a longer-term regressive trend. The relatively similar nature of reflections within seismic package 1 to the underlying regressional Unit I act to confirm this. The upper boundary of Unit II, and corresponding sequence boundary, is located somewhere within seismic package 2. This horizon was (initially) not observed in the seismic, and thus does not correspond to any mapped reflections (see below for an exception). In most of the study area, Reflection C approximates the upper boundary of the transgressive Unit III where, similar to reflection B, an acoustic impedance contrast is produced at the boundary between sandstone and mudstone. Because reflections C and D are not present in most of the wells, due in part to their relatively shallow occurrence and the fact that well logs are not recorded for the upper 200-300 metres of the wells (in the casing), the exact nature of R_C is difficult to determine precisely. R_C may represent one of the many layers of intermingling mudstone and sandstone underlying the boundary, or it may in fact represent the actual boundary between the mudstone and sandstone (as observed in the Demascota and Moheida wells). An exception to this interpretation is found near the centre of the study area, where the mapped Reflection C is much deeper

8624-S006-005E,006E Line 0-101-70/1

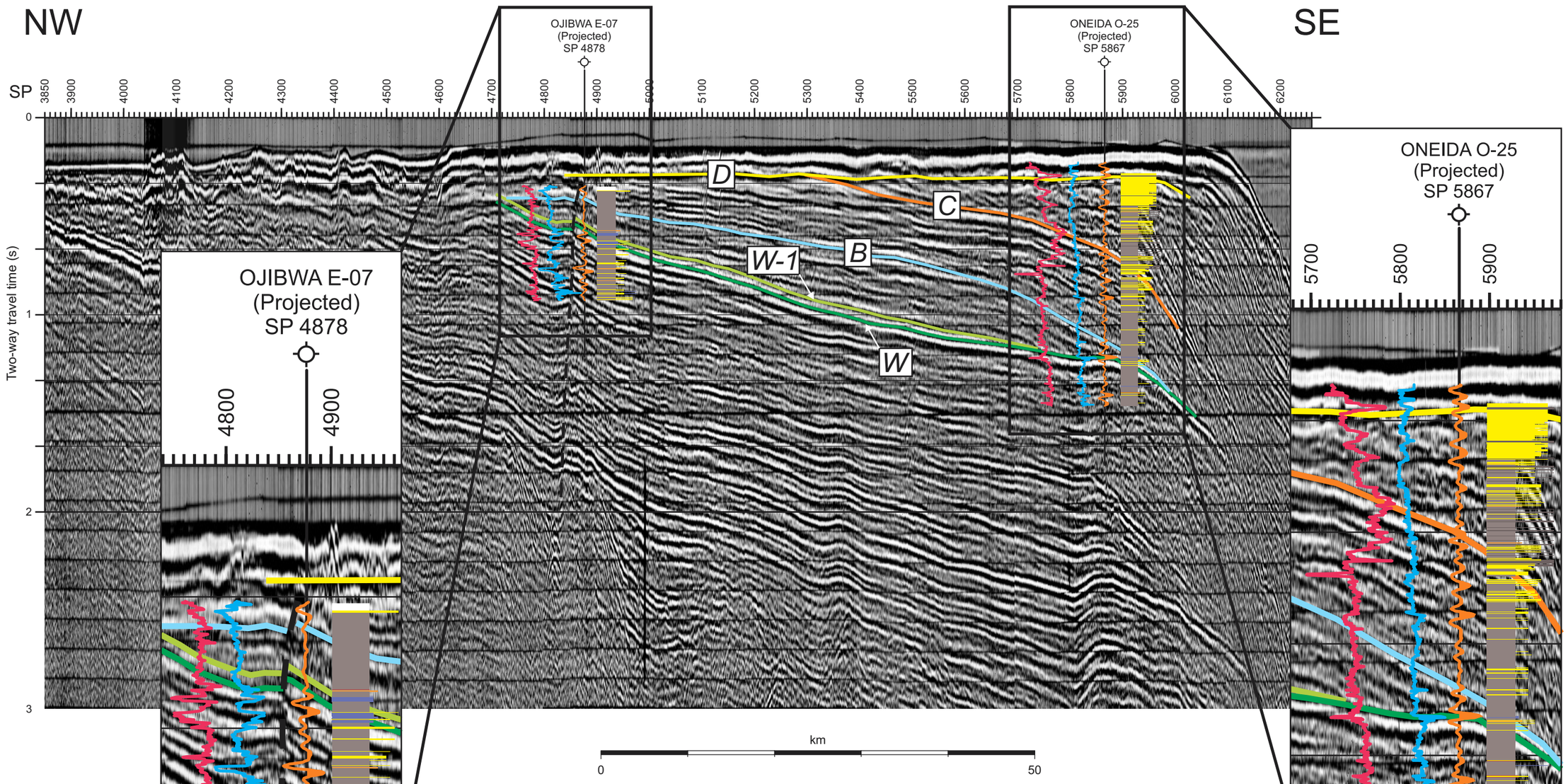

Figure 4.14 Synthesis of well log and seismic stratigraphy. Italicized letters represent interpreted seismic horizons. Well logs include the gamma ray log (red), sonic log (blue), synthetic trace (orange), and cuttings log for each well (well logs obtained from BASIN, courtesy of the CNSOPB, 2002; wireline data courtesy of QC Data Inc.; lithostratigraphy courtesy of CanStrat Ltd.; synthetic seismograms prepared using GeoSyn version 4.8.1.5).

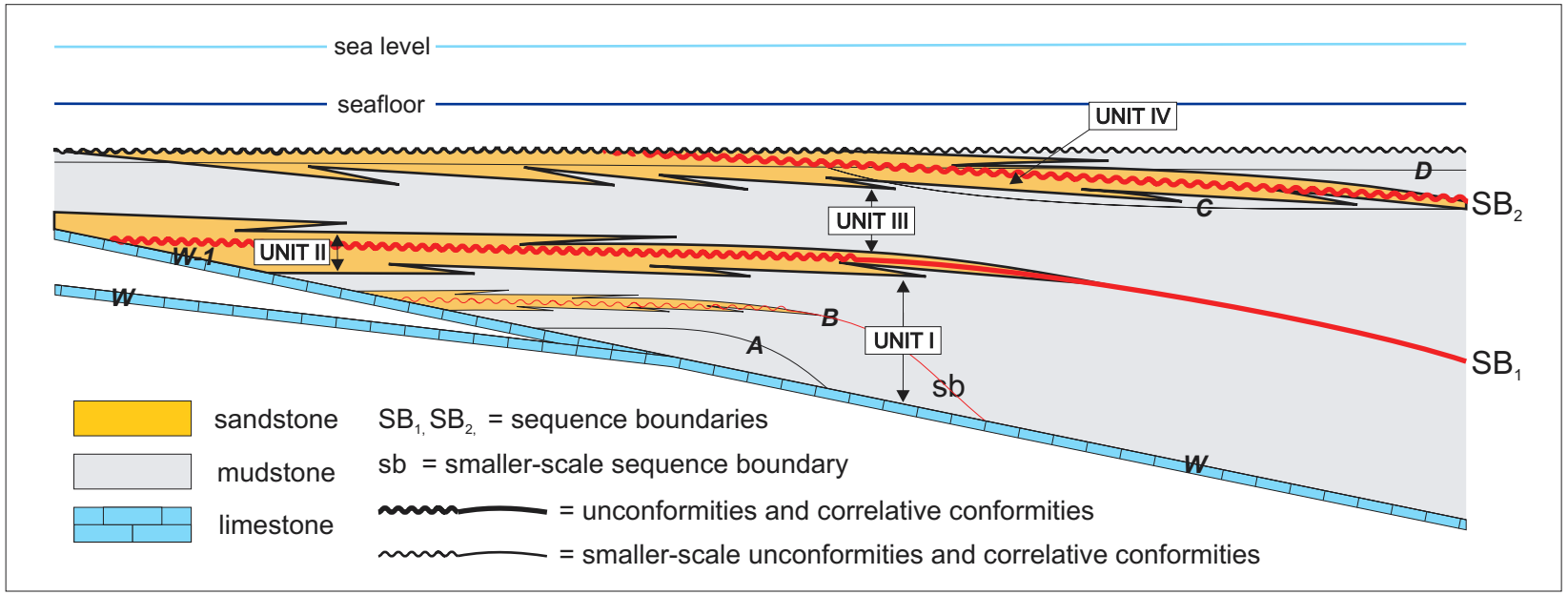

Figure 4.15 Diagrammatic representation of the synthesis of well log and seismic stratigraphy. Italicized letters represent interpreted seismic horizons. For respective seismic packages, refer to Figure 4.1.

in the interval and actually corresponds to the boundary between well log Units I and II, and thus sequence boundary 2 (as observed at the Oneida well, illustrated in Figure 4.14). This inconsistency should be considered an error in the interpretation of the reflection, but because it was detected late in the preparation of this report, the inaccurate seismic lines were not reinterpreted. It is useful to note that, upon further inspection, this reflection is observed in the remainder of the study area, so that the recognized sequence boundary 2 could be interpreted over most of the study area. Also, it should be noted that the imprecise measurements do not significantly affect the geometry, and thus interpretation of, the depositional units. Reflection D correlates within the coarse-grained material in Unit IV, which (together with the toplap relationship of R_C into the reflection) suggests that R_D is probably an erosional surface (and thus sequence boundary) developed during the regression of the depositional system.

4.4.1 Canyon Incision

The canyons on the shelf edge in the eastern portion of the project area were not studied in detail due to the large number (and complexity) of the canyons, and the relatively few seismic lines used for this project in that area. Although those canyons were not studied, their intersections with interpreted reflections were mapped when observed (Figure 4.8). The Moheida well illustrates that the oldest fill in the canyon penetrated by the well is Oligocene-Miocene (based on biostratigraphic ages reported by the Bujak Davies Group, 1988), thus the minimum age of the incision is Oligocene-Miocene. This corresponds (approximately) to the second major maximum regression in the study interval (culminating in SB_2). Based on correlations made between adjacent canyons on the seismic lines, all of the other canyon fill in the area appears to correspond

to the same depositional period, including the canyon that intersects the Mohican well, informally referred to as the ‘Mohican Canyon’. The oldest fill observed in the Mohican well is Middle Miocene (based on Gradstein, 1976, Williams, 1977, and Williams, 1979), which also corresponds to the second maximum regression, suggesting that a single main phase of canyon incision took place.

5. Discussion and Conclusions

5.1 Overview of Latest Cretaceous-Tertiary Stratigraphy

Wade and MacLean (1990) have previously interpreted the Scotian Basin to have undergone a long-term transgression during the latest Cretaceous and Paleogene, followed by regression during the Neogene. In this study the latest Cretaceous-Tertiary stratigraphy on the LaHave Platform is interpreted as regression during the post-Wyandot Campanian, the maximum regression occurring in the Maastrichtian-Paleocene, followed by transgression and subsequent regression in the Eocene-Oligocene and Miocene, respectively. A comparison of these two interpretations is made in Table 4.1. The differences between the two models can be accepted if we acknowledge the fact that Wade and MacLean's results were part of a generalized interpretation based on the entire Scotian Basin, whereas the study area and interval examined in this project were much smaller and more specific, allowing for a more detailed interpretation. It is plausible that the regression-transgression-regression-transgression cycle observed in the study interval is part of the overall transgression of the region that occurred during the latest Cretaceous-Neogene described by Wade and MacLean.

<table>
<tr><th colspan="2">Geological Time</th><th rowspan="2">Wade & MacLean (1990)</th><th rowspan="2">This Study</th></tr>
<tr><th>Period</th><th>Epoch</th></tr>
<tr><td rowspan="2">Quaternary</td><td>Holocene</td><td></td><td></td></tr>
<tr><td>Pleistocene</td><td></td><td></td></tr>
<tr><td rowspan="2">Neogene</td><td>Pliocene</td><td rowspan="2">regression</td><td></td></tr>
<tr><td>Miocene</td><td rowspan="2">regression</td></tr>
<tr><td rowspan="3">Paleogene</td><td>Oligocene</td><td rowspan="5">transgression</td></tr>
<tr><td>Eocene</td><td>transgression</td></tr>
<tr><td>Paleocene</td><td rowspan="2">regression</td></tr>
<tr><td rowspan="5">Cretaceous</td><td>Maastrichtian</td></tr>
<tr><td>Campanian</td><td rowspan="2">transgression</td></tr>
<tr><td>Santonian</td><td></td></tr>
<tr><td>Coniacian</td><td></td><td></td></tr>
<tr><td>Turonian</td><td></td><td></td></tr>
<tr><td>Cenomanian</td><td></td><td></td></tr>
</table>

Table 4.1 Comparison between Wade and MacLean's (1990) regional stratigraphic interpretation and this study.

The well log units identified correspond approximately to Hardy's (1975) informal subdivisions of the Banquereau Formation relating to the filling of the Sable Subbasin (Section 2.3). With small variation, Unit I corresponds with Hardy's "Maskonomet beds" (mudstone-dominated), Unit II with the "Nashwauk beds" (sandstone-dominated), Unit III with the "Manhasset beds" (mudstone-dominated), and Unit IV with the "Esperanto beds" (sandstone-dominated). Although Wade and MacLean (1990) have noted the difficulty correlating these units with the seismic data and the nomenclature has not been widely adopted or subsequently formalized, within the study area the units appear to correlate with the seismic data.

Previous authors (King et al., 1974; Wade and MacLean, 1990; MacRae et al., 2002) have also noted the evidence of significant erosion on the Wyandot horizon, in some cases reducing the formation to less than half its original thickness in the area immediately southwest of Sable Island (MacRae et al., 2002). This erosion is apparent on the time-structure maps of the present study area as a north-trending 'trough' where the erosion cut into the Wyandot, as previously noted by Wade and MacLean (1990). The erosion has resulted in the top of the Wyandot appearing at a slightly greater two-way time within the affected area. Erosion may also be responsible for the apparent convergence/divergence of the Wyandot-related seismic horizons (R_W and R_{W-1}) and the distribution of the two chalk units seen in the western portion of the study area, discussed in Section 4.2.2. It is possible that two chalk units were once present over the entire LaHave Platform, but that the upper unit was eroded in the eastern portion of the study area, leaving a single Wyandot chalk unit. Although the origin of the erosion is

unknown, it is possible that it is due to an additional regressive event prior to the beginning of the Banquereau Formation deposition.

5.2 Depositional History and Paleoenvironment

The Wyandot and Wyandot-1 reflections represent two similar episodes of chalk deposition during maximum transgression in the early Campanian, in a relatively deep-water, but still shelf, environment where clastic sediment deposition is greatly reduced and the fine-grained limestone can accumulate without dilution by other lithotypes (Elder et al., 1994). The deposition of the Wyandot chalk was followed by several periodic episodes of regression (such as Subunit IA) within an overall regressive period (Unit I) during the Campanian, characterized in the well logs as mudstone grading to sandstone. This regression of the system represents a decrease in relative sea level (RSL), either by an actual decrease in global sea level, tectonic uplift of the underlying bedrock, or an increase in sediment supply. The maximum regression, or lowest stage of relative sea level, and subsequent rise of RSL (during the following transgression), of the system occurred during the Maastrichtian-Paleocene, within the sandstone Unit II which overlies the mudstone and sandstone. This transgressive-regressive cycle was followed by another regressional episode, represented in Units III and IV, deposited during the Oligocene-Eocene and Miocene, respectively.

This depositional series may represent deposition in a delta at the mouth of a large fluvial system. During the first active phase of deposition (i.e. the Maastrichtian-Paleocene regressive episode), the study area progressed from a prodelta (mud) to beach (sand) facies as the shoreline prograded. The lobe-shaped geometry of the depocentre suggests that the paleocoast was relatively close to the centre of the study area. During

the second phase of active deposition (i.e. the Oligocene-Miocene regressive episode), a similar progression from prodelta to beach facies is observed, but with a more seaward depocentre. This suggests that the paleocoast was also further from the modern coast, which would be expected as the delta grew and prograded seaward.

5.3 Implications for Scotian Slope Stratigraphy

The geometry of the seismic packages and canyons in the study area indicate the location of the main depocentres and sediment transport directions. The thickest accumulations of Campanian-Paleocene mudstones and sandstones (450 m) were deposited near the centre of the study interval, in the area between the Ojibwa, Oneida, and Demascota wells (Figure 5.1).

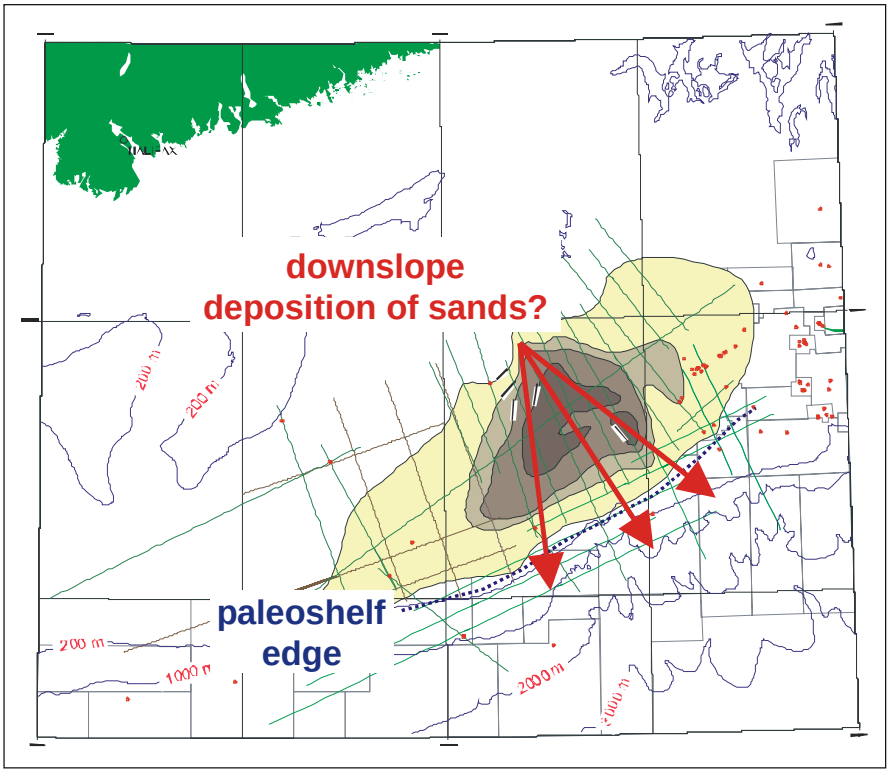

Figure 5.1 Campanian-Paleocene depocentre and speculated transport directions. For data sources refer to Figure 4.3.

If transported over the paleoshelf edge, significant accumulations of sandstone-dominated units may be expected on the slope adjacent to this depocentre, and areas further to the

southwest and northeast would have received less sediment. The depocentre of the Eocene-Miocene sandstones (up to 274 m) was slightly seaward of the Oneida well, and was more evenly distributed long the shelf margin (Figure 5.2).

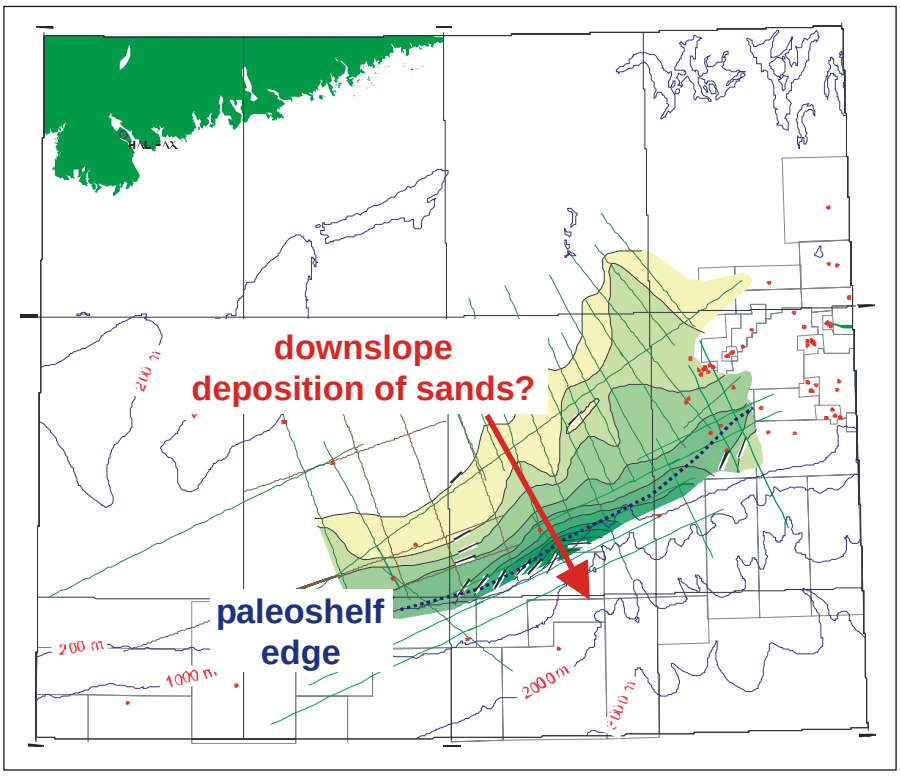

Figure 5.2 Eocene-Miocene depocentre and speculated transport direction. For data sources refer to Figure 4.6.

The thickest accumulation of these later sandstones should therefore occur on the slope beyond Oneida. Furthermore, canyons in the southwest portion of the study area were probably initially cut during the Oligocene-Miocene regression, implying that coeval prograding sandstones may have been intermittently transported through the canyons and onto the slope. Future oil and gas exploration efforts should therefore concentrate on these areas as sites of potentially significant hydrocarbon reservoirs, especially in the interval of the Maastrichtian-Paleocene and Oligocene-Miocene sands on the shelf.

5.4 Summary

- At least two successive transgressive-regressive episodes can be identified using seismic and well log data in the latest Cretaceous-Tertiary interval of the LaHave Platform: regression during the Campanian-Paleocene, with maximum regression during the Maastrichtian-Paleocene, then transgression during the Eocene-Oligocene, and finally regression during the Oligocene-Miocene.
- Two main sediment depocentres are observed in the study area/interval. One depocentre is a lenticular lobe-shape located near the centre of the study interval, in the area between the Ojibwa, Oneida, and Demascota wells, and was deposited during the Campanian-Paleocene with maximum thickness 450 m. The other is a seaward-thickening wedge with maximum thickness 275 m, located seaward of the Oneida well, and was deposited during the Eocene-Miocene.
- Canyon incisions are observed near the shelf edge where they continue onto the slope. A single main phase of canyon incision was observed, during the Oligocene-Miocene. This episode coincides with the maximum regression of the system.

5.5 Recommendations for Future Work

More work could be completed in and around the study area to further investigate and define the depositional packages within the Banquereau Formation. The main effort should be to examine more data so that a more complete picture of the area can be achieved. This project has illustrated the fact that data from separate exploration surveys can be successfully merged together to create a larger and denser grid. If possible, effort should be made to obtain digital copies of the surveys, as digital data is easier to work

with and manipulate, thus making the interpretation process more efficient. Digital data would also allow a wavelet to be extracted directly from the data, which could be used to explain the unexpected and unconventional response produced at the top of the Wyandot Formation (discussed in Section 3.2.3).

It is also worthwhile to note that in the summer of 2001 WesternGeco acquired a 2D survey that they are currently marketing as a multiclient dataset (WesternGeco, 2002). This survey almost directly covers the project area, and would be a significant improvement on both the quality and quantity of data in and around the study area. A request could be made to WesternGeco for access to the shallow part of the data for educational purposes. Access to these modern 2D data would allow a much more detailed and precise 'picture' of the Latest Cretaceous-Tertiary stratigraphy to be constructed in the LaHave Platform area.

Shallow single-channel seismic data available directly from the GSC could also be used to investigate the more shallow features (less than 0.5 seconds) that are masked and/or disturbed by seafloor multiples and other effects of multi-channel industry seismic data. This would permit a more reliable interpretation of the Neogene depositional system and features near the erosional edge of older units.

Furthermore, a more complete velocity model could be developed for the depositional packages to allow conversion from time to depth for the entire study area to produce a true geologic model. Because of the fact that time is a function of velocity, which is not constant, the time to depth conversion of seismic data can alter the apparent form of the bodies that had been initially identified in time (Badley, 1985). Thus, to

properly depict the subsurface features, the time/depth relationship must be properly understood.

References

Amoco Canada Petroleum Company Limited and Imperial Oil Limited, 1973. Regional Geology of the Grand Banks. Canadian Petroleum Geology, Bulletin v. 21, pp. 479-503.

Ascoli, P. 1988. Mesozoic-Cenozoic foraminiferal, ostracod and calpionellid zonation of the North Atlantic margin of North America: Georges Bank-Scotian Basins and northeastern Grand Banks (Jeanne d'Arc, Carson and Flemish Pass Basins). Biostratigraphic correlation of 51 wells. GSC Open File 1791.

Atlantic Geoscience Centre, 1991. Introduction 2: Bathymetry and physiographic features. *In* East Coast Basin Atlas Series: Scotian Shelf, Atlantic Geoscience Centre, Geological Survey of Canada, p. 3.

Badley, M.E. 1985. Practical Seismic Interpretation. International Human Resources Development Corporation, Boston.

Bates, J.L. (ed.) 1991. East Coast Basin Atlas Series: Scotian Shelf. Atlantic Geoscience Centre, Geological Survey of Canada, Dartmouth.

Berggren, W., Kent, D., Swicher III, C., and Aubry, M. 1995. A revised Cenozoic geochronology and chronostratigraphy. *In* Geochronology Time Scales and Global Stratigraphic Correlation, *Edited by* W. Berggren, D. Kent, M. Aubry, and J. Hardenbol. Society of Economic Paleontologists and Mineralogists, Special Publication No. 54, p. 129-212.

Boggs, S. 1987. Principles of Sedimentology and Stratigraphy. Merrill Publishing Company, Toronto.

Bujak Davies Group, 1988. Palynological Analysis of the Interval 1140-14100 Ft, Moheida P-15 well, Scotian Shelf. GSC Open File Report 1862.

Elder, W.P., Gustasaon, E.R., and Sageman, B.B. 1994. Correlation of basinal carbonate cycles to nearshore parasequences in the Late Cretaceous Greenhorn seaway, Western Interior U.S.A. Geological Society of America, Bulletin No. 106, p. 892-902.

Gradstein, F.M. 1976. Cenozoic biostratigraphy (Foraminifera) and depositioinal environment of Shell Mohican I-100, Scotian Shelf. Unpublished GSC (Atlantic) Internal Report No. EPGS-PAL.30-76FMG.

Gradstein, F., Agterberg, F., Ogg, J., Hardenbol, J, van Veen, P., Thierry, J. and Huang, Z. 1995. A Triassic, Jurassic, and Cretaceous time scale. *In* Geochronology Time Scales and Global Stratigraphic Correlation, *Edited by* W. Berggren, D. Kent, M.

Aubry, and J. Hardenbol. Society of Economic Paleontologists and Mineralogists, Special Publication No. 54, p. 95-126.

Hardy, I.A. 1974. Lithostratigraphy of the Banquereau Formation on the Scotian Shelf; Geological Survey of Canada, Paper 74-30, v. 2, pp. 163-174.

Haq, B.U., Hardenbol, J., and Vail, P.R. 1987. Chronology of fluctuating sea levels since the Triassic (250 million years ago to present). Science, v. 235, pp. 1156-1167.

Jansa, L.F., and Wade, J.A. 1975. Geology of the continental margin off Nova Scotia and Newfoundland. *In* Offshore Geology of Eastern Canada, *Edited by* W.J.M. van der Linden and J.A. Wade. Geological Survey of Canada, Paper 74-30, v. 2, pp. 51-105.

King, L.H., MacLean, B.C., and Fader, G.B. 1974. Unconformities on the Scotian Shelf. Canadian Journal of Earth Sciences, v. 11, pp. 89-100.

MacLean, B. C., and Wade, J.A. 1993. East Coast Basin Atlas Series: Seismic markers and stratigraphic picks in Scotian Basin Wells. Atlantic Geoscience Centre, Geological Survey of Canada, Dartmouth.

MacRae, A., Shimeld, J., and Fensome, R. 2002. Cryptic erosion on the Upper Cretaceous Wyandot Formation, Sable Island area, Scotian Shelf. Atlantic Geoscience Society: Colloquium & Annual General Meeting, 2002 - Program and Abstracts.

McIver, N.L. 1972. Cenozoic and Mesozoic stratigraphy of the Nova Scotia Shelf. Canadian Journal of Earth Sciences, v. 9, pp. 54-70.

Mitchum Jr., R.M., Vail, P.R., and Thompson, S. 1977. Seismic Stratigraphy and Global Changes of Sea Level, Part 2: Sequence as a Unit for Analysis. *In* Seismic Stratigraphy - applications to hydrocarbon exploration, Edited by C.W. Payton. American Association of Petroleum Geologists Memoir 26, pp. 53-62.

Moir, P. N. 1999. BASIN: A Hydrocarbon Exploration Database and Model for Data Distribution. Bedford Institute of Oceanography Science Review 1996 & 97. Department of Fisheries and Oceans, Dartmouth.
[http://agcwww.bio.ns.ca/BASIN]

Payton, C.E. (ed.) 1977. Seismic Stratigraphy - applications to hydrocarbon exploration. American Association of Petroleum Geologists Memoir 26.

Prothero, D.R. and Schwab, F. 1997. Sedimentary Geology. W.H. Freeman and Company, New York.

Sanford, B.V., Fader, G.B.J. and Moir, P.N. 1991. Regional geology and geophysics 8: bedrock geology. *In* East Coast Basin Atlas Series: Scotian Shelf, Atlantic Geoscience Centre, Geological Survey of Canada, p. 23.

Sherwin, D.F., 1972. Scotian Shelf and Grand Banks. *In* Future Petroleum Provinces of Canada, *Edited by* R.G. McCrossan. Canadian Society of Petroleum Geologists, Memoir 1, pp. 519-559.

Vail, P.R. and Mitchum Jr., R.M. 1977. Seismic Stratigraphy and Global Changes of Sea Level, Part 1: Overview. *In* Seismic Stratigraphy - applications to hydrocarbon exploration, Edited by C.W. Payton. AAPG Memoir 26, pp. 51-52.

Vail, P.R., Mitchum Jr., R.M., and Thompson, S. 1977. Seismic Stratigraphy and Global Changes of Sea Level, Part 3: Relative Changes in Sea Level from Coastal Onlap. *In* Seismic Stratigraphy - applications to hydrocarbon exploration, Edited by C.W. Payton. American Association of Petroleum Geologists Memoir 26, pp. 63-82.

Van Wagoner, J.C., Posamentier, H.W., Mitchum, R.M., Vail, P.R., Sarg, J.F., Loutit, T.S., and Hardenbol, J. 1988. An overview of the fundamentals of sequence stratigraphy and key definitions. *In* Sea-level changes: an integrated approach, *Edited by* C.K. Wilgus, B.S. Hastings, C.G.St.C. Kendall, H.W. Posamentier, C.A. Ross, and J.C. Van Wagoner. Society of Economic Paleontologists and Mineralogists, Special Publication No. 42, pp. 39-45.

Wade, J.A. 1991. Lithostratigraphy 7: Dawson Canyon and Wyandot formations. *In* East Coast Basin Atlas Series: Scotian Shelf, Atlantic Geoscience Centre, Geological Survey of Canada, p. 63.

Wade, J.A. and MacLean, B.C., 1990. Chapter 5: The geology of the southeastern margin of Canada. *In* Geology of the Continental Margin of Eastern Canada, *Edited by* M.J. Keen and G.L. Williams. Geological Survey of Canada, Geology of Canada Series No. 2, pp. 167-238.

Walker, R., 1992, Chapter 1: Facies, Facies Models and Modern Stratigraphic Concepts. *In* Facies Models: Response to Sea Level Change, *Edited by* R. Walker and N. James. Geological Association of Canada, p. 1-14.

Wessel, P. and Smith, W.H.F. 1998. New, improved version of Generic Mapping Tools released. EOS Transactions of the American Geophysical Union, vol. 79 (47).

WesternGeco, 2002. Ocean Resources Advertisement.

Wilgus, C.K., Hastings, B.S., Kendall, C.G.St.C, Posamentier, H.W., Ross, C.A., and Van Wagoner, J.C. (eds.) 1988, Sea-level changes: an integrated approach. Society of Economic Paleontologists and Mineralogists, Special Publication No. 42.

Williams, G.L. and Bujak, J.P. 1977. Cenozoic palynostratigraphy of offshore eastern Canada. American Association of Stratigraphic Palynologists, Contributions Series 5A, p. 14-47.

Williams, G.L., Barss, M.S., and Bujak, J.P. 1979. Palynological zonation and correlation of sixty-seven wells, eastern Canada. Geological Survey of Canada, Paper 78-24.

Williams G.L., Fyffe, L.R., Wardle R.J., Colman-Sadd S.P., and Boehner, R.C. 1985. Lexicon of Canadian Stratigraphy Volume VI: Atlantic Region. Canadian Society of Petroleum Geologists, Calgary.

Williams, H. and Grant, A.C. 1998. Tectonic assemblages map, Atlantic Region, Canada, scale 1:3,000,000. Geological Survey of Canada, Open File 3657.

Yilmaz, Ö. 1987. Seismic Data Processing, Series: Investigations in Geophysics, Volume 2. Society of Exploration Geophysicists, Tulsa.

Appendix A. Seismic Programs and Lines Used

Seismic survey data and well locations were obtained from BASIN, courtesy of the CNSOPB. In the figures, dark blue contours represent bathymetry (courtesy of the Atlantic Geoscience Centre, 1991), and gray boxes represent active exploration licences (courtesy of the CNSOPB). The project area is outlined in purple.

Project Number 8624-P028-049E
Year 1982
Company ..... Petro-Canada
Contractor..... Sefel
Area ..... Scotian Shelf/Scotian Slope
Minimum Latitude..... 42.66
Maximum Latitude..... 44.36
Minimum Longitude ..... -63.94
Maximum Longitude..... -60.54

Line	Start SP	End SP	Distance (km)
3501-82A	1880	4966	76.952
3501-82P	0	960	24.04
3502-82P	0	2334	58.279
3503-82P	0	1220	30.47
3504-82A	1600	3066	36.579
3504-82P	0	621	15.573
3505-82P	1	10062	250.435
3506-82P	0	3615	90.496
3507-82P	0	5516	138.049
3508-82A	2762	3842	27.056
3508-82P	0	1841	45.94
3510-82P	0	3552	88.86
3512-82P	0	2631	65.771
3514-82P	0	2911	72.872
3516-82A	2021	3471	36.348
3516-82B	4411	7057	66.154
3516-82P	0	1081	27.015
3518-82A	3000	3788	19.719
3518-82P	0	2041	50.96
3520-82A	0	1478	36.853
3520-82B	1400	4956	89.118
3520-82P	0	456	11.394
3522-82P	0	2307	57.715
3524-82P	0	2118	52.978
3526-82P	0	561	13.936
3528-82A	0	2667	66.576
3528-82B	3000	3775	19.332
3528-82P	1	2582	64.787
3530-82A	4381	5915	38.437
3530-82P	0	3461	86.582
3532-82P	0	3415	85.533
3534-82P	0	4313	107.942
3536-82A	1331	3915	64.248
3536-82P	0	400	10.138

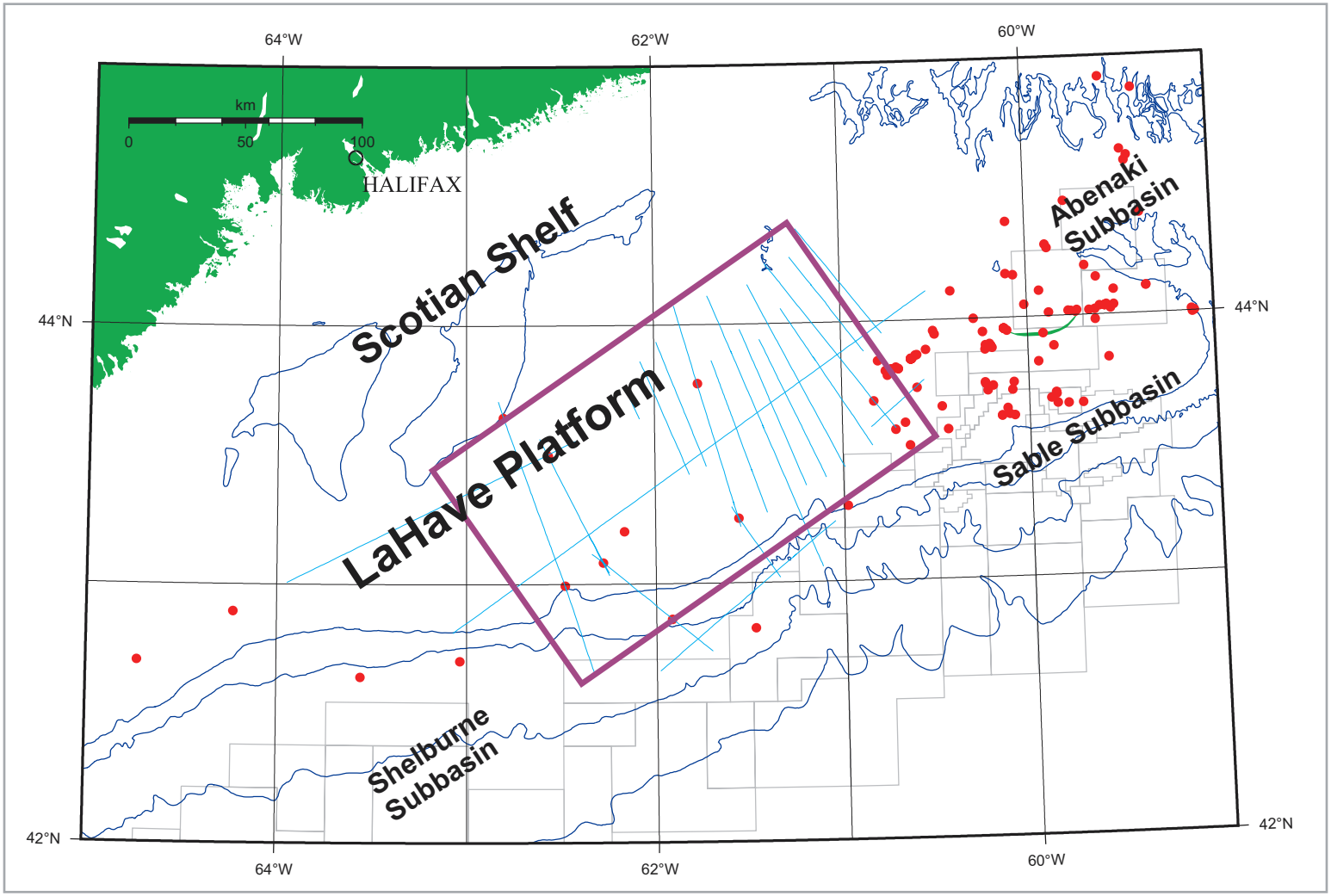

Figure A.1 Selected seismic lines used from 8624-P028-049E.

Project Number 8620-S014-006E
Year 1983
Company ..... PAREX/Soquip
Contractor..... GSI
Area ..... Scotian Shelf/Scotian Slope
Minimum Latitude..... 42.34
Maximum Latitude..... 44.76
Minimum Longitude ..... -63.96
Maximum Longitude..... -57.02

Line	Start SP	End SP	Distance (km)
83-598AA			
83-790C	101	2179	52.037
83-838C	101	1963	46.609
83-854C	101	3378	82.123
83-4369AB	4873	6601	43.224
83-4369BC	6645	10195	88.766
83-4385AA	2028	5090	76.422
83-4385BB	5091	6628	38.362
83-4401BD	2425	7294	121.882
83-4417A	101	1871	44.228
83-4417AA	1896	2315	10.454
83-4417AB	2955	4554	39.885
83-4417B	101	11269	279.715
83-4417BC	4460	5250	29.83
83-4417BD	5279	5468	4.689
83-4433BD	2516	4930	60.359

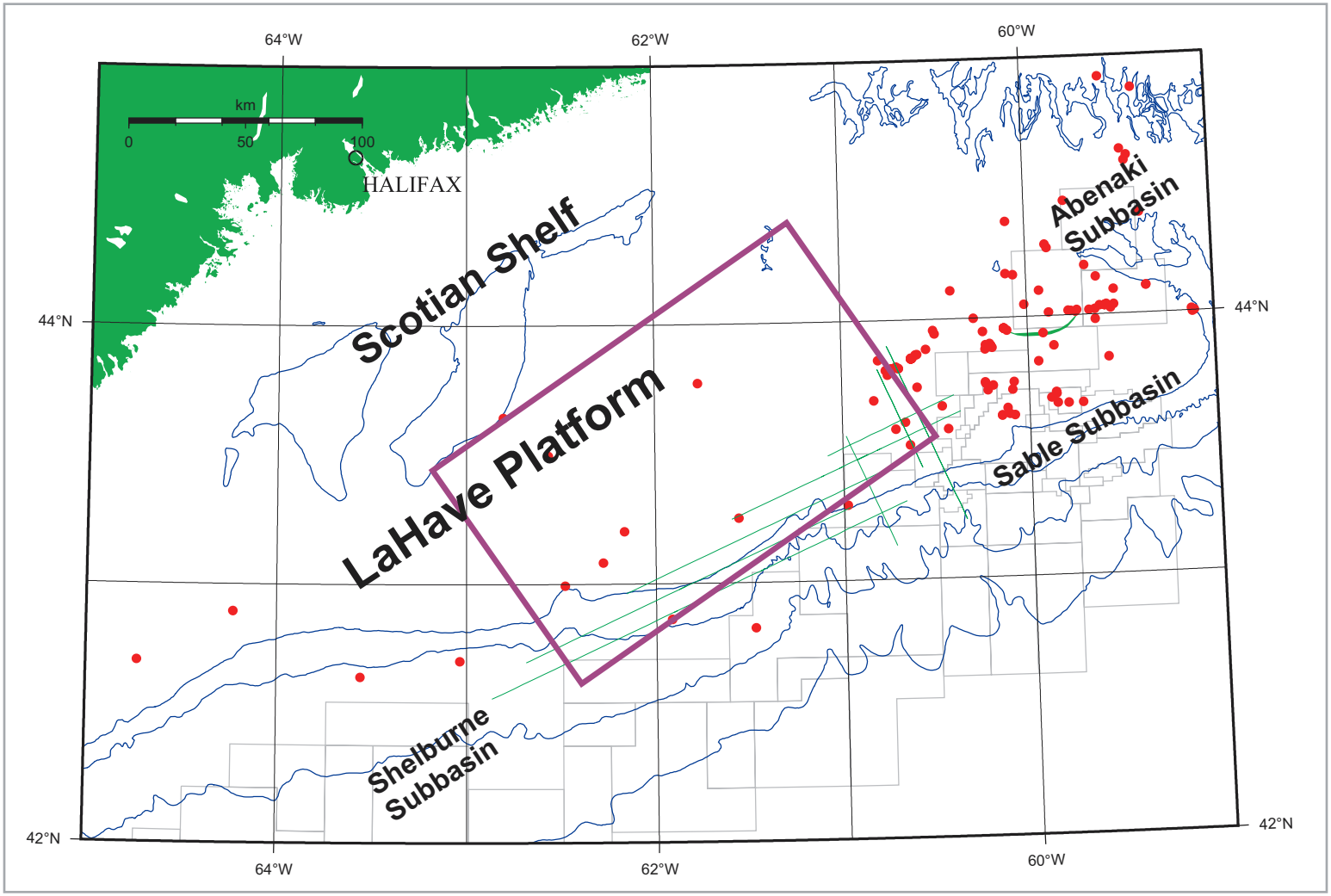

Figure A.2 Selected seismic lines used from 8620-S014-006E.

Project Number 8624-S006-005E,6E
Year 1970
Company ..... Shell Canada
Contractor..... Shell Oil
Area ..... Scotian Shelf/Scotian Slope
Minimum Latitude..... 41.55
Maximum Latitude..... 43.95
Minimum Longitude ..... -65.91
Maximum Longitude..... -58.99

Line	Start SP	End SP	Distance (km)
202-70/2	2400	3810	86.636
214-70/1	2400	3909	92.482
226-70/1	3150	3936	48.222
2800-70/4	4455	5850	85.433
3500-70/2,3	3375	5610	136.624
3700-70/3A	3969	5550	96.313

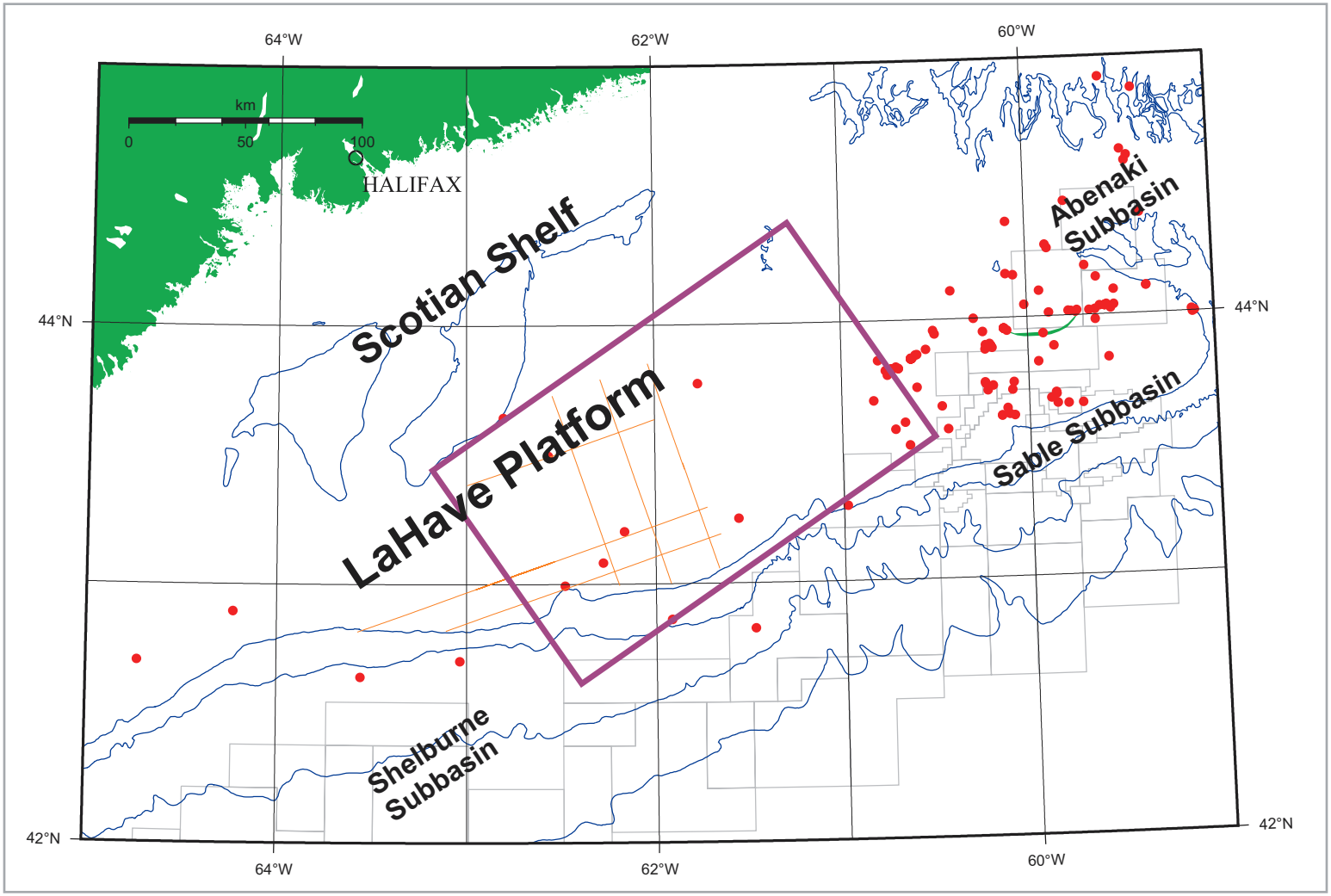

Figure A.3 Selected seismic lines used from 8624-S006-005E,6E.

Appendix B. Wells Used

Well data was obtained from BASIN, with data available courtesy of the CNSOPB. All well depth measurements are measured depth, kelly bushing datum.

Well Name..... Alma K-85
GSC #..... D267
Spud Date..... January 29th, 1985
Company ..... Shell/Petro-Canada/others
Well Class ..... Delineation
Gas..... gas (C)
Oil..... unrated
Status..... plugged & abandoned
Rotary Table..... 24.0 m
Water Depth ..... 65.3 m
Total Depth..... 3602.0 m
Location (NAD 27 geographic datum):
Latitude..... 43.57897
Longitude ..... -60.71714
Location (NAD 83 geographic datum):
Latitude..... 43.579047
Longitude ..... -60.7164

Well Name..... Cree E-35
GSC #..... D006
Spud Date..... September 08th, 1970
Company ..... Shell/Petro-Canada/others
Well Class ..... Exploratory
Gas..... show
Oil..... unrated
Status..... plugged & abandoned
Rotary Table..... 31.4 m
Water Depth ..... 53.3 m
Total Depth..... 3983.7 m
Location (NAD 27 geographic datum):
Latitude..... 43.73909
Longitude ..... -60.59886
Location (NAD 83 geographic datum):
Latitude..... 43.739161
Longitude ..... -60.598117

Well Name..... Demascota G-32
GSC #..... D125
Spud Date..... March 1st, 1974
Company ..... Shell
Well Class ..... Exploratory
Gas..... show
Oil..... unrated
Status..... plugged & abandoned
Rotary Table..... 29.9 m
Water Depth ..... 54.3 m

Total Depth..... 4672.3 m
Location (NAD 27 geographic datum):
Latitude..... 43.69089
Longitude ..... -60.83167
Location (NAD 83 geographic datum):
Latitude..... 43.690964
Longitude ..... -60.830928

Well Name..... Moheida P-15
GSC #..... D168
Spud Date..... November 18th, 1976
Company ..... Petro-Canada/Shell
Well Class ..... Exploratory
Gas..... unrated
Oil..... unrated
Status..... plugged & abandoned
Rotary Table..... 29.9 m
Water Depth ..... 111.9 m
Total Depth..... 4297.7 m
Location (NAD 27 geographic datum):
Latitude..... 43.08231
Longitude ..... -62.27898
Location (NAD 83 geographic datum):
Latitude..... 43.082386
Longitude ..... -62.278267

Well Name..... Mohican I-100
GSC #..... D074
Spud Date..... December 28th, 1971
Company ..... Shell
Well Class ..... Exploratory
Gas..... unrated
Oil..... trace
Status..... plugged & abandoned
Rotary Table..... 29.9 m
Water Depth ..... 153.3 m
Total Depth..... 4393.4 m
Location (NAD 27 geographic datum):
Latitude..... 43.99418
Longitude ..... -62.48092
Location (NAD 83 geographic datum):
Latitude..... 43.994253
Longitude ..... -62.480211

Well Name..... Naskapi N-30
GSC #..... D004

Spud Date ..... February 16th, 1970
Company ..... Husky/Bow Valley/others
Well Class ..... Exploratory
Gas..... trace
Oil..... trace
Status ..... plugged & abandoned
Rotary Table..... 25.9 m
Water Depth ..... 95.1 m
Total Depth..... 2205.2 m
Location (NAD 27 geographic datum):
Latitude..... 43.49619
Longitude ..... -62.56684
Location (NAD 83 geographic datum):
Latitude..... 43.496261
Longitude ..... -62.566139

Well Name..... Ojibwa E-07
GSC #..... D121
Spud Date ..... February 4th, 1974
Company ..... Husky/Bow Valley/others
Well Class ..... Exploratory
Gas..... trace
Oil..... unrated
Status ..... plugged & abandoned
Rotary Table..... 29.9 m
Water Depth ..... 75.6 m
Total Depth..... 2329.6 m
Location (NAD 27 geographic datum):
Latitude..... 43.77214
Longitude ..... -61.76959
Location (NAD 83 geographic datum):
Latitude..... 43.772217
Longitude ..... -61.768872

Well Name..... Oneida O-25
GSC #..... D003
Spud Date ..... November 16h, 1969
Company ..... Shell
Well Class ..... Exploratory
Gas..... trace
Oil..... unrated
Status ..... plugged & abandoned
Rotary Table..... 25.9 m
Water Depth ..... 82.3 m
Total Depth..... 4109.9 m
Location (NAD 27 geographic datum):

Latitude..... 43.2493
Longitude ..... -61.5601
Location (NAD 83 geographic datum):
Latitude..... 43.249381
Longitude ..... -61.559375

Appendix C. Well Logs and Synthetic Seismograms for Study Interval – In Time

Well logs were obtained from BASIN. Wireline data is provided courtesy of QC Data Inc., and lithostratigraphic data courtesy of CanStrat Ltd. Data was plotted with "lithoplot3.perl", a program written by A. MacRae (GSC (Atlantic)) that extracted and plotted the data from BASIN to a scale of 2.5 inches per second using a time to depth conversion. For biostratigraphic age data refer to Appendix D.

Synthetic seismograms and depth to time tables were produced using GeoSyn, version 4.8.1.5, a synthetic and modelling software package created by IHS AccuMap Limited of Calgary, Alberta.

Plots are shown from the top of the wireline logs to just below the top of the Logan Canyon Formation (thereby encompassing the entire study interval).

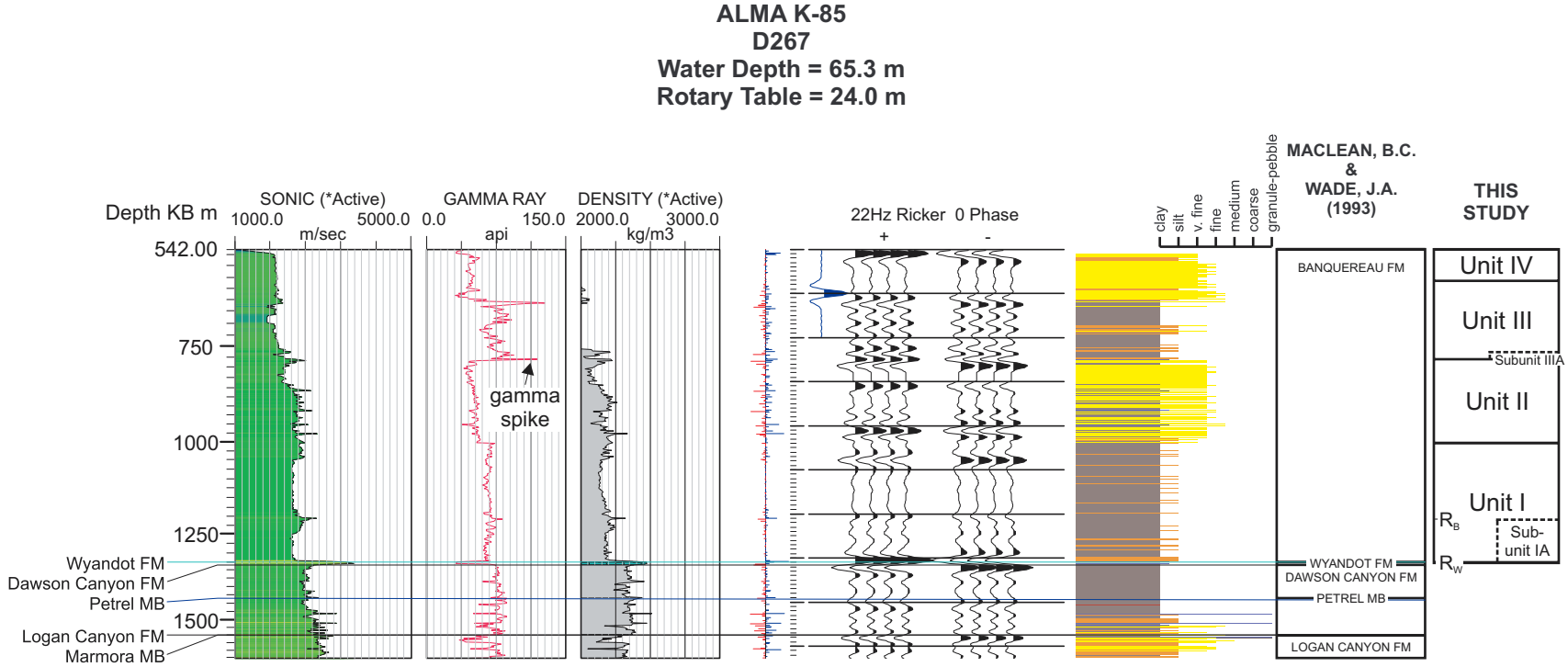

Figure C.1 Well log and synthetic seismogram for Alma K-85.

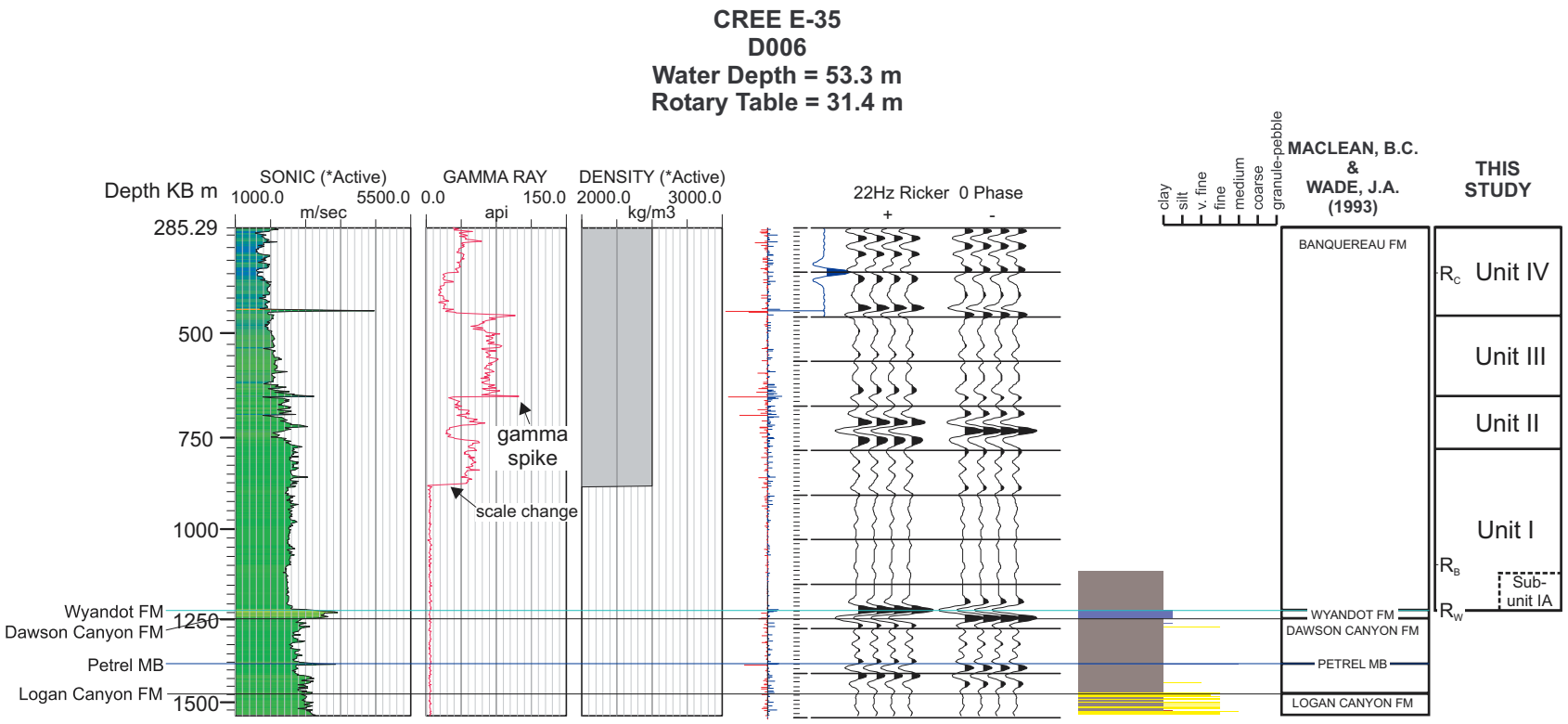

Figure C.2 Well log and synthetic seismogram for Cree E-35. Note the uncorrected scale change in the gamma log at approximately 875 m.

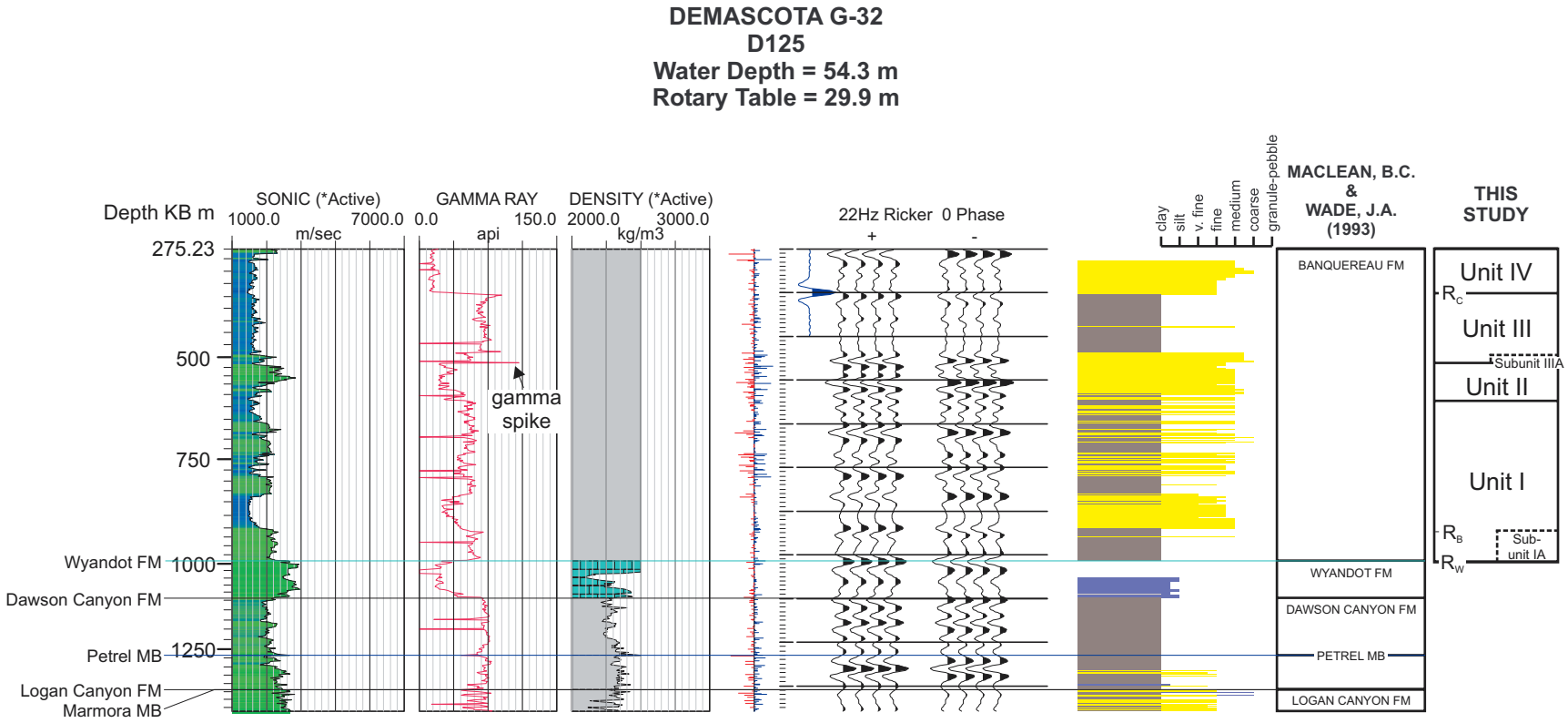

Figure C.3 Well log and synthetic seismogram for Demascota G-32.

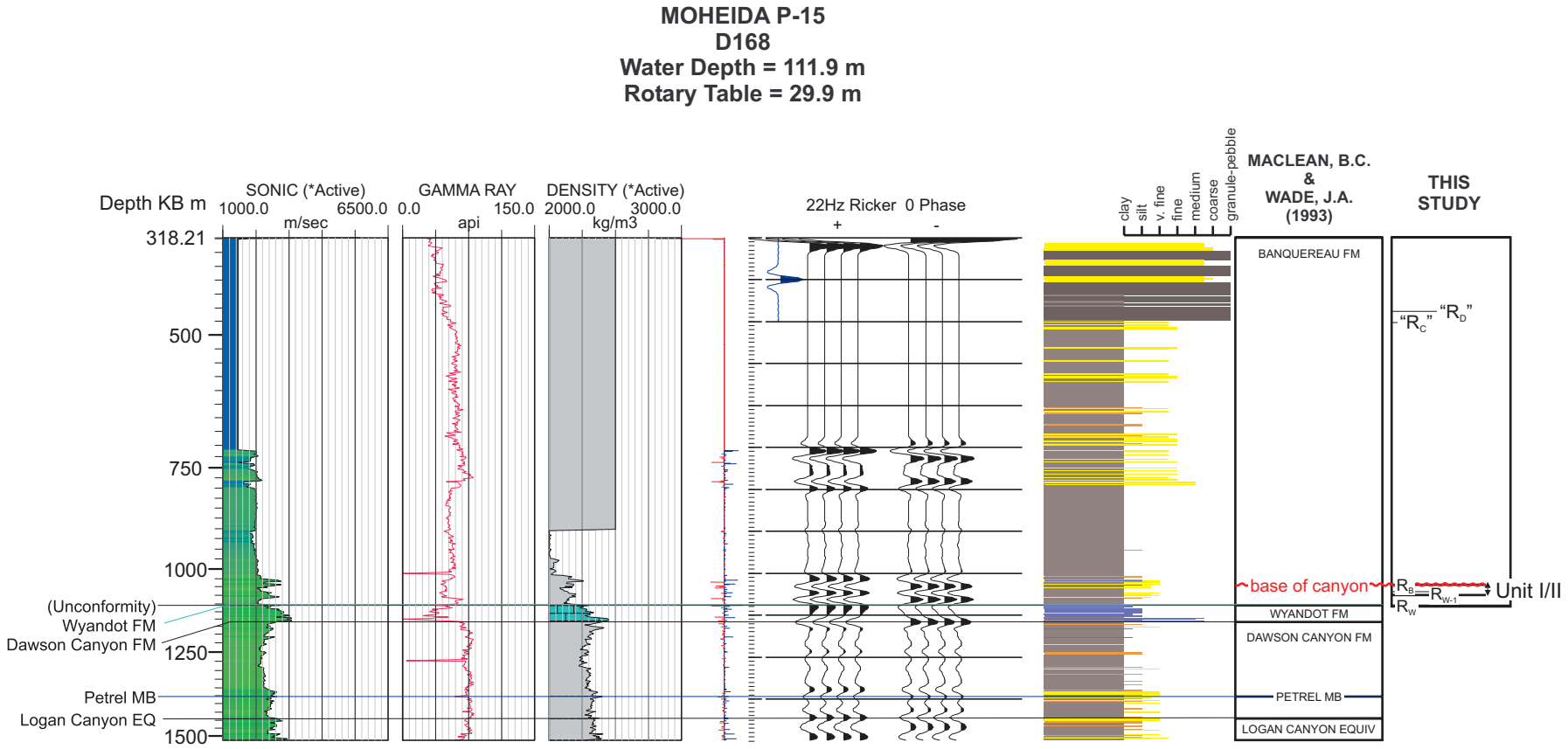

Figure C.4 Well log and synthetic seismogram for Moheida P-15. Quotation marks represent reflections that, although mapped, are probably not present in the canyon fill.

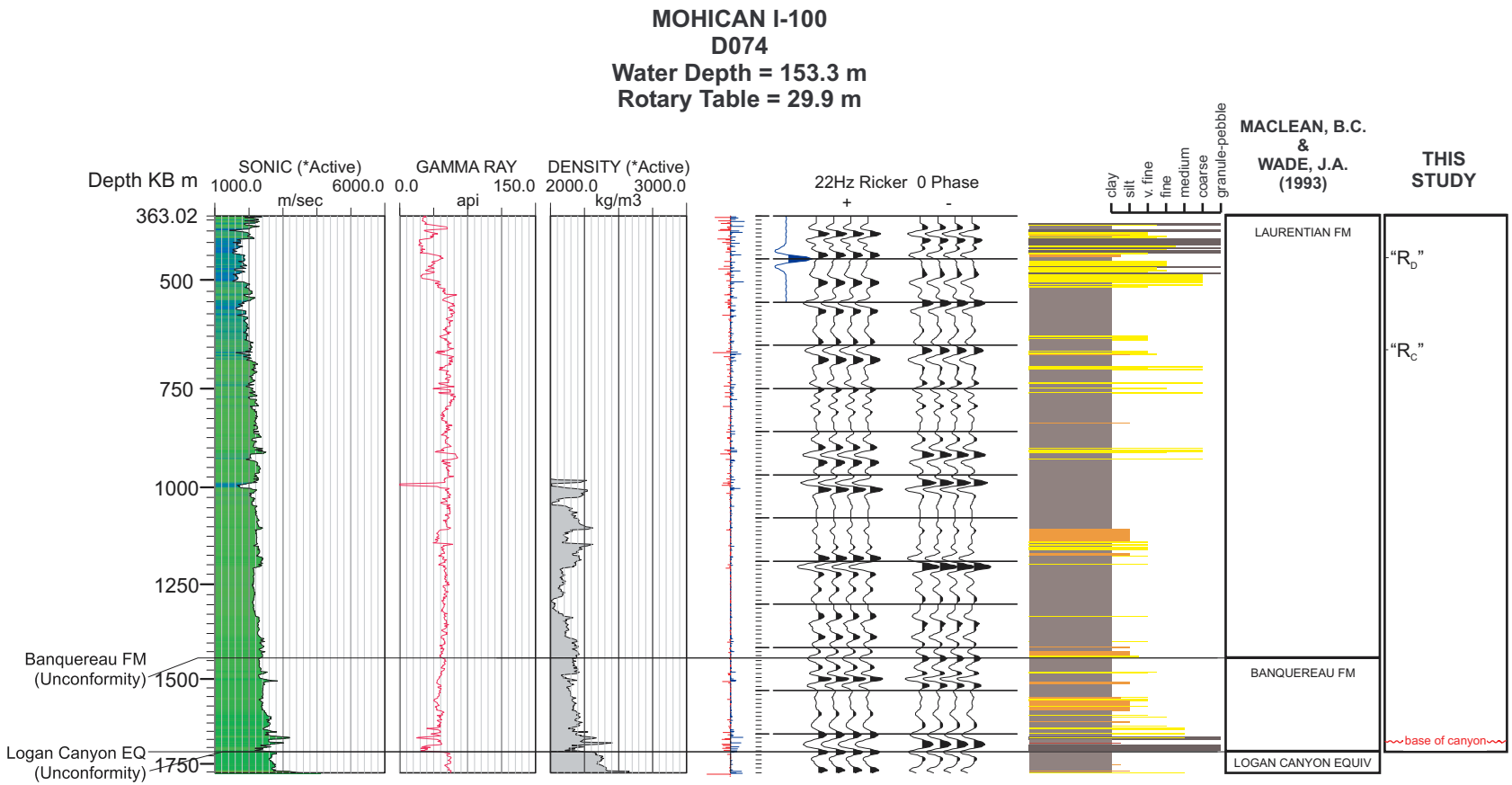

Figure C.5 Well log and synthetic seismogram for Mohican I-100. Quotation marks represent reflections that, although mapped, are probably not present in the canyon fill.

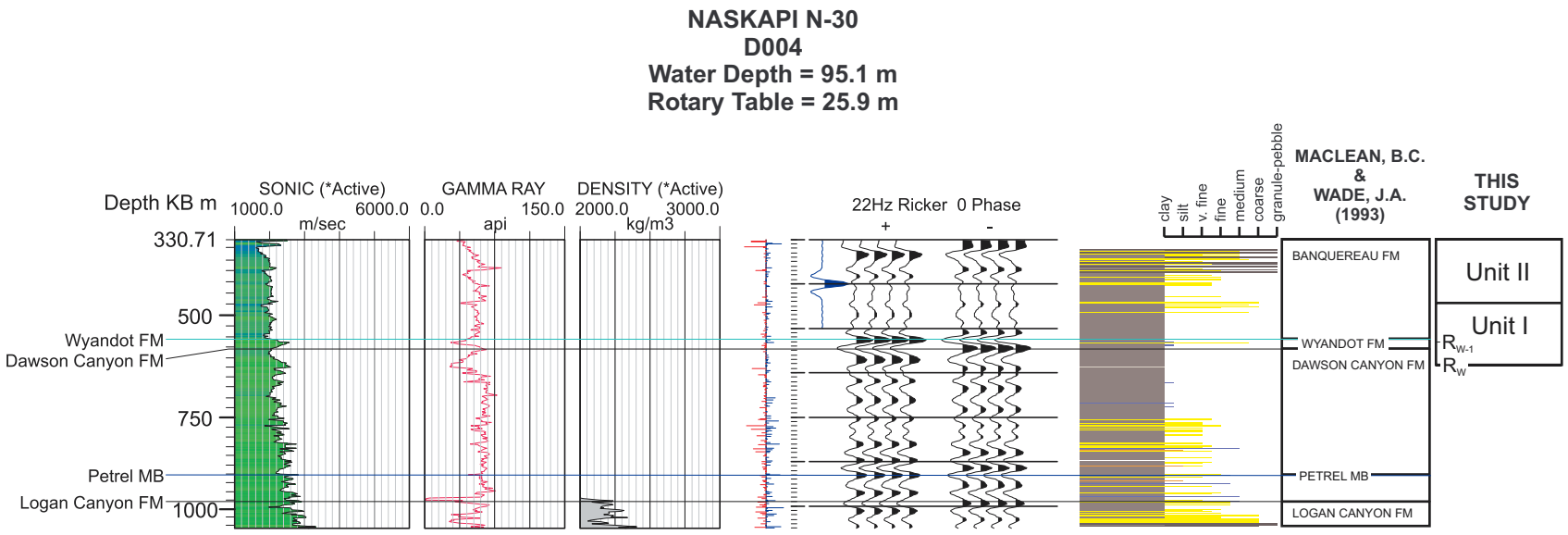

Figure C.6 Well log and synthetic seismogram for Naskapi N-30.

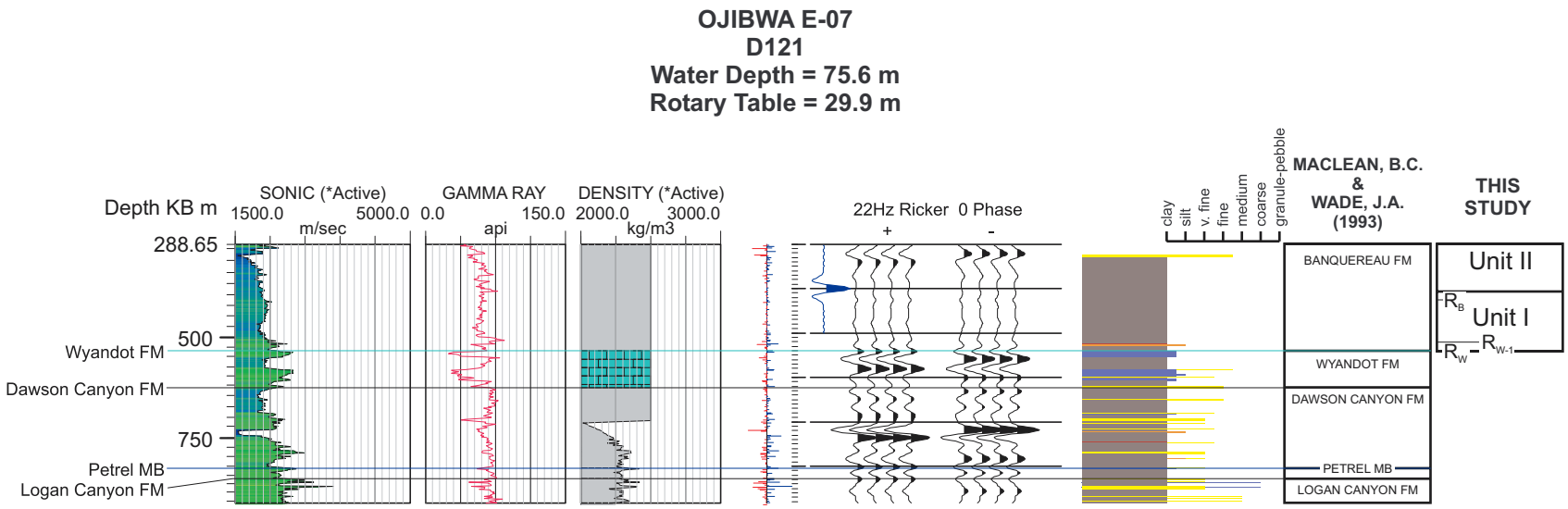

Figure C.7 Well log and synthetic seismogram for Ojibwa E-07.

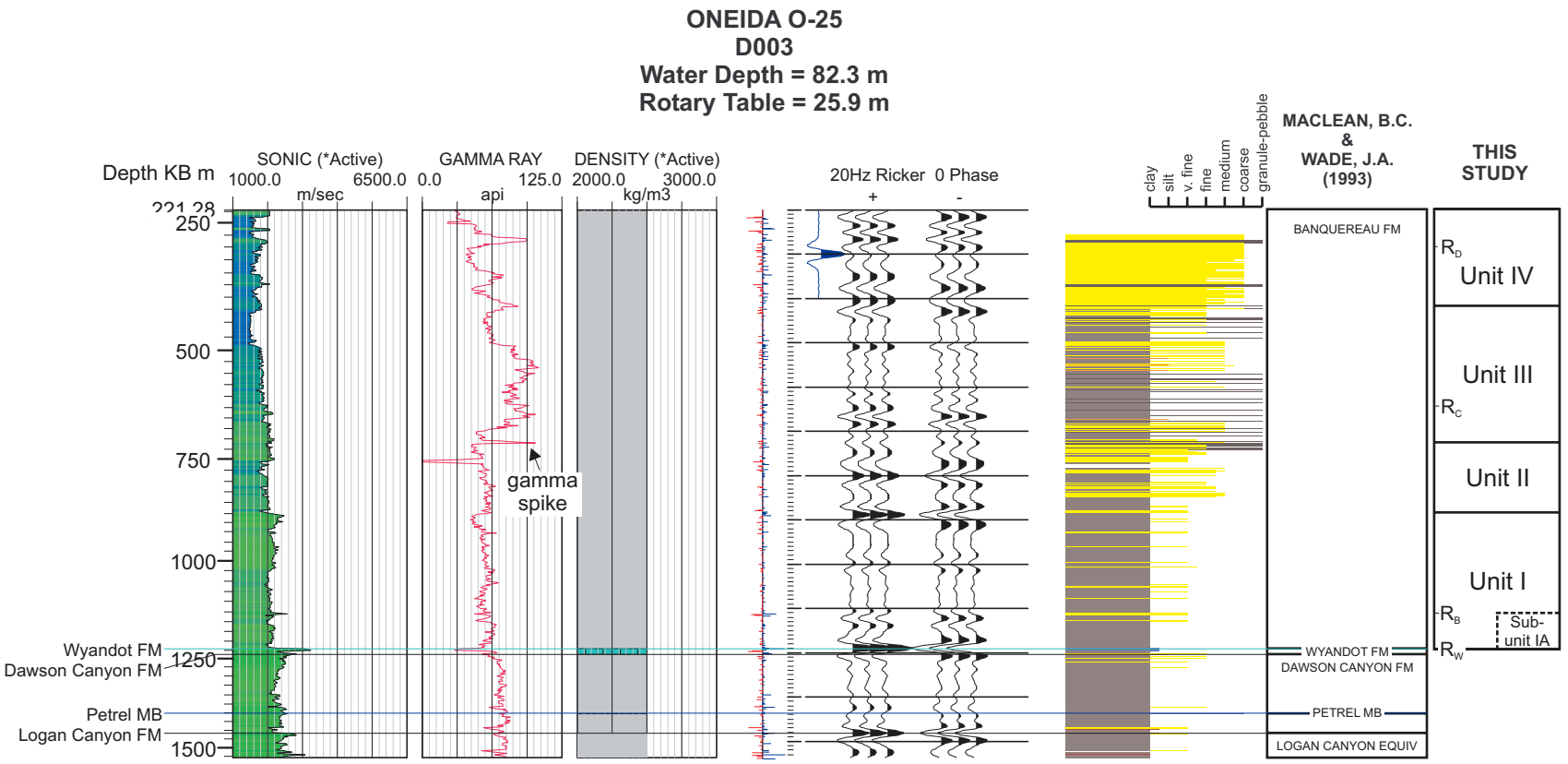

Figure C.8 Well log and synthetic seismogram for Oneida O-25.

Appendix D. Well Logs – In Depth

Well logs were obtained from BASIN, with data available courtesy of the CNSOPB. Wireline data is provided courtesy of QC Data Inc., lithostratigraphic data courtesy of CanStrat Ltd., and biostratigraphic data courtesy of the individual authors. Data was plotted with "lithoplot3.perl", a program written by A. MacRae (GSC (Atlantic)) that extracted and plotted the data from BASIN. For approximate biostratigraphic ages, refer to the legend below:

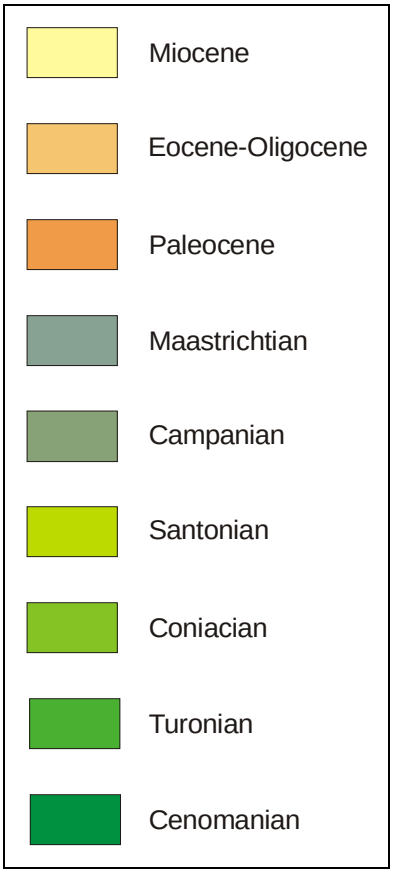

Abbreviations used are listed below:

ALB.	Albian
BOUND.	boundary
CAMP.	Campanian
CENO.	Cenomanian
CON.	Coniacian

CRET.	Cretaceous
E	Early
EOC.	Eocene
GLAC.	glacial
GSC	Geological Survey of Canada
INDET.	indeterminate
INT.	inter
L	Late
M	Middle
MAAS.	Maastrichtian
MIO.	Miocene
OLIG.	Oligocene
PAL.	Paleocene
PLIO.	Pliocene
PLST.	Pleistocene
POSS.	possible
REWRKD.	reworked
SANT.	Santonian
SEN.	Senonian
TERT.	Tertiary
TUR.	Turonian
UNC.	Unconformity

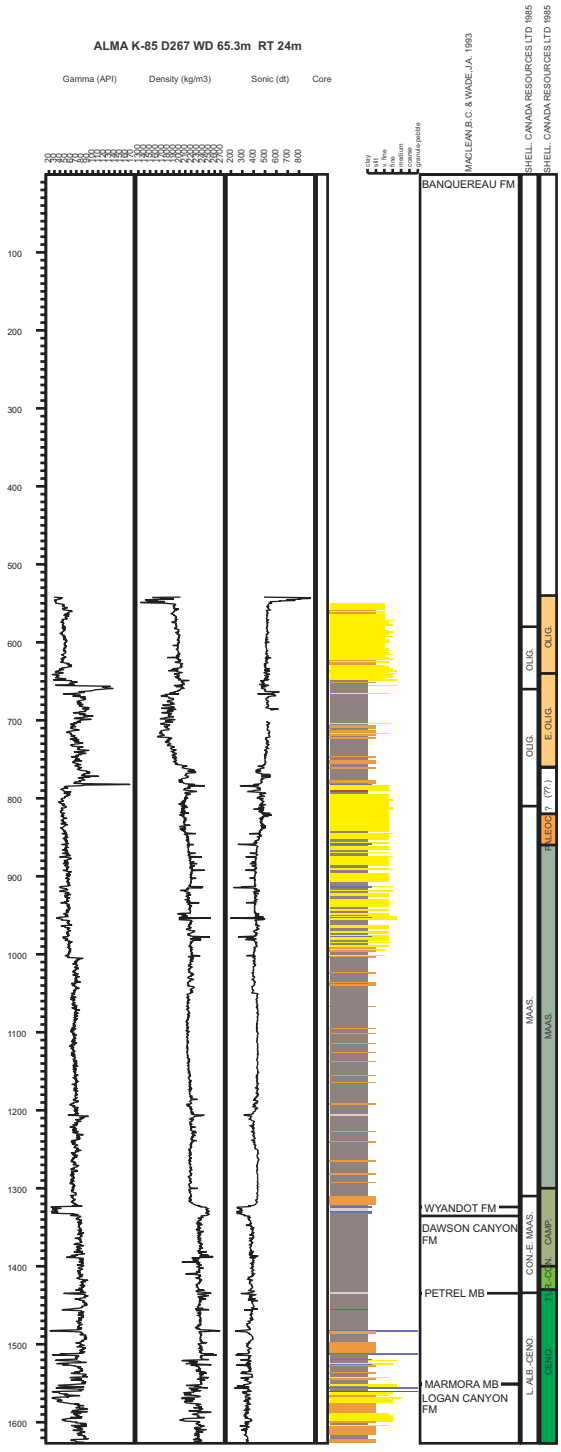

FigurE. D.1 WelL. log for Alma K-85.

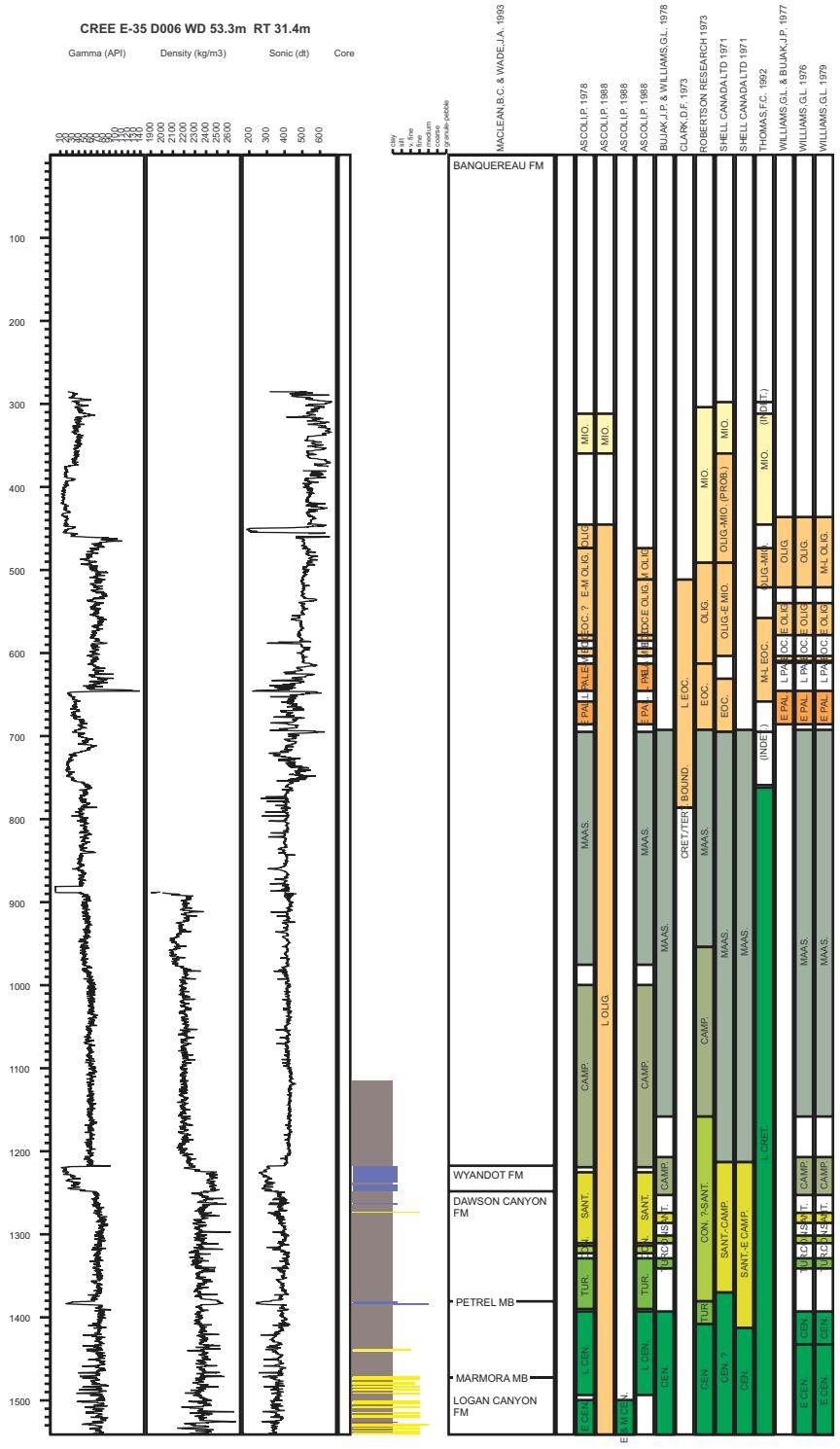

Figure D.2 Well log for Cree E-35.

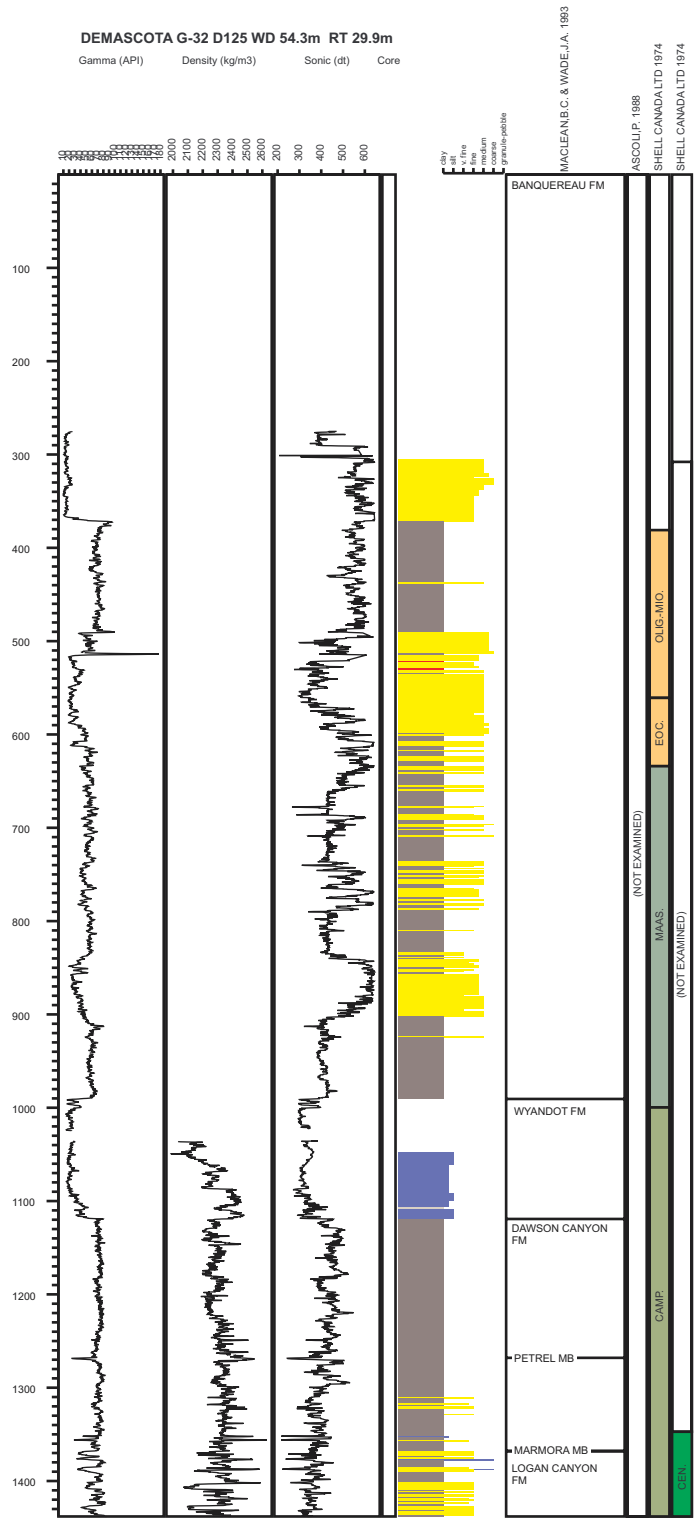

Figure D.3 Well log for Demascota G-32.

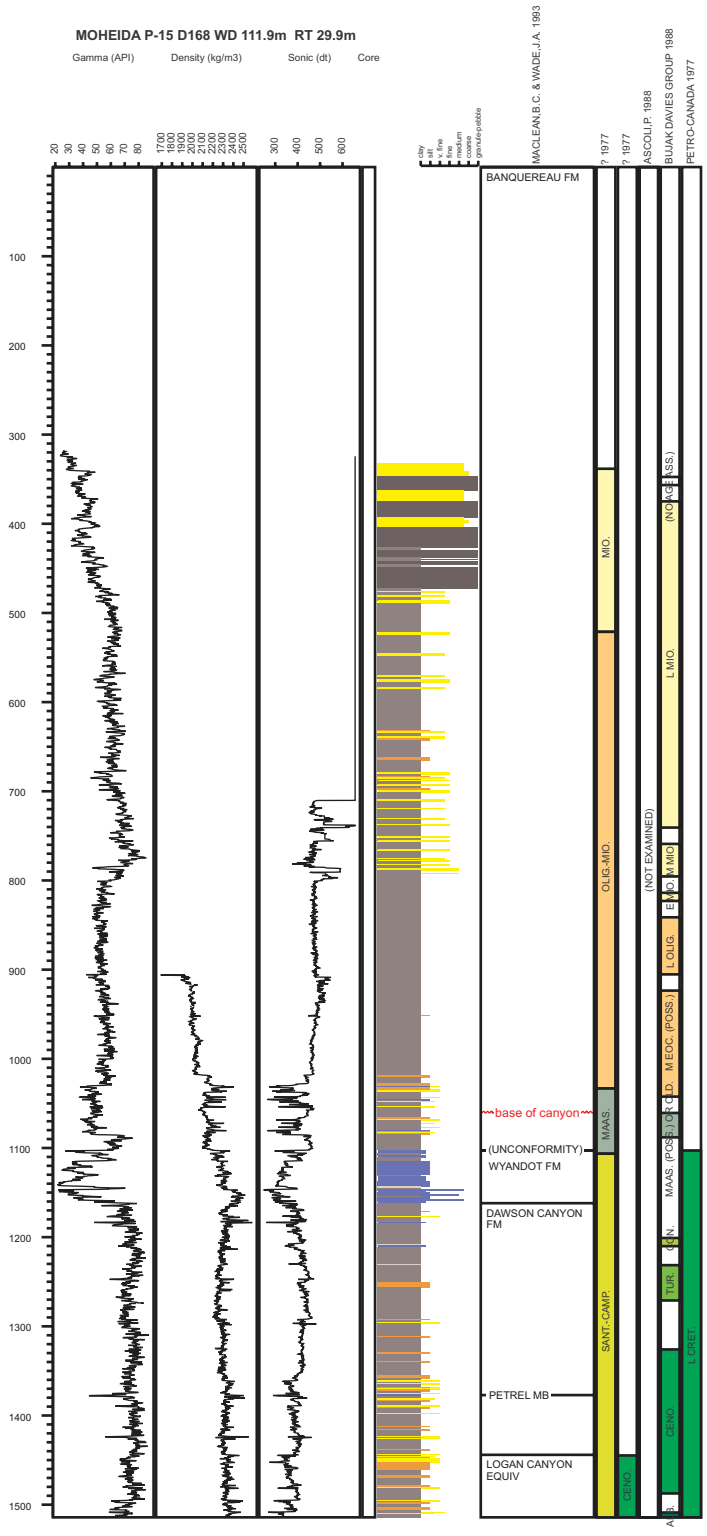

Figure D.4 Well log for Moheida P-15. Base of canyon is interpreted to occur at about 1060 m.

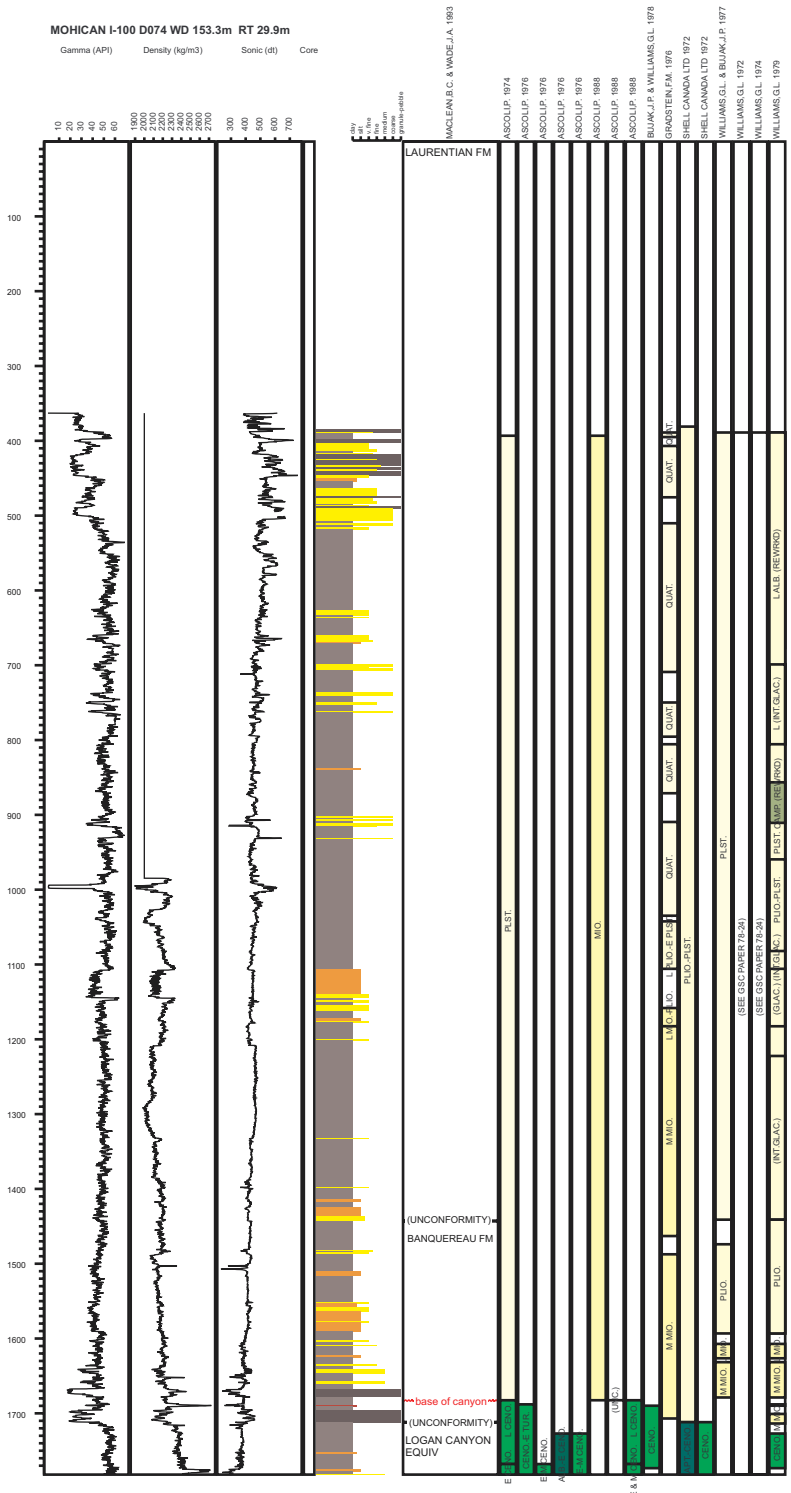

Figure D.5 Well log for Mohican I-100. Base of canyon is interpreted to occur at about 1680 m.

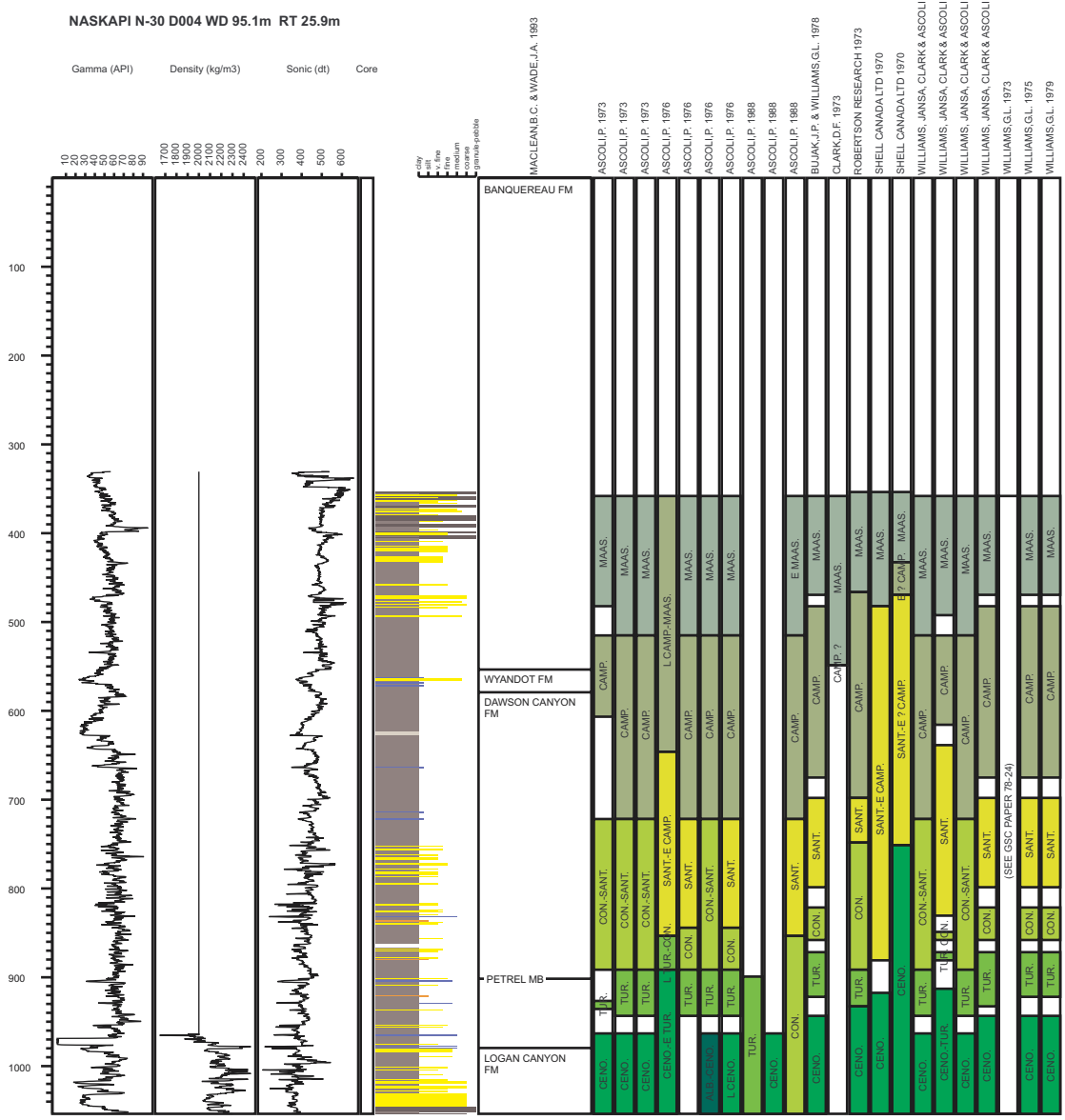

Figure D.6 Well log for Naskapi N-30.

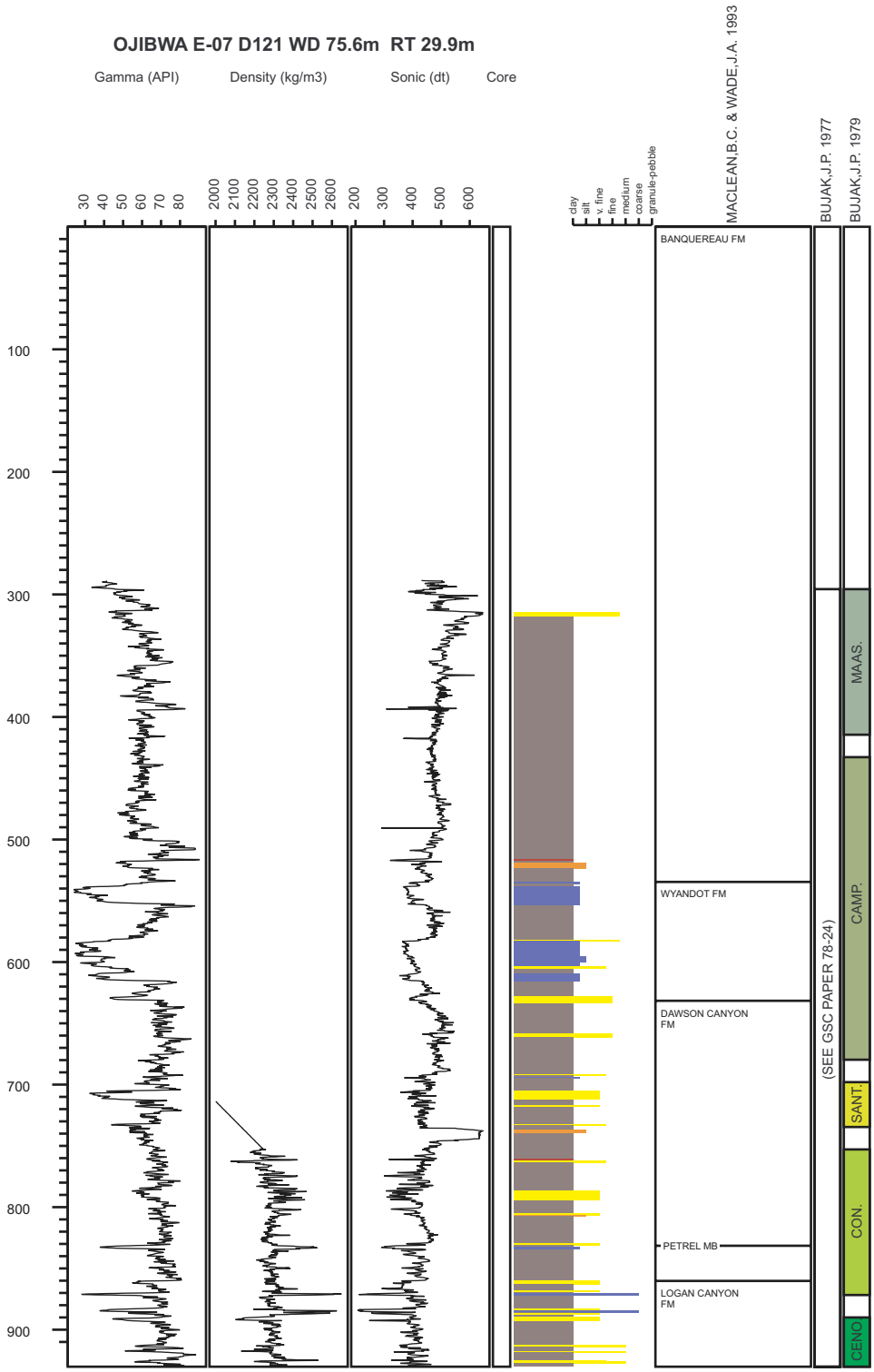

Figure D.7 Well log for Ojibwa E-07.

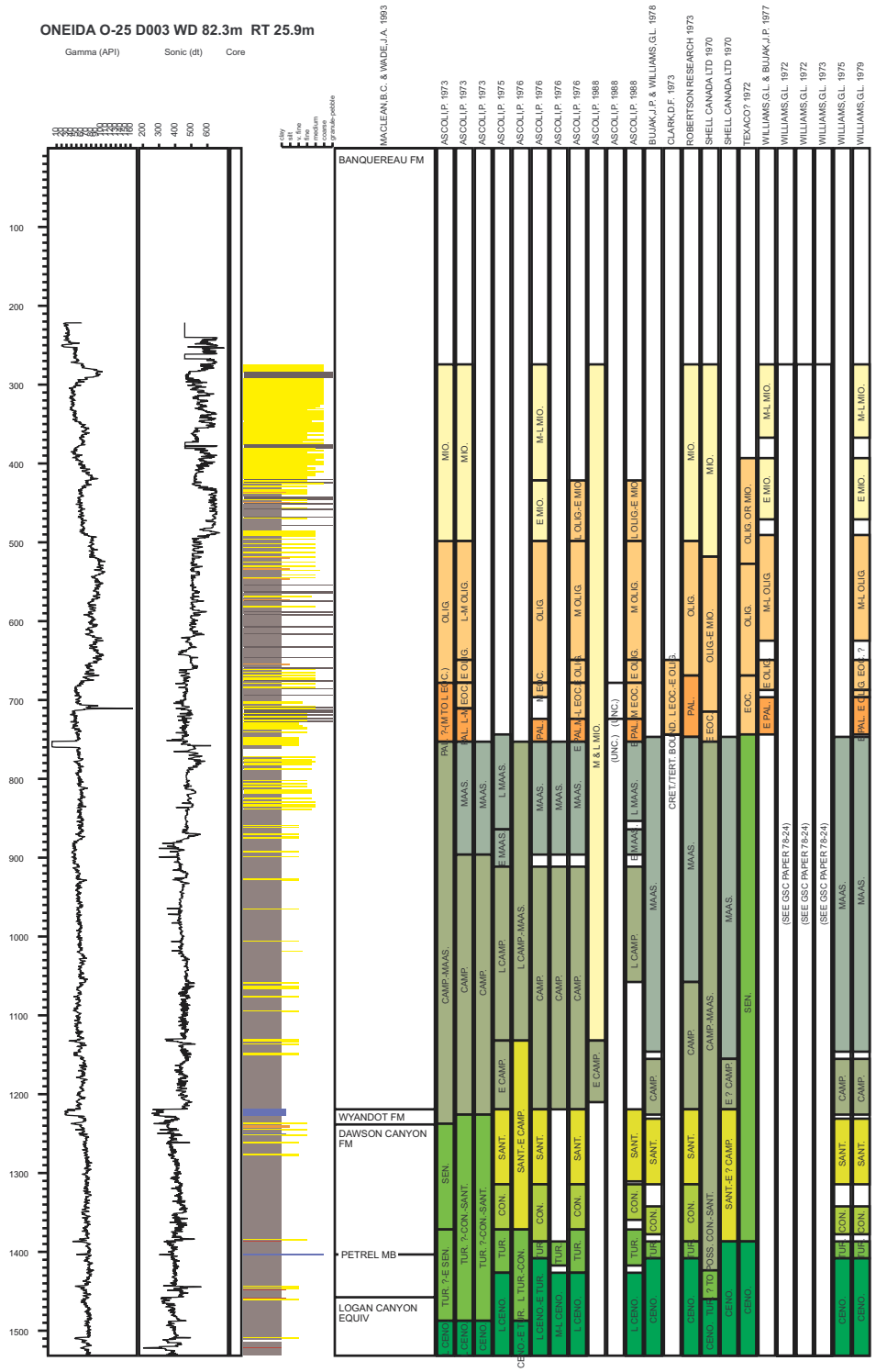

Figure D.8 Well log for Oneida O-25.

Appendix E. Synthetic Seismograms – Entire Well

Synthetic seismograms were produced using GeoSyn, version 4.8.1.5, a synthetic and modelling software package created by IHS AccuMap Limited of Calgary, Alberta.

Note that on the synthetic seismograms, seismic time is the linear scale, while the depth scale is variable as a result of its dependency on velocity for depth conversion. Also note that although the time plotted is two-way time (TWT), the scale is set at zero where the well log commences, which is different than the time recorded on corresponding seismic sections, which are recorded from sea level. These plots were originally scaled at 2.5 inches/second to correspond to the seismic sections. They are reproduced here at a smaller scale. For 2.5 in/sec plots for the study interval, refer to Appendix C.

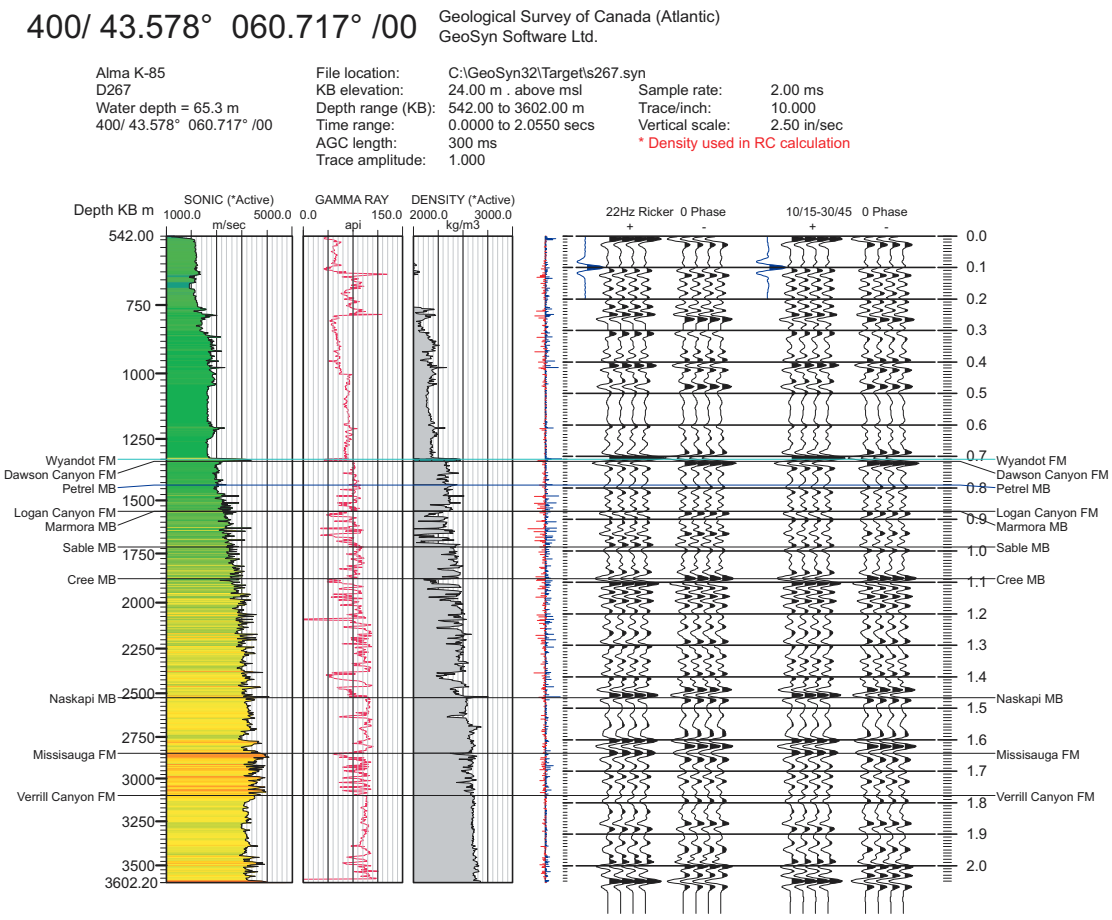

400/ 43.578° 060.717° /00

Tops	Depth KB m	Depth SS m	Time 2 way sec	Vav. m/sec	Vint. m/sec	Isochron sec	Isopach m
Kelly Bushing = 24.00 (m) above msl							
Tops Author: MacLean & Wade (1993)							
Top of Log	542.00	-518.00	0.00000	---	2205.0	0.70930	782.00
Wyandot FM	1324.00	-1300.00	0.70930	2205.0	3564.9	0.00645	11.50
Dawson Canyon FM	1335.50	-1311.50	0.71575	2217.3	2626.7	0.07546	99.10
Petrel MB	1434.60	-1410.60	0.79121	2256.3	2760.8	0.08432	116.40
Logan Canyon FM	1551.00	-1527.00	0.87553	2304.9	---	0.00000	0.00
Marmora MB	1551.00	-1527.00	0.87553	2304.9	2980.7	0.11239	167.50
Sable MB	1718.50	-1694.50	0.98792	2381.8	3140.2	0.10095	158.50
Cree MB	1877.00	-1853.00	1.08887	2452.1	3431.0	0.37785	648.20
Naskapi MB	2525.20	-2501.20	1.46672	2704.3	3608.5	0.17614	317.80
Missisauga FM	2843.00	-2819.00	1.64286	2801.2	3872.1	0.13481	261.00
Verrill Canyon FM	3104.00	-3080.00	1.77767	2882.4	3594.9	0.27706	498.00
Bottom of Log	3602.00	-3578.00	2.05473	2978.5			

Figure E.1 Synthetic seismogram for Alma K-85 (indicated vertical scale not accurate).

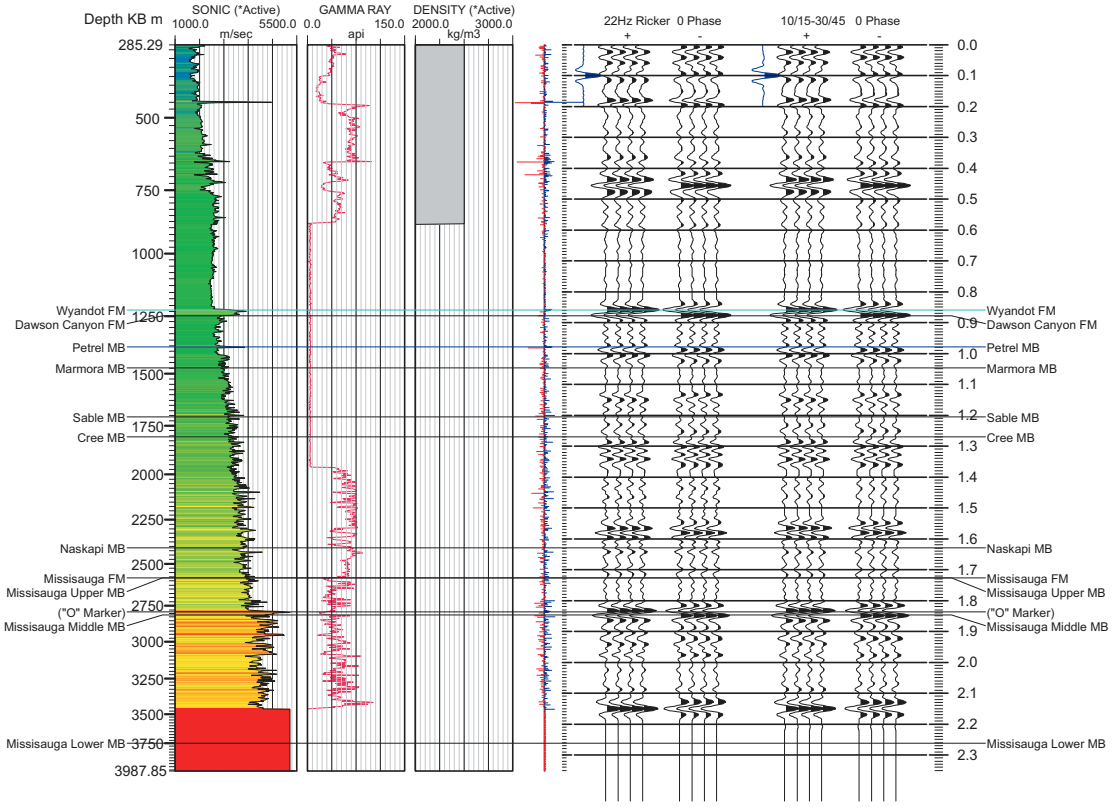

400/ 43.739° 060.598° /00

Tops	Depth KB m	Depth SS m	Time 2 way sec	Vav. m/sec	Vint. m/sec	Isochron sec	Isopach m
Kelly Bushing = 31.40 (m) above msl							
Tops Author: MacLean & Wade (1993)							
Top of Log	285.29	-253.89	0.00000	---	2170.5	0.85885	932.08
Wyandot FM	1217.37	-1185.97	0.85885	2170.5	3319.5	0.01855	30.79
Dawson Canyon FM	1248.16	-1216.76	0.87740	2194.8	2599.8	0.10199	132.58
Petrel MB	1380.74	-1349.34	0.97940	2237.0	2754.0	0.06663	91.75
Marmora MB	1472.49	-1441.09	1.04603	2269.9	2932.1	0.15884	232.87
Sable MB	1705.36	-1673.96	1.20487	2357.2	3076.3	0.06480	99.67
Cree MB	1805.03	-1773.63	1.26967	2393.9	3359.9	0.35887	602.89
Naskapi MB	2407.92	-2376.52	1.62854	2606.8	3528.2	0.09849	173.74
Missisauga FM	2581.66	-2550.26	1.72703	2659.3	---	-0.00000	0.00
Missisauga Upper MB	2581.66	-2550.26	1.72703	2659.3	3771.3	0.10991	207.26
("O" Marker)	2788.92	-2757.52	1.83694	2725.9	4810.9	0.01014	24.38
Missisauga Middle MB	2813.30	-2781.90	1.84707	2737.3	4511.7	0.41548	937.26
Missisauga Lower MB	3750.56	-3719.16	2.26256	3063.1	5245.6	0.09041	237.14
Bottom of Log	3987.70	-3956.30	2.35297	3147.0			

Figure E.2 Synthetic seismogram for Cree E-35 (indicated vertical scale not accurate).

400/ 43.691° 060.832° /00 Geological Survey of Canada (Atlantic)
GeoSyn Software Ltd.

Demascota G-32
D125
Water Depth = 54.3 m
400/ 43.691° 060.832° /00

File location: C:\GeoSyn32\Target\s125.syn
KB elevation: 29.90 m . above msl
Depth range (KB): 275.23 to 4676.24 m
Time range: 0.0000 to 2.6010 secs
AGC length: 600 ms
Trace amplitude: 1.000

Sample rate: 2.00 ms
Trace/inch: 10.000
Vertical scale: 2.50 in/sec
* Density not used in RC calculation

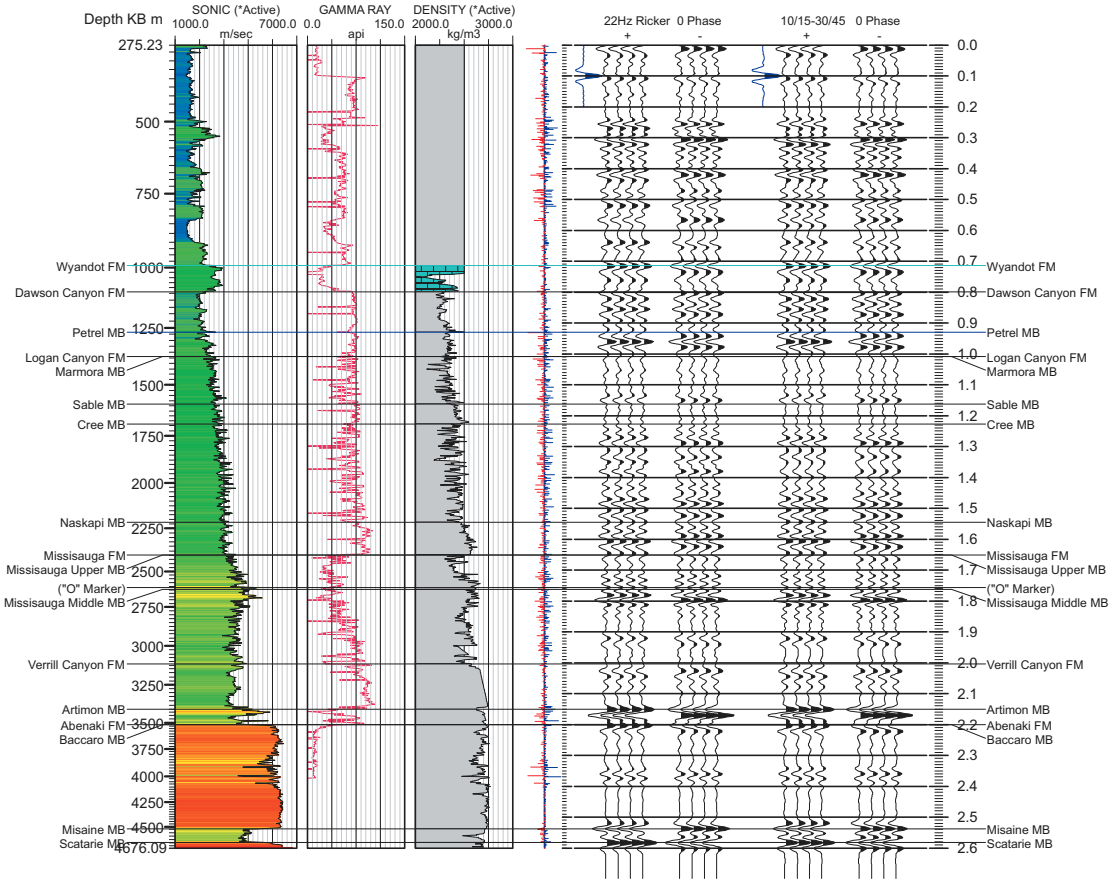

400/ 43.691° 060.832° /00

Tops	Depth KB m	Depth SS m	Time 2 way sec	Vav. m/sec	Vint. m/sec	Isochron sec	Isopach m
Kelly Bushing = 29.90 (m) above msl							
Tops Author: MacLean & Wade (1993)							
Top of Log	275.23	-245.33	0.00000	---	2004.4	0.71378	715.37
Wyandot FM	990.60	-960.70	0.71378	2004.4	3024.7	0.08503	128.60
Dawson Canyon FM	1119.20	-1089.30	0.79882	2113.0	2266.5	0.13130	148.80
Petrel MB	1268.00	-1238.10	0.93012	2134.7	2558.2	0.07810	99.90
Logan Canyon FM	1367.90	-1338.00	1.00822	2167.5	---	0.00000	0.00
Marmora MB	1367.90	-1338.00	1.00822	2167.5	2895.3	0.15418	223.20
Sable MB	1591.10	-1561.20	1.16240	2264.0	3071.5	0.06544	100.50
Cree MB	1691.60	-1661.70	1.22784	2307.1	3299.5	0.31817	524.90
Naskapi MB	2216.50	-2186.60	1.54601	2511.3	3444.6	0.10515	181.10
Missisauga FM	2397.60	-2367.70	1.65116	2570.8	---	-0.00000	0.00
Missisauga Upper MB	2397.60	-2367.70	1.65116	2570.8	3973.0	0.10491	208.40
("O" Marker)	2606.00	-2576.10	1.75607	2654.5	4879.4	0.00627	15.30
Missisauga Middle MB	2621.30	-2591.40	1.76234	2662.4	4096.4	0.24109	493.80
Verrill Canyon FM	3115.10	-3085.20	2.00343	2835.0	3885.1	0.14702	285.60
Artimon MB	3400.70	-3370.80	2.15046	2906.8	4506.1	0.05073	114.30
Abenaki FM	3515.00	-3485.10	2.20119	2943.7	---	0.00000	0.00
Baccaro MB	3515.00	-3485.10	2.20119	2943.7	5977.6	0.33733	1008.20
Misaine MB	4523.20	-4493.30	2.53852	3346.8	4455.0	0.04323	96.30
Scatarie MB	4619.50	-4589.60	2.58175	3365.4	5885.6	0.01928	56.74
Bottom of Log	4676.24	-4646.34	2.60103	3384.0			

Figure E.3 Synthetic seismogram for Demascota G-32 (indicated vertical scale not accurate).

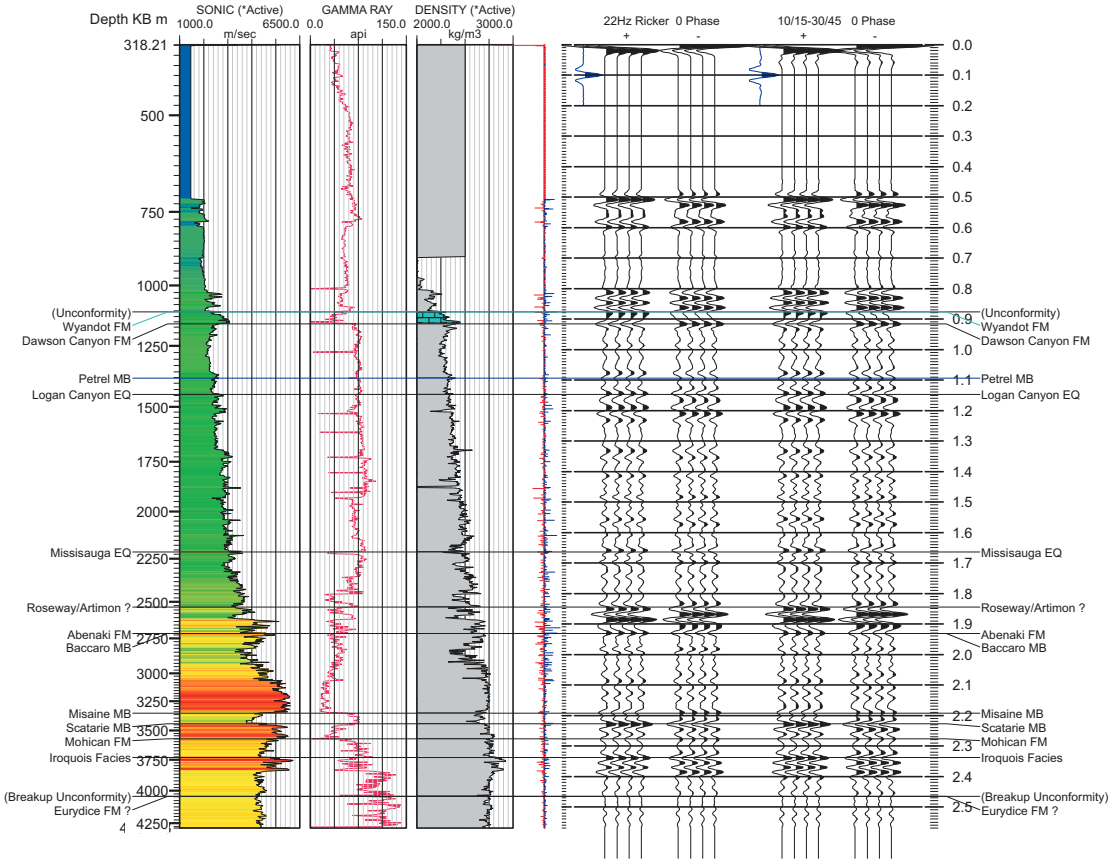

400/ 43.082° 062.279° /00

Tops	Depth KB m	Depth SS m	Time 2 way sec	Vav. m/sec	Vint. m/sec	Isochron sec	Isopach m
Kelly Bushing = 29.90 (m) above msl							
Tops Author: MacLean & Wade (1993)							
Top of Log	318.21	-288.31	0.00000	---	1790.9	0.87619	784.59
(Unconformity)	1102.80	-1072.90	0.87619	1790.9	---	0.00000	0.00
Wyandot FM	1102.80	-1072.90	0.87619	1790.9	2941.9	0.04018	59.10
Dawson Canyon FM	1161.90	-1132.00	0.91637	1841.4	2420.0	0.17785	215.20
Petrel MB	1377.10	-1347.20	1.09422	1935.4	2557.2	0.05240	67.00
Logan Canyon EQ	1444.10	-1414.20	1.14662	1963.8	2965.3	0.51685	766.30
Missisauga EQ	2210.40	-2180.50	1.66347	2275.0	3553.9	0.18183	323.10
Roseway/Artimon ?	2533.50	-2503.60	1.84529	2401.0	4154.0	0.08556	177.70
Abenaki FM	2711.20	-2681.30	1.93085	2478.7	---	0.00000	0.00
Baccaro MB	2711.20	-2681.30	1.93085	2478.7	4984.5	0.26233	653.80
Misaine MB	3365.00	-3335.10	2.19318	2778.4	4435.6	0.03422	75.90
Scatarie MB	3440.90	-3411.00	2.22741	2803.9	5526.5	0.04951	136.80
Mohican FM	3577.70	-3547.80	2.27691	2863.1	4916.4	0.06102	150.00
Iroquois Facies	3727.70	-3697.80	2.33793	2916.7	4974.5	0.12685	315.50
(Breakup Unconformity)	4043.20	-4013.30	2.46478	3022.6	---	0.00000	0.00
Eurydice FM ?	4043.20	-4013.30	2.46478	3022.6	4674.1	0.10654	248.99
Bottom of Log	4292.19	-4262.29	2.57132	3091.0			

Figure E.4 Synthetic seismogram for Mohedia P-15 (indicated vertical scale not accurate).

400/ 42.994° 062.481° /00

Geological Survey of Canada (Atlantic)
GeoSyn Software Ltd.

Mohican I-100
D074
Water Depth = 153.3 m
400/ 42.994° 062.481° /00

File location: C:\GeoSyn32\Target\s074.syn
KB elevation: 29.90 m . above msl
Depth range (KB): 363.02 to 4393.39 m
Time range: 0.0000 to 2.5100 secs
AGC length: 250 ms
Trace amplitude: 1.000

Sample rate: 2.00 ms
Trace/inch: 10.000
Vertical scale: 2.50 in/sec
* Density not used in RC calculation

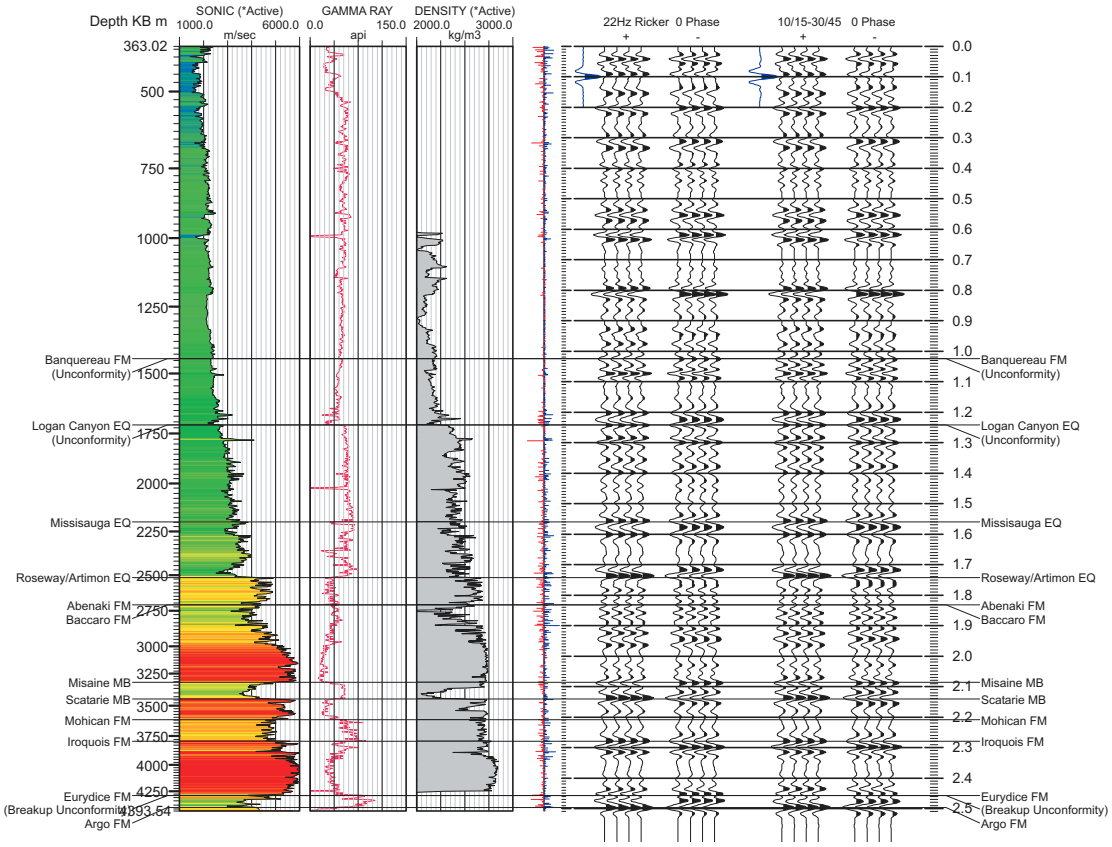

400/ 42.994° 062.481° /00

Tops	Depth KB m	Depth SS m	Time 2 way sec	Vav. m/sec	Vint. m/sec	Isochron sec	Isopach m
Kelly Bushing = 29.90 (m) above msl							
Tops Author: MacLean & Wade (1993)							
Top of Log	363.02	-333.12	0.00000	---	2106.9	1.02511	1079.88
Banquereau FM	1442.90	-1413.00	1.02511	2106.9	---	-0.00000	0.00
(Unconformity)	1442.90	-1413.00	1.02511	2106.9	2479.9	0.21686	268.90
Logan Canyon EQ	1711.80	-1681.90	1.24197	2172.0	---	-0.00000	0.00
(Unconformity)	1711.80	-1681.90	1.24197	2172.0	3063.2	0.31758	486.40
Missisauga EQ	2198.20	-2168.30	1.55955	2353.5	3442.9	0.18345	315.80
Roseway/Artimon EQ	2514.00	-2484.10	1.74300	2468.1	4424.5	0.08941	197.80
Abenaki FM	2711.80	-2681.90	1.83241	2563.6	---	0.00000	0.00
Baccaro FM	2711.80	-2681.90	1.83241	2563.6	4873.8	0.25303	616.60
Misaine MB	3328.40	-3298.50	2.08544	2843.9	4048.9	0.05572	112.80
Scatarie MB	3441.20	-3411.30	2.14116	2875.3	5367.0	0.06793	182.30
Mohican FM	3623.50	-3593.60	2.20909	2951.9	4695.7	0.06981	163.90
Iroquois FM	3787.40	-3757.50	2.27890	3005.3	5606.7	0.17811	499.30
Eurydice FM	4286.70	-4256.80	2.45701	3193.9	---	0.00000	0.00
(Breakup Unconformity)	4286.70	-4256.80	2.45701	3193.9	3939.2	0.03991	78.60
Argo FM	4365.30	-4335.40	2.49691	3205.8	4305.0	0.01305	28.09
Bottom of Log	4393.39	-4363.49	2.50996	3211.5			

Figure E.5 Synthetic seismogram for Mohican I-100 (indicated vertical scale not accurate).

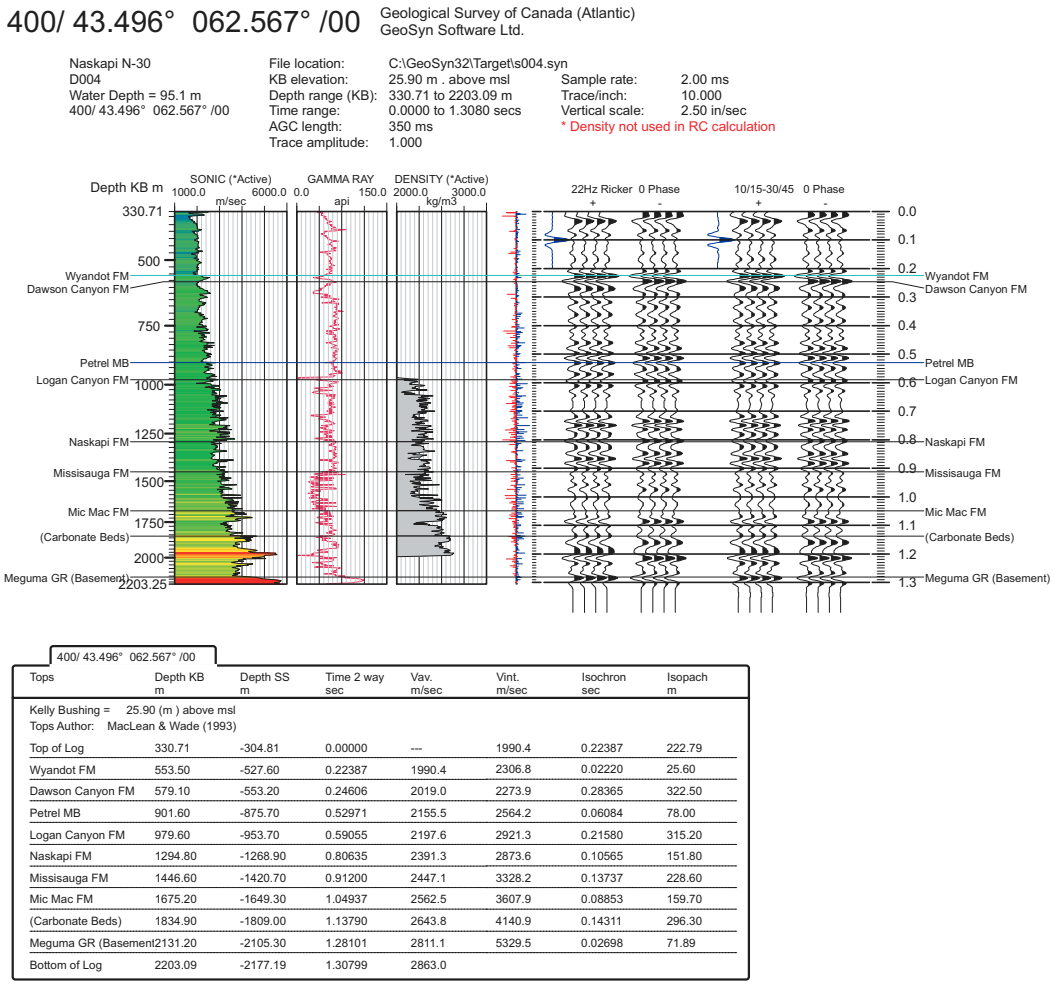

400/ 43.496° 062.567° /00

Tops	Depth KB m	Depth SS m	Time 2 way sec	Vav. m/sec	Vint. m/sec	Isochron sec	Isopach m
Kelly Bushing = 25.90 (m) above msl							
Tops Author: MacLean & Wade (1993)							
Top of Log	330.71	-304.81	0.00000	---	1990.4	0.22387	222.79
Wyandot FM	553.50	-527.60	0.22387	1990.4	2306.8	0.02220	25.60
Dawson Canyon FM	579.10	-553.20	0.24606	2019.0	2273.9	0.28365	322.50
Petrel MB	901.60	-875.70	0.52971	2155.5	2564.2	0.06084	78.00
Logan Canyon FM	979.60	-953.70	0.59055	2197.6	2921.3	0.21580	315.20
Naskapi FM	1294.80	-1268.90	0.80635	2391.3	2873.6	0.10565	151.80
Missisauga FM	1446.60	-1420.70	0.91200	2447.1	3328.2	0.13737	228.60
Mic Mac FM	1675.20	-1649.30	1.04937	2562.5	3607.9	0.08853	159.70
(Carbonate Beds)	1834.90	-1809.00	1.13790	2643.8	4140.9	0.14311	296.30
Meguma GR (Basement	2131.20	-2105.30	1.28101	2811.1	5329.5	0.02698	71.89
Bottom of Log	2203.09	-2177.19	1.30799	2863.0			

Figure E.6 Synthetic seismogram for Naskapi N-30 (indicated vertical scale not accurate).

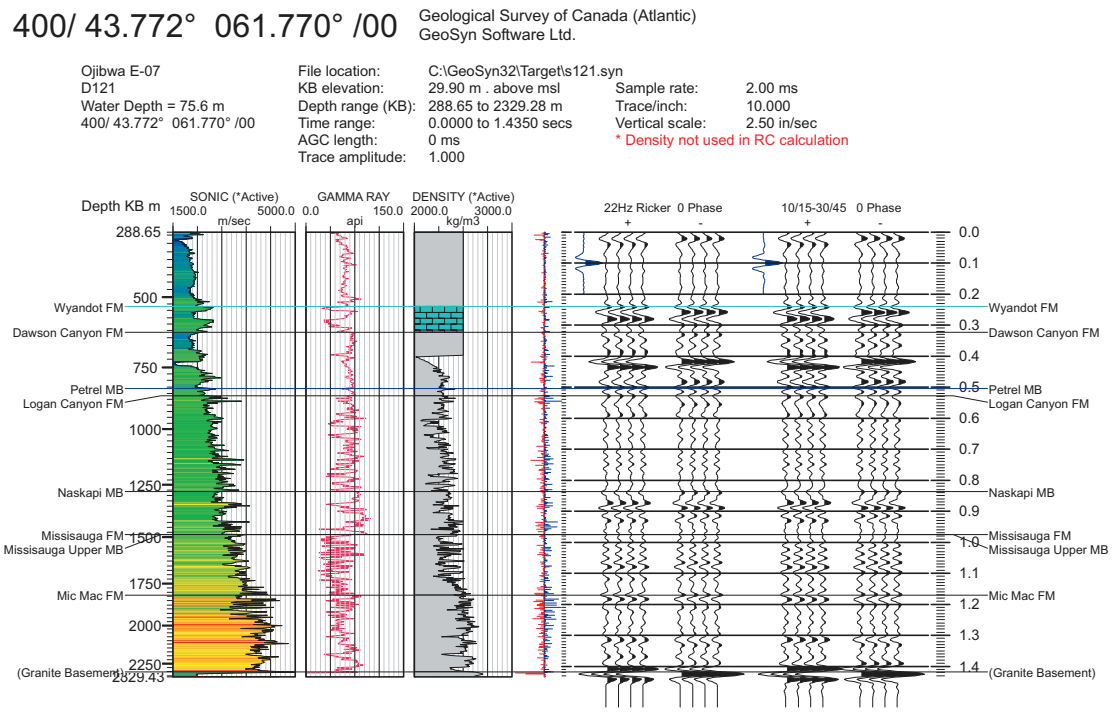

400/ 43.772° 061.770° /00

Tops	Depth KB m	Depth SS m	Time 2 way sec	Vav. m/sec	Vint. m/sec	Isochron sec	Isopach m
Kelly Bushing = 29.90 (m) above msl							
Tops Author: MacLean & Wade (1993)							
Top of Log	288.65	-258.75	0.00000	---	2041.6	0.24094	245.95
Wyandot FM	534.60	-504.70	0.24094	2041.6	2359.9	0.08212	96.90
Dawson Canyon FM	631.50	-601.60	0.32306	2122.5	2193.4	0.18237	200.00
Petrel MB	831.50	-801.60	0.50543	2148.1	2438.8	0.02345	28.60
Logan Canyon FM	860.10	-830.20	0.52889	2161.0	2742.6	0.30810	422.50
Naskapi MB	1282.60	-1252.70	0.83699	2375.1	2940.4	0.13889	204.20
Missisauga FM	1486.80	-1456.90	0.97588	2455.5	---	-0.00000	0.00
Missisauga Upper MB	1486.80	-1456.90	0.97588	2455.5	3406.5	0.19527	332.60
Mic Mac FM	1819.40	-1789.50	1.17115	2614.1	3919.8	0.24741	484.90
(Granite Basement)	2304.30	-2274.40	1.41856	2841.8	3066.2	0.01629	24.98
Bottom of Log	2329.28	-2299.38	1.43486	2844.4			

Figure E.7 Synthetic seismogram for Ojibwa E-07 (indicated vertical scale not accurate).

400/ 43.249° 061.560° /00 Geological Survey of Canada (Atlantic)
GeoSyn Software Ltd.

Oneida O-25
D003
Water Depth = 82.3 m
400/ 43.249° 061.560° /00

File location: C:\GeoSyn32\Target\s003.syn
KB elevation: 25.90 m . above msl
Depth range (KB): 221.28 to 4103.52 m
Time range: 0.0000 to 2.5230 secs
AGC length: 350 ms
Trace amplitude: 1.200

Sample rate: 2.00 ms
Trace/inch: 10.000
Vertical scale: 2.50 in/sec
* Density not used in RC calculation

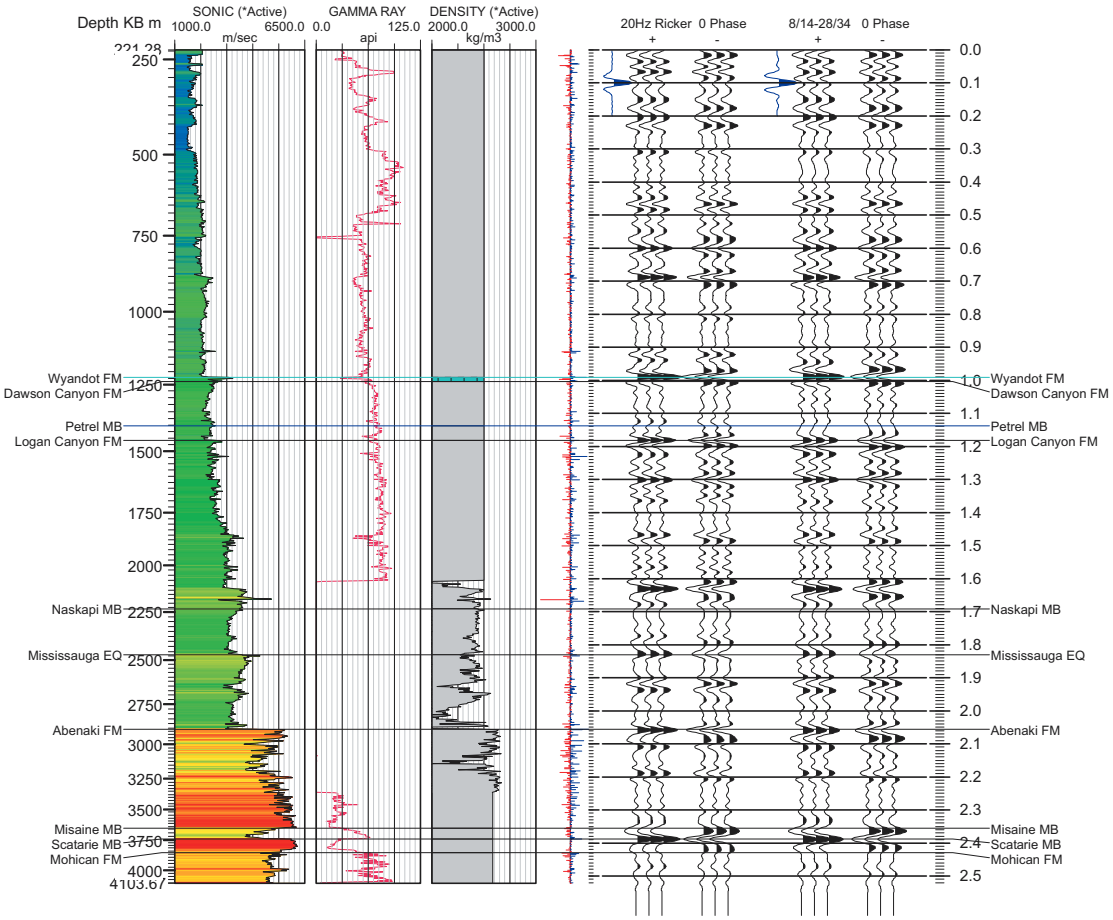

400/ 43.249° 061.560° /00

Tops	Depth KB m	Depth SS m	Time 2 way sec	Vav. m/sec	Vint. m/sec	Isochron sec	Isopach m
Kelly Bushing = 25.90 (m) above msl							
Tops Author: MacLean & Wade (1993)							
Top of Log	221.28	-195.38	0.00000	---	2012.6	0.99169	997.92
Wyandot FM	1219.20	-1193.30	0.99169	2012.6	2986.9	0.01286	19.20
Dawson Canyon FM	1238.40	-1212.50	1.00455	2025.0	2462.0	0.13395	164.90
Petrel MB	1403.30	-1377.40	1.13850	2076.4	2461.5	0.04412	54.30
Logan Canyon FM	1457.60	-1431.70	1.18262	2090.8	3045.3	0.50904	775.10
Naskapi MB	2232.70	-2206.80	1.69166	2378.0	3378.5	0.13983	236.20
Mississauga EQ	2468.90	-2443.00	1.83149	2454.4	3673.5	0.22502	413.30
Abenaki FM	2882.20	-2856.30	2.05650	2587.8	5247.6	0.29899	784.50
Misaine MB	3666.70	-3640.80	2.35550	2925.4	4623.1	0.03245	75.00
Scatarie MB	3741.70	-3715.80	2.38794	2948.5	5963.3	0.04132	123.20
Mohican FM	3864.90	-3839.00	2.42926	2999.8	5116.9	0.09327	238.62
Bottom of Log	4103.52	-4077.62	2.52253	3078.1			

Figure E.8 Synthetic seismogram for Oneida O-25 (indicated vertical scale not accurate).

Appendix F. Seismic Picks

The following tables contain the seismic times picked for the horizons in this study. Refer to the enclosed CD-ROM for the electronic files.

# Data file containing reflection (TWT) measurements							
# West of Sable Island, Scotian Shelf							
# Water depth measured in metres							
# Seismic reflectors measured in milliseconds							
# Measurements by Stephan Bigg, March 2002							
# Project 8624-P028-049E Line 3502-82P							
# Shot	**Water**	**Wyandot**	**Wyandot-1**	**Reflection A**	**Reflection B**	**Reflection C**	**Reflection D**
# Point	**Depth**						
1	40	765		650	606	315	278
50		760		623	595	320	280
100	40	750		612	572	332	283
150		732		595	555	328	280
200	40	720		590	543	312	272
250		710		572	520	300	269
300	40	700		563	505	310	265
350		683		542	480	320	260
400	40	661		515	450	314	270
450		642		496	455	312	265
500	40	620		475	450	313	270
550		610		463	439	310	270
600	42	601		450	415	300	275
650		602		447	415	320	295
700	45	598		448	418	322	300
750		590		455	418	328	300
800	50	596		480	410	335	312
850		570		455	398	319	304
900	50	552		430	395	325	298
950		545		430	372	330	302
1000	55	518		435	359	330	300
1050		520		465	355	330	310
1100	55	512		470	398	360	340
1150		490		470	360	332	300
1200	60	472		SP 1190=470	392	345	305
1250		478			400	365	340
1300	65	468			410	358	320
1350		470			410	342	328
1400	67	473			435	377	345
1450		405			SP 1440=420	365	342
1500	70	400				370	338
1550		385				SP 1540=385	340
1600	65	370					335
1650		338					SP 1640=338
1700	70	337					
1750		335					
1800	75	350					
1850		345					
1900	80	348					
1950		368					
2000	82	361					
2050		355					
2100	82	355					
2150		358					
2200	85	345					
2250		338					
2300	80	335					
# Line 3503-82P							
# Shot	**Water**	**Wyandot**	**Wyandot-1**	**Reflection A**	**Reflection B**	**Reflection C**	**Reflection D**
# Point	**Depth**						
1	52	1198			1075	395	241
50		1203			1075	404	248
100	52	1195			1070	400	245
150		1189			1075	403	253
200	52	1186			1091	403	255
250		1200			1085	410	255
300	55	1202			1078	405	260
350		1218			1097	395	260
400	54	1215			1095	395	259
450		1213			1090	400	254
500	56	1205			1088	408	255
550		1200			1100	415	255
600	57	1198			1092	410	255
650		1182			1088	406	255

700	57	1185			1080	418	260
750		1180			1065	430	268
800	59	1150			1053	438	277
850		1140			1044	445	295
900	60	1134			1025	453	297
950		1115			1015	478	303
1000	62	1168			1022	482	305
1050		1148			1005	490	310
1100	62	1128			1000	480	312
1150		1125			1014	485	325
1200	62	1123			1015	489	327
# Line 3504-82P							
# Shot	**Water**	**Wyandot**	**Wyandot-1**	**Reflection A**	**Reflection B**	**Reflection C**	**Reflection D**
# Point	**Depth**						
1	100	492					343
50		490					340
100	95	490					342
150		482					340
200	90	488					348
250		475				SP 250=330	330
300	80	458				350	322
350		455				364	325
400	75	438				360	315
450		420				365	308
500	70	428			SP 520=430	350	300
550		449			414	370	311
600	70	448			410	375	310
# Line 3504-82A							
# Shot	**Water**	**Wyandot**	**Wyandot-1**	**Reflection A**	**Reflection B**	**Reflection C**	**Reflection D**
# Point	**Depth**						
1550	74	447			410	352	305
1600	72	453			412	380	296
1650		461			400	376	300
1700	71	488		SP 1710=485	409	380	310
1750		510		450	409	372	315
1800	67	530		435	405	365	303
1850		540		422	400	368	292
1900	63	522		428	400	359	280
1950		538		420	397	372	278
2000	59	555		422	398	358	275
2050		560		428	400	364	278
2100	61	578		435	407	371	285
2150		591		458	422	380	305
2200	54	595		459	422	380	318
2250		610		464	438	365	305
2300	52	628		455	435	365	305
2350		640		470	435	360	302
2400	52	625		465	431	360	297
2450		635		495	460	362	308
2500	51	653		503	468	383	310
2550		678		540	490	403	320
2600	50	690		565	510	420	335
2650		695		570	520	405	332
2700	48	710		580	530	385	320
2750		718		577	515	369	305
2800	45	725		580	538	352	290
2850		735		576	539	315	280
2900	44	752		600	555	315	278
2950		765		610	560	315	275
3000	41	780		613	565	312	260
3050		788		604	568	300	260
# Line 3505-82P							
# Shot	**Water**	**Wyandot**	**Wyandot-1**	**Reflection A**	**Reflection B**	**Reflection C**	**Reflection D**
# Point	**Depth**						
1900							
1950							
2000							
2050							
2100							
2150							
2200							

2250		1094	1043		960	518	440
2300	105	1090	1033		955	502	430
2350		1080	1025		945	478	420
2400	105	1072	1017		945	473	410
2450		1070	1010		937	460	405
2500	100	1071	1010		935	451	400
2550		1070	1005		926	454	405
2600	100	1070	1005		935	448	401
2650		1061	1000		933	447	403
2700	100	1060	1002		935	440	405
2750		1070	1000		935	439	402
2800	100	1071	1000		936	440	402
2850		1058	993		928	432	405
2900	100	1050	989		918	431	400
2950		1059	992		930	432	400
3000	100	1050	981		920	426	405
3050		1040	967		915	432	405
3100	100	1032	970		915	427	405
3150		1022	956		895	442	405
3200	100	1030	954		880	433	400
3250		1030	955		873	432	400
3300	100	1031	955		860	435	405
3350		1030	951		852	447	405
3400	100	1025	950		860	437	407
3450		1022	945		867	432	413
3500	100	1018	943		853	428	410
3550		1020	944		852	426	406
3600	100	1011	939		847	426	410
3650		1012	934		825	425	410
3700	100	1010	930		825	427	400
3750		1010	928		833	423	400
3800	100	1010	932		822	416	395
3850		1001	928		820	416	395
3900	100	1000	920		813	412	390
3950		997	915		805	406	380
4000	95	991	912		805	405	381
4050		990	912		800	408	383
4100	95	990	905		796	406	381
4150		982	900		797	410	385
4200	95	988	903		795	410	386
4250		979	902		795	408	382
4300	90	973	898		792	405	382
4350		970	893		793	403	375
4400	90	970	891		795	405	375
4450		975	900		798	402	380
4500	90	975	903		795	407	380
4550		982	910		795	410	380
4600	90	975	905		795	410	378
4650		978	910		792	397	367
4700	90	982	912		793	380	366
4750		975	900		783	376	360
4800	85	977	900		770	373	350
4850		978	888		770	370	346
4900	85	980	895		775	369	343
4950		982	902	SP 4965=902	775	368	341
5000	80	988	912	885	772	365	340
5050		990	915	870	772	368	342
5100	80	990	920	867	769	372	348
5150		986	928	865	762	375	342
5200	80	988	930	865	759	380	352
5250		985	935	855	748	385	355
5300	80	990	938	850	740	375	350
5350		1005	941	835	732	380	350
5400	80	1000	940	830	735	378	345
5450		1000	950	830	730	382	350
5500	75	1002	955	825	725	380	350
5550		1005	970	820	727	378	347
5600	75	1010	978	822	712	383	350
5650		1005	986	820	705	382	345
5700	75	1002	980	808	694	378	345
5750		1000	982	800	692	383	345
5800	70	998	979	783	690	372	342
5850		980	SP 5830=983	780	688	374	340
5900	70	980		773	682	370	338

5950		982		766	683	370	330
6000	65	982		760	684	371	340
6050		980		750	675	370	332
6100	65	977		742	670	368	330
6150		975		735	662	362	330
6200	60	972		730	660	365	322
6250		970		725	653	360	315
6300	60	960		710	642	358	310
6350		952		700	638	365	317
6400	55	950		702	637	358	312
6450		950		695	630	359	315
6500	55	950		690	635	355	305
6550		948		690	635	355	300
6600	50	948		685	622	352	300
6650		950		685	620	359	301
6700	55	950		685	630	355	310
6750		940		688	625	348	300
6800	55	938		688	625	352	300
6850		932		690	621	350	302
6900	50	925		663	614	349	294
6950		923		657	612	348	290
7000	50	924		660	603	341	292
7050		921		655	595	345	290
7100	50	920		657	596	351	292
7150		915		652	595	350	295
7200	50	907		650	598	354	298
7250		900		645	590	355	308
7300	50	890		648	595	375	310
7350		885		641	590	378	320
7400	50	875		630	585	360	305
7450		867		625	590	360	300
7500	50	855		622	585	362	300
7550		842		619	580	368	305
7600	55	835		620	577	355	310
7650		830		630	566	365	310
7700	55	822		640	565	365	308
7750		820		639	569	345	300
7800	55	820		632	570	370	310
7850		810		630	570	372	310
7900	55	803		625	570	370	308
7950		800		622	567	368	310
8000	55	795		618	565	367	310
8050		791		600	563	363	306
8100	50	790		598	564	366	300
8150		785		592	564	365	305
8200	50	778		595	565	366	301
8250		788		600	570	375	310
8300	50	775		600	575	375	308
8350		763		585	568	365	308
8400	50	760		590	560	360	290
8450		762		590	558	368	320
8500	45	755		580	552	355	290
8550		750		585	556	363	315
8600	45	738		582	548	355	280
8650		730		578	540	350	290
8700	45	727		575	543	342	283
8750		722		566	536	342	280
8800	40	720		572	530	330	287
8850		728		578	550	325	270
8900	40	738		597	560	312	278
8950		740		600	558	305	270
9000	35	752		605	555	300	275
9050		738		603	560	290	260
9100	35	730		595	558	288	252
9150		740		613	580	300	265
9200	35	740		610	575	283	250
9250		730		605	573	290	245
9300	30	732		612	575	275	240
9350		726		610	587	270	230
9400	25	720		605	588	265	230
9450		712		603	580	255	227
9500	30	710		602	570	260	230
9550		710		605	575	255	230
9600	30	715		610	582	255	230

9650		720		620	591	282	255
9700	40	725		635	600	286	260
9750		730		650	607	295	262
9800	40	730		658	613	290	270
9850		730		660	626	292	245
9900	45	736		680	642	295	265
9950		740		685	650	299	260
10000	50	738		695	660	302	265
10050		735		705	672	300	265
# Line 3506-82P							
# Shot	**Water**	**Wyandot**	**Wyandot-1**	**Reflection A**	**Reflection B**	**Reflection C**	**Reflection D**
# Point	**Depth**						
1	65	1335			1284	558	339
50		1320			1256	554	337
100	65	1270			1230	564	340
150		1251			1152	540	322
200	70	1225			1102	513	313
250		1178			1047	480	302
300	60	1129			1002	460	300
350		1095			961	450	283
400	65	1070			920	458	280
450		1050			881	423	275
500	60	1025		SP 500=1025	842	390	253
550		1010		953	810	368	240
600	55	997		930	795	388	248
650		998		900	769	368	235
700	45	978		864	760	362	240
750		974		845	745	350	245
800	45	968		835	745	355	262
850		964		815	735	358	270
900	40	954		798	714	360	265
950		940		775	700	345	262
1000	45	930		750	680	343	273
1050		915		735	675	333	283
1100	45	902		714	662	342	280
1150		890		702	644	338	287
1200	45	887		688	645	351	292
1250		880		675	640	355	297
1300	45	862		665	624	350	290
1350		845		646	610	350	292
1400	45	836		617	595	353	284
1450		820		625	585	342	280
1500	50	800		607	572	345	278
1550		803		620	595	382	310
1600	50	770		590	551	355	290
1650		758		593	552	353	283
1700	50	753		585	547	353	245
1750		732		570	537	358	288
1800	50	720		565	530	349	290
1850		708		555	522	353	300
1900	55	700		552	510	352	290
1950		690		545	505	357	295
2000	55	670		525	490	352	298
2050		658		520	475	355	303
2100	60	655		513	462	348	300
2150		643		510	460	335	302
2200	60	630		490	437	360	302
2250		620		475	433	365	302
2300	60	614		485	440	365	300
2350		600		490	450	378	320
2400	65	589		498	459	391	318
2450		581		500	453	380	320
2500	65	568		500	440	371	315
2550		553		495	473	362	303
2600	70	547		510	475	370	330
2650		550		SP 2620=540	495	365	336
2700	75	539			SP 2690=535	372	342
2750		513				375	345
2800	80	492				SP 2790=370	372
2850		480					378
2900	95	502					392
2950		512					408
3000	105	530					420

3050		515					425
3100	110	512					438
3150		545					475
3200	115	530					472
3250		522					470
3300	120	508					468
3350		492					SP 3335=490
3400	125	488					
3450		472					
3500	135	480					
3550		495					
3600	190	520					
# Line 3507-82P							
# Shot	**Water**	**Wyandot**	**Wyandot-1**	**Reflection A**	**Reflection B**	**Reflection C**	**Reflection D**
# Point	**Depth**						
2250							
2300	135						
2350							
2400	130						
2450							
2500	140						
2550							
2600	145						
2650							
2700	150						
2750							
2800	145						
2850							
2900	130						
2950							
3000	130						
3050							
3100	120	820	795				385
3150		818	805				390
3200	120	828	803				395
3250		833	805				413
3300	110	835	805				405
3350		837	798				392
3400	105	832	803				367
3450		834	808				376
3500	105	833	803				373
3550		834	808				374
3600	105	836	806				372
3650		830	800				368
3700	100	825	790				355
3750		820	795				358
3800	100	815	786				369
3850		810	780				367
3900	105	810	778				367
3950		805	773				369
4000	100	797	759				370
4050		795	763				367
4100	100	792	754				370
4150		795	753				368
4200	100	783	745				363
4250		754	722				368
4300	100	745	716				365
4350		733	695				373
4400	100	734	702				368
4450		733	693				379
4500	100	725	692				375
4550		720	685				375
4600	100	705	665				370
4650		697	651				357
4700	100	679	642				355
4750		672	632				355
4800	100	668	630				340
4850		669	635				345
4900	100	656	621				335
4950		670	620				338
5000	95	663	620				323
5050		648	608				305
5100	90	649	605				303

5150		650	605				305
5200	85	648	595				295
5250		640	595				285
5300	80	628	590				285
5350		619	592				295
5400	80	615	575				275
5450		614	570				280
5500	80	612	555				285
# Line 3508-82P							
# Shot	**Water**	**Wyandot**	**Wyandot-1**	**Reflection A**	**Reflection B**	**Reflection C**	**Reflection D**
# Point	**Depth**						
1	65	1309			1240	590	325
50		1290			1200	570	330
100	70	1238			1155	550	333
150		1184			1115	522	335
200	70	1155			1070	523	330
250		1123			1032	500	320
300	65	1100			999	480	315
350		1080		SP 380=1060	958	490	318
400	65	1068		1040	926	488	320
450		1058		1020	908	510	330
500	60	1042		992	912	495	328
550		1021		960	885	475	325
600	60	1014		938	870	492	325
650		1000		910	838	483	320
700	60	990		848	813	487	330
750		990		890	800	462	318
800	45	980		873	785	460	316
850		970		855	782	458	310
900	45	960		830	762	463	310
950		952		825	759	460	315
1000	50	932		805	750	450	310
1050		922		803	722	435	308
1100	50	920		798	720	438	312
1150		908		780	695	424	303
1200	45	904		770	680	412	305
1250		890		758	664	400	302
1300	50	881		738	646	393	308
1350		872		724	636	390	315
1400	50	860		710	619	400	315
1450		851		690	610	397	320
1500	55	842		668	600	405	323
1550		828		663	588	395	323
1600	55	817		645	573	380	316
1650		798		630	552	390	320
1700	55	783		605	543	380	320
1750		760		582	542	378	305
1800	55	750		575	538	395	315
# Line 3508-82A							
# Shot	**Water**	**Wyandot**	**Wyandot-1**	**Reflection A**	**Reflection B**	**Reflection C**	**Reflection D**
# Point	**Depth**						
2762	55	760		580	542	382	312
2800	55	754		575	542	392	315
2850		744		570	540	390	312
2900	55	730		563	533	372	312
2950		719		570	518	380	318
3000	55	710		548	513	378	316
3050		694		543	512	372	312
3100	55	684		530	510	350	310
3150		668		520	503	350	310
3200	60	655		540	511	349	316
3250		650		545	515	358	315
3300	60	633		537	512	342	315
3350		635		542	520	352	322
3400	65	614		540	517	350	322
3450		604		560	527	350	318
3500	70	600		580	535	352	320
3550		598		SP 3550=598	535	358	323
3600	75	596			540	358	335
3650		595			570	375	332
3700	100	590			SP 3660=590	403	370
3750		590				412	375

3800	115	552				388	350
# Line 3510-82P							
# Shot	**Water**	**Wyandot**	**Wyandot-1**	**Reflection A**	**Reflection B**	**Reflection C**	**Reflection D**
# Point	**Depth**						
1	130	370					
50		430					SP 75=452
100	150	469					430
150		482					453
200	145	442					390
250		415					346
300	145	468					439
350		500					440
400	135	510					423
450		518					435
500	140	490					440
550		473					410
600	115	530					446
650		534					435
700	105	552			SP 745=580		435
750		590			577		420
800	95	612			550		423
850		640			540		405
900	80	620		SP 900=620	520		345
950		620		570	498		338
1000	65	638		562	490		338
1050		653		560	487		339
1100	60	663		551	482	SP 1100=335	335
1150		662		545	468	345	322
1200	60	670		540	460	370	339
1250		683		535	465	342	305
1300	55	699		530	470	371	305
1350		700		535	468	365	308
1400	50	718		543	459	362	300
1450		726		554	455	356	302
1500	45	735		561	485	352	305
1550		751		576	495	355	310
1600	45	765		580	485	348	295
1650		782		580	493	340	300
1700	45	805		595	515	350	302
1750		834		613	545	365	305
1800	50	847		630	559	377	300
1850		860		639	570	380	293
1900	50	874		637	580	362	302
1950		888		645	585	375	305
2000	50	898		644	598	384	288
2050		910		662	600	393	298
2100	50	913		668	605	400	295
2150		918		683	620	304	300
2200	50	928		690	623	407	293
2250		935		720	625	410	300
2300	50	940		722	642	415	297
2350		948		732	650	418	298
2400	50	948		736	652	413	299
2450		956		748	655	417	292
2500	45	967		755	662	417	285
2550		975		763	668	421	295
2600	50	988		773	663	425	303
2650		995		790	675	430	305
2700	60	1010		790	688	440	308
2750		1013		800	690	445	310
2800	65	1020		822	692	455	305
2850		1042		840	700	450	315
2900	60	1044		865	708	450	320
2950		1074		896	728	460	320
3000	65	1090		915	763	460	325
3050		1072		915	798	471	330
3100	65	1086		951	820	492	338
3150		1098		988	844	500	338
3200	70	1112		1028	875	525	340
3250		1130		1060	898	512	332
3300	70	1145		1095	910	523	333
3350		1160		1130	935	535	335
3400	70	1183		1148	968	555	347

3450		1200		SP 3440=1190	998	580	362
3500	70	1210			1020	605	383
# Line 3512-82P							
# Shot	**Water**	**Wyandot**	**Wyandot-1**	**Reflection A**	**Reflection B**	**Reflection C**	**Reflection D**
# Point	**Depth**						
1	55	637		470	430		299
50		650		468	430		298
100	50	660		485	432		295
150		669		475	430		295
200	50	678		470	428		300
250		679		475	425		295
300	50	686		472	434		295
350		702		482	446		300
400	50	720		503	462	SP 405=293	290
450		730		521	490	300	276
500	45	748		525	490	295	275
550		763		532	496	290	280
600	40	773		538	490	295	260
650		792		540	495	298	263
700	45	804		545	513	299	262
750		809		555	520	298	270
800	45	834		580	540	312	268
850		865		605	560	334	265
900	45	880		620	572	338	266
950		900		638	590	350	296
1000	45	914		652	595	347	292
1050		930		665	595	334	292
1100	50	940		680	615	358	300
1150		952		700	643	365	300
1200	50	970		730	662	365	320
1250		972		738	674	378	325
1300	50	982		747	684	395	343
1350		988		755	696	420	331
1400	50	996		770	703	435	342
1450		1000		780	705	435	342
1500	50	1008		795	710	432	339
1550		1010		803	725	423	340
1600	55	1015		816	744	423	340
1650		1018		832	758	425	340
1700	60	1030		850	760	435	356
1750		1030		860	770	439	362
1800	65	1037		865	780	443	368
1850		1040		875	790	454	378
1900	70	1050		879	800	460	374
1950		1057		891	813	475	380
2000	70	1063		900	810	483	380
2050		1072		918	820	512	390
2100	70	1080		930	832	510	392
2150		1090		960	853	531	380
2200	75	1110		995	882	560	395
2250		1120		1022	905	570	400
2300	70	1130		1055	920	582	400
2350		1140		1082	940	608	395
2400	70	1143		1115	951	610	400
2450		1160		1148	995	638	405
2500	75	1174		SP 2460=1155	1023	663	400
2550		1189			1055	680	400
2600	80	1220			1105	692	410
# Line 3514-82P							
# Shot	**Water**	**Wyandot**	**Wyandot-1**	**Reflection A**	**Reflection B**	**Reflection C**	**Reflection D**
# Point	**Depth**						
1	80	1222			1125	677	444
50		1196			1083	640	400
100	75	1180		SP 120=1165	1044	598	393
150		1170		1145	1005	574	380
200	70	1150		1110	968	557	380
250		1140		1082	930	539	363
300	70	1130		1072	923	520	365
350		1125		1052	905	517	360
400	70	1121		1026	895	508	368
450		1110		1003	866	495	364
500	70	1100		972	853	477	366

550		1094		948	838	462	365
600	75	1097		926	833	478	364
650		1090		914	825	486	370
700	70	1090		905	810	480	370
750		1083		884	810	470	345
800	65	1079		870	795	453	325
850		1070		855	782	435	315
900	60	1059		840	770	422	320
950		1055		830	760	420	320
1000	60	1050		826	735	412	320
1050		1042		820	730	405	322
1100	60	1030		805	725	405	320
1150		1018		805	727	403	315
1200	60	1010		797	732	405	341
1250		1000		798	731	392	345
1300	60	995		774	720	398	355
1350		980		750	700	400	343
1400	50	968		734	672	385	325
1450		954		720	650	362	303
1500	50	950		707	633	355	288
1550		935		690	628	355	292
1600	50	928		650	600	335	287
1650		900		650	583	345	282
1700	50	878		638	568	342	285
1750		855		610	545	338	282
1800	55	850		592	515	332	282
1850		832		560	498	309	275
1900	50	812		549	502	300	275
1950		803		533	495	295	262
2000	50	795		515	480	290	260
2050		779		500	465	280	256
2100	50	758		495	451	SP 2090=280	280
2150		752		490	446		291
2200	50	738		473	430		295
2250		719		465	421		320
2300	50	712		465	408		322
2350		701		468	410		340
2400	50	690		449	405		353
2450		676		445	420		360
2500	50	653		445	418		358
2550		636		438	408		340
2600	50	625		448	420		350
2650		610		443	418		352
2700	50	605		440	410		353
2750		603		440	410		364
2800	55	575		446	415		380
2850		550		465	432		398
2900	65	535		480	445		403
# Line 3516-82P							
# Shot	**Water**	**Wyandot**	**Wyandot-1**	**Reflection A**	**Reflection B**	**Reflection C**	**Reflection D**
# Point	**Depth**						
1	155	485	450				
50		480	448				
100	145	470	433				
150		455	415				
200	140	450	410				
250		440	400				SP 280=380
300	120	430	410				382
350		435	412				373
400	90	451	408				360
450		469	442				360
500	85	475	440				350
550		487	443		SP 560=440		348
600	80	480	452		425		340
650		493	450		420		350
700	75	493	460		418		330
750		505	477		415		316
800	70	528	502	SP 830=502	405		312
850		550	522	498	395		295
900	60	582	555	490	395		300
950		605	573	485	387		303
1000	55	621	589	480	385		302
1050		648	612	465	402		302

# Line 3516-82A							
# Shot	**Water**	**Wyandot**	**Wyandot-1**	**Reflection A**	**Reflection B**	**Reflection C**	**Reflection D**
# Point	**Depth**						
2021	55	630	598	446	396		310
2050		648	612	443	402		305
2100	55	683	650	462	412		298
2150		705	673	478	427		300
2200	55	730	700	495	445		298
2250		745	718	514	463		295
2300	55	745	723	520	458		289
2350		750	730	525	448		292
2400	55	762	740	525	465	SP 2420=300	291
2450		770	752	535	472	311	300
2500	55	790	765	555	489	320	290
2550		800	779	560	501	322	292
2600	55	790	SP 2560=795	553	498	318	290
2650		800		553	492	325	302
2700	50	806		558	510	330	298
2750		818		563	515	322	290
2800	55	828		580	520	324	282
2850		845		600	538	325	291
2900	50	865		605	558	328	302
2950		882		625	578	333	300
3000	50	895		640	590	344	310
3050		905		656	600	341	320
3100	55	922		657	613	350	310
3150		938		682	622	350	305
3200	55	945		695	640	350	300
3250		970		705	655	351	306
3300	50	977		726	668	355	300
3350		1000		740	685	350	293
3400	55	1010		770	695	348	302
3450		1016		792	705	362	300
# Line 3516-82B							
# Shot	**Water**	**Wyandot**	**Wyandot-1**	**Reflection A**	**Reflection B**	**Reflection C**	**Reflection D**
# Point	**Depth**						
4411	50	1010		792	710	345	310
4450		1015		790	722	348	298
4500	60	1024		795	730	350	315
4550		1038		810	725	352	292
4600	55	1046		820	734	380	308
4650		1050		833	745	375	302
4700	65	1065		860	747	390	310
4750		1075		890	772	398	318
4800	70	1084		905	785	418	325
4850		1089		912	792	430	328
4900	75	1100		920	803	443	342
4950		1110		942	816	456	355
5000	80	1105		941	820	472	353
5050		1110		930	828	495	363
5100	75	1112		942	836	493	351
5150		1120		968	855	505	354
5200	75	1129		994	865	530	363
5250		1130		1020	885	540	355
5300	75	1132		1019	903	553	354
5350		1140		1037	932	563	355
5400	75	1150		1064	958	578	353
5450		1160		1083	960	588	356
5500	75	1162		1105	988	592	358
5550		1180		1130	1015	605	360
5600	70	1186		1160	1068	631	368
5650		1200		SP 5610=1180	1105	652	380
5700	80	1222			1145	685	395
5750		1235			1189	705	410
5800	90	1280			1240	757	427
5850		1315			1288	820	438
5900	110	1365			1341	959	475
5950		1422			1400	1059	530
6000	130	1480			SP 5960=1425	1165	572
6050		1563				1245	640
6100	175	1670					
6150		1832					

6200	290	1938					
6250		2070					
6300	620						
6350							
6400	920						
6450							
6500	990						
6550							
6600	1260						
# Line 3518-82P							
# Shot	**Water**	**Wyandot**	**Wyandot-1**	**Reflection A**	**Reflection B**	**Reflection C**	**Reflection D**
# Point	**Depth**						
1	70	605	562				330
50		626	591	SP 95=590			336
100	70	640	605	580			333
150		657	623	590	SP 190=600		330
200	80	680	648	610	600		335
250		692	663	595	568		332
300	65	710	681	585	560		332
350		720	693	573	540		331
400	65	738	714	570	545	SP 410=335	332
450		755	730	570	537	352	335
500	65	771	746	573	532	360	330
550		782	760	585	532	362	325
600	65	795	775	593	535	360	325
650		792	798	605	543	357	325
700	60	800	SP 660=795	605	535	355	320
750		807		603	532	346	315
800	60	820		620	547	352	326
850		830		630	554	352	320
900	65	855		655	570	358	330
950		880		674	582	360	320
1000	60	899		685	598	353	315
1050		913		695	624	349	315
1100	65	925		710	635	360	320
1150		938		722	645	340	310
1200	60	955		730	648	345	312
1250		972		742	666	352	320
1300	65	990		760	680	351	318
1350		993		765	695	349	315
1400	65	1001		773	700	348	320
1450		1019		782	710	356	322
1500	60	1024		793	711	350	323
1550		1039		809	740	347	323
1600	65	1052		828	760	355	315
1650		1070		853	769	357	325
1700	75	1080		875	777	370	340
1750		1092		886	779	370	333
1800	75	1102		900	800	375	340
1850		1112		932	810	375	335
1900	75	1121		932	818	373	338
1950		1130		935	830	388	358
2000	80	1134		940	835	402	353
# Line 3518-82A							
# Shot	**Water**	**Wyandot**	**Wyandot-1**	**Reflection A**	**Reflection B**	**Reflection C**	**Reflection D**
# Point	**Depth**						
2981	80	1132		932	840	400	362
3000	80	1137		947	845	410	361
3050		1131		962	850	430	370
3100	80	1140		970	862	445	367
3150		1146		988	872	462	370
3200	80	1150		1000	880	478	371
3250		1165		1020	900	490	365
3300	80	1170		1044	925	497	372
3350		1177		1070	945	519	370
3400	80	1177		1095	971	537	362
3450		1180		1112	995	562	359
3500	80	1188		1134	1032	580	365
3550		1200		1160	1075	620	353
3600	80	1211		1185	1103	650	350
3650		1220		SP 3630=1202	1140	680	340
3700	80	1230			1175	705	333

3750		1252			1210	730	342
3770		1270			1240	761	350
# Line 3520-82P							
# Shot	**Water**	**Wyandot**	**Wyandot-1**	**Reflection A**	**Reflection B**	**Reflection C**	**Reflection D**
# Point	**Depth**						
1	85	1300			1267	830	398
50		1270			1222	778	378
100	95	1251			1190	735	378
150		1225			1150	702	368
200	85	1220		SP 205=1215	1125	670	362
250		1220		1178	1095	650	362
300	85	1220		1155	1064	625	362
350		1218		1135	1035	592	373
400	85	1208		1120	1000	580	370
450							
# Line 3520-82A							
# Shot	**Water**	**Wyandot**	**Wyandot-1**	**Reflection A**	**Reflection B**	**Reflection C**	**Reflection D**
# Point	**Depth**						
1	1510						
50							
100	1330						
150							
200	1180						
250							
300	950						
350							
400	775						
450							
500	720						
550							
600	465						
650							
700	190	1880				1658	580
750		1680				1450	438
800	105	1590				1332	410
850		1538				1270	390
900	95	1490				1200	385
950		1435				1095	388
1000	85	1365			SP 1000=1365	975	368
1050		1338			1310	880	360
1100	80	1300			1262	822	355
1150		1277			1222	773	355
1200	80	1260			1186	735	358
1250		1222			1150	700	355
1300	80	1218			1122	668	360
1350		1218			1090	645	358
1400	80	1219			1065	619	351
1450		1210			1025	592	350
# Line 3520-82B							
# Shot	**Water**	**Wyandot**	**Wyandot-1**	**Reflection A**	**Reflection B**	**Reflection C**	**Reflection D**
# Point	**Depth**						
1400		1202		1119	980	578	368
1450		1192		1085	936	555	375
1500	80	1185		1040	915	532	363
1550		1182		1025	902	520	363
1600	85	1170		1015	900	511	372
1650		1160		1000	875	496	354
1700	80	1150		970	866	484	370
1750		1142		955	850	470	360
1800	80	1131		930	845	460	365
1850		1128		916	830	448	368
1900	80	1122		915	825	452	365
1950		1110		905	820	450	375
2000	85	1100		902	810	444	378
2050		1080		890	795	430	362
2100	70	1075		872	787	425	342
2150		1060		878	765	418	345
2200	75	1052		862	768	418	345
2250		1042		855	758	410	360
2300	75	1033		855	748	398	364
2350		1017		840	730	395	363

2400	80	1010	SP 2430=1000	832	722	386	358
2450		1005	990	828	715	380	352
2500	80	1018	990	826	708	380	348
2550		1000	965	810	693	393	358
2600	80	970	930	785	692	395	355
2650		940	918	785	690	382	350
2700	80	920	892	780	682	380	353
2750		908	878	765	685	375	354
2800	75	890	858	739	672	375	352
2850		875	842	730	665	360	356
2900	75	852	820	710	642	SP 2860=355	350
2950		843	798	705	645		360
3000	75	832	783	700	633		350
3050		818	770	690	630		355
3100	75	803	750	678	610		350
3150		790	737	685	585		360
3200	75	778	720	690	575		353
3250		758	700	676	575		348
3300	75	740	680	SP 3300=680	575		360
3350		725	660		560		345
3400	80	708	640		550		338
3450		690	625		542		358
3500	70	664	595		530		330
3550		640	555		530		335
3600	75	618	545		SP 3580=542		333
3650		647	570				368
3700	75	665	580				375
3750		660	565				362
3800	80	640	552				365
3850		618	520				385
3900	80	583	490				392
3950		548	448				400
4000	90	522	434				402
4050		533	438				406
4100	95	582	510				475
4150		600	530				502
4200	135	600	536				505
4250		585	515				SP 4250=515
4300	140	570	495				
4350		495	385				
4400	145	472	370				
4450		465	362				
4500	95	457	352				
4550		465	354				
4600	95	490	370				
4650		525	430				
4700	100	538	442				
4750		510	430				
4800	140	535	435				
4850		555	445				
4900	140	558	432				
4950							
# Line 3522-82P							
# Shot	**Water**	**Wyandot**	**Wyandot-1**	**Reflection A**	**Reflection B**	**Reflection C**	**Reflection D**
# Point	**Depth**						
1	140	482	450				
50		502	468				
100	135	520	472				
150		522	480				
200	130	530	460				SP 240=440
250		525	445				435
300	130	540	490				452
350		550	503				460
400	125	570	500				448
450		575	540				438
500	120	580	475				400
550		592	492				385
600	110	613	480				378
650		651	515				370
700	100	683	533				365
750		700	565		SP 755=562		372
800	95	725	580		555		383
850		723	589		550		390

900	95	725	590		555		395
950		715	598		560		392
1000	90	700	592		550		390
1050		685	585		550		385
1100	85	678	580		545		372
1150		682	600		558		372
1200	80	688	605		544		365
1250		700	600		550		363
1300	80	710	625		568		360
1350		722	638		567		368
1400	75	746	660		590		362
1450		770	680		603		351
1500	75	788	700		605	SP 1510=370	361
1550		807	723		615	390	360
1600	80	829	748	SP 1640=755	630	397	355
1650		842	768	752	623	395	355
1700	80	860	783	760	640	389	350
1750		879	805	772	655	380	351
1800	80	892	825	770	665	380	348
1850		918	850	785	690	395	351
1900	80	930	870	802	695	392	352
1950		945	885	820	711	395	357
2000	90	958	908	830	725	395	360
2050		978	933	850	735	395	364
2100	80	1000	950	851	735	396	356
2150		1010	969	858	733	392	350
2200	80	1020	990	865	738	388	352
2250		1042	1020	870	730	380	343
# Line 3524-82P							
# Shot	**Water**	**Wyandot**	**Wyandot-1**	**Reflection A**	**Reflection B**	**Reflection C**	**Reflection D**
# Point	**Depth**						
2	85	1030	977	925	813	372	342
50		1011	952	915	795	372	342
100	85	1000	933	903	782	368	345
150		991	920	895	777	365	345
200	85	978	895	885	765	368	342
250		962	880	SP 210=890	760	370	355
300	85	945	856		740	365	342
350		932	842		732	368	345
400	85	921	825		725	SP 400=345	345
450		910	810		720		360
500	85	900	805		708		368
550		892	805		700		368
600	80	880	800		692		368
650		858	780		675		364
700	80	835	765		652		358
750		820	754		632		372
800	85	805	738		620		368
850		785	708		610		372
900	85	770	690		592		378
950		752	670		580		380
1000	90	732	650		562		369
1050		722	644		558		362
1100	95	710	631		545		355
1150		715	638		558		345
1200	90	720	638		548		326
1250		722	642		SP 1240=570		322
1300	105	747	662				332
1350		750	670				323
1400	105	750	670				335
1450		733	655				335
1500	105	718	645				332
1550		700	629				322
1600	105	680	612				315
1650		652	596				335
1700	105	629	579				338
1750		608	545				345
1800	115	588	542				362
1850		562	518				360
1900	120	550	510				362
# Line 3528-82P							
# Shot	**Water**	**Wyandot**	**Wyandot-1**	**Reflection A**	**Reflection B**	**Reflection C**	**Reflection D**

# Point	Depth						
1	115	1322			1270	578	517
50		1290			1249	558	505
100	110	1258	SP 130=1240		1221	542	495
150		1240	1215		1183	529	479
200	110	1205	1167		1139	534	480
250		1183	1153		1115	532	482
300	105	1172	1134		1100	525	479
350		1169	1130		1085	500	456
400	105	1135	1105		1053	500	453
450		1128	1084		1030	487	448
500	100	1097	1048		990	480	441
550		1085	1032		967	478	438
600	100	1092	1035		980	473	435
650		1090	1029		972	464	432
700	95	1082	1020		954	463	430
750		1059	995		930	437	405
800	95	1021	956		890	440	403
850		1033	964		903	437	405
900	95	1004	942		878	433	402
950		1003	941		878	432	398
1000	95	985	925		850	431	402
1050		964	910		840	426	405
1100	95	942	889		830	433	398
1150		941	880		820	431	399
1200	95	929	880		822	429	405
1250		917	871		816	422	403
1300	95	894	850		798	410	397
1350		877	837		790	SP 1320=405	400
1400	95	856	805		789		400
1450		830	780		SP 1450=780		403
1500	95	807	765				405
1550		788	751				410
1600	90	775	740				400
1650		767	732				405
1700	90	764	727				395
1750		763	725				405
1800	95	754	715				400
1850		751	703				392
1900	90	737	699				383
1950		727	695				361
2000	90	723	683				355
2050		714	675				353
2100	90	700	663				342
2150		696	653				345
2200	90	680	640				340
2250		673	630				323
2300	95	667	632				313
2350		678	645				314
2400	90	682	640				310
2450		694	645				305
2500	90	685	633				307
2550		685	622				295
# Line 3528-82A							
# Shot	**Water**	**Wyandot**	**Wyandot-1**	**Reflection A**	**Reflection B**	**Reflection C**	**Reflection D**
# Point	**Depth**						
450							
500	1165						
550							
600	1140						
650							
700	1030						
750							
800	950						
850							
900	860						
950							
1000	770						
1050							
1100	745						
1150							
1200	645						
1250							

1300	525						
1350		1970					
1400	435	1900					
1450		1830					
1500	330	1795					
1550		1740					
1600	250	1670				1250	
1650		1625				1168	1061
1700	175	1590				1085	932
1750		1548				1010	833
1800	140	1500				923	725
1850		1465			SP 1850=1465	867	675
1900	125	1438			1415	829	596
1950		1375			1365	788	525
2000	125	1363			1330	755	512
2050		1350			1323	748	500
2100	120	1300			1270	721	498
2150		1265			1230	692	489
2200	115	1235			1195	685	484
2250		1240			1200	645	480
2300	110	1200	SP 2340=1210		1180	637	477
2350		1218	1200		1173	634	475
2400	105	1215	1165		1150	613	475
2450		1222	1198		1160	600	476
2500	105	1192	1160		1120	580	473
2550		1175	1133		1100	566	465
2600	100	1165	1131		1078	565	465
2650		1155	1110		1053	565	458
# Line 3528-82B							
# Shot	**Water**	**Wyandot**	**Wyandot-1**	**Reflection A**	**Reflection B**	**Reflection C**	**Reflection D**
# Point	**Depth**						
3001	95	1068	1000		945	458	427
3050		1090	1022		970	475	432
3100	95	1092	1038		977	505	425
3150		1080	1024		968	505	425
3200	95	1088	1045		982	508	425
3250		1122	1079		1020	511	438
3300	100	1158	1128		1029	530	450
3350		1195	1150		1075	554	460
3400	105	1178	1150		1063	566	465
3450		1205	1185		1110	580	477
3500	110	1203	1185		1123	600	489
3550		1230	SP 3550=1230		1165	590	485
3600	105	1270			1209	599	495
3650		1311			1252	597	495
3700	110	1345			1302	620	510
3750		1376			1340	649	530
# Line 3530-82P							
# Shot	**Water**	**Wyandot**	**Wyandot-1**	**Reflection A**	**Reflection B**	**Reflection C**	**Reflection D**
# Point	**Depth**						
1	210	474	420				
50		467	423				
100	205	463	414				
150		457	415				SP 195=425
200	200	462	429				425
250		485	453				425
300	180	505	466				435
350		495	463				433
400	160	498	463				432
450		503	465				432
500	130	510	471				400
550		535	485				397
600	110	563	505				382
650		588	528				378
700	110	602	555				377
750		626	583				382
800	100	655	613				371
850		673	620				368
900	100	692	648				373
950		694	654				361
1000	100	696	658				358
1050		700	659				363

1100	100	708	673				362
1150		723	687				360
1200	100	730	700				365
1250		753	719				367
1300	100	740	718				356
1350		740	710				345
1400	100	737	710				335
1450		753	710				335
1500	95	756	728				334
1550		775	737				340
1600	100	773	747				358
1650		782	745				357
1700	95	793	766				355
1750		795	768				379
1800	90	815	780				384
1850		815	789				385
1900	100	830	800				385
1950		838	805			SP 1950=389	389
2000	95	849	820			400	385
2050		858	828			423	375
2100	100	900	863			425	383
2150		908	875			426	367
2200	100	925	892			427	374
2250		971	920			433	377
2300	100	979	948			440	378
2350		1011	978			442	383
2400	100	1050	1009			444	389
2450		1040	998			453	385
2500	100	1083	1050			452	383
2550		1078	1028			456	380
2600	105					469	385
2650						481	384
2700	105					498	385
2750						505	405
2800	105	1100	1047		962	520	425
2850		1090	1038		950	514	425
2900	105	1110	1060		978	518	423
2950						529	420
3000	105					545	415
3050						560	421
3100	110					582	452
3150						602	458
3200	120					634	460
3250						692	480
3300	140					752	510
3350						806	570
3400	200						655
3450							680
# Project 8620-S014-006E Line 83-790C							
# Shot	**Water**	**Wyandot**	**Wyandot-1**	**Reflection A**	**Reflection B**	**Reflection C**	**Reflection D**
# Point	**Depth**						
101	63	1065		995	845	468	355
150	64	1076		1000	875	463	350
200	65	1095		1032	905	460	355
250	66	1105		1065	937	470	355
300	67	1124		1094	980	510	365
350	68	1159		1125	1022	555	367
400	69	1210		1188	1097	586	358
450	70	1220		SP 420=1210	1155	583	362
500	71	1247			1188	600	372
550	72	1323			1261	640	395
600	74	1348			1290	690	412
650	80	1375			1345	762	460
700	84	1440			1423	838	520
750	86	1480			SP 715=1432	932	590
800	88	1502				1038	655
850	90	1555				1140	740
900	82	1588				1202	800
950	89	1620				1295	877
1000	107	1655				1390	963
1050	119						
1100	133						
1150	151						

1200	172						
1250	209						
1300	257						
1350	312						
1400	364						
1450	446						
1500	571						
1550	731						
1600	831						
1650	950						
1700	1012						
1750	1086						
1800	1052						
1850	1138						
1900	1018						
1950	1090						
2000	1260						
2050	1296						
2100	1244						
# Line 83-838C							
# Shot	**Water**	**Wyandot**	**Wyandot-1**	**Reflection A**	**Reflection B**	**Reflection C**	**Reflection D**
# Point	**Depth**						
101	39						
150	39						
200	35						
250	35						
300	40						
350	44						
400	45						
450	48						
500	56						
550	56						
600	56						
650	60						
700	60						
750	60						
800	61						
850	61	1193			1125	460	280
900	63	1215			1152	485	297
950	65	1238			1180	505	305
1000	65	1250			1200	505	310
1050	66	1318			1269	500	330
1100	66	1320			1270	533	357
1150	66	1330			1295	562	390
1200	66	1365			1330	595	408
1250	66	1372			1356	633	420
1300	68	1433			SP 1260=1375	692	475
1350	72	1466				782	580
1400	75	1570				874	663
1450	77	1568				923	718
1500	79	1595				995	785
1550	79	1624				1031	830
1600	79	1640				1055	890
1650	84	1660				1149	958
1700	89	1700				1230	1046
1750	93	1770				1288	1132
1800	99	1850				1407	1265
1850	109	1898				1450	1368
# Line 83-854C							
# Shot	**Water**	**Wyandot**	**Wyandot-1**	**Reflection A**	**Reflection B**	**Reflection C**	**Reflection D**
# Point	**Depth**						
101	39						
150	35						
200	35						
250	39						
300	37						
350	37						
400	44						
450	46						
500	44						
550	39						
600	39						

650	39						
700	46						
750	52						
800	54						
850	56						
900	57	1150			996	395	255
950	57	1195			1062	385	260
1000	57	1200			1082	390	259
1050	57	1209			1105	407	263
1100	60	1220			1133	420	271
1150	61	1235			1169	444	278
1200	63	1258			1210	480	289
1250	68	1283			SP 1240=1260	503	317
1300	68	1306				522	333
1350	68	1330				568	353
1400	68	1380				628	390
1450	68	1402				703	442
1500	68	1405				710	278
1550	68	1440				780	535
1600	70	1465				772	567
1650	72	1482				812	613
1700	74	1496				814	663
1750	76	1532				838	706
1800	71	1550				891	770
1850	72	1580				920	853
1900	79	1611				963	905
1950	84	1625				1005	968
2000	88	1730				1065	1032
2050	91	1755				1140	1120
2100	101	1821				1235	1205
2150	113	1900				1352	1305
2200	118	1944				1468	1422
2250	129	2000					
2300	146	2052					
2350	166	2080					
# Line 83-4401BD							
# Shot	**Water**	**Wyandot**	**Wyandot-1**	**Reflection A**	**Reflection B**	**Reflection C**	**Reflection D**
# Point	**Depth**						
2425	257	1648					
2450		1642					
2500	228	1623					
2550	211	1588					
2600	195	1574					942
2650	180	1559					900
2700	166	1557					842
2750	155	1548					807
2800	147	1540					758
2850	141	1531					702
2900	136	1516					664
2950	132	1520					643
3000	129	1508					959
3050	126	1513					609
3100	123	1501					605
3150	122	1508					578
3200	119	1492					553
3250	117	1499					543
3300	116	1470					529
3350	113	1468					519
3400	112	1471					505
3450	111	1453					495
3500	110	1457					495
3550	109	1455					475
3600	108	1450					463
3650	106	1440					455
3700	105	1482					451
3750	104	1481					442
3800	103	1445					445
3850	104	1450				940	438
3900	103	1457				970	444
3950	103	1462				992	443
4000	103	1440				1035	433
4050	102	1448				1048	432
4100	102	1438				1056	411

4150	101	1447				1073	406
4200	101	1433				1045	403
4250	100	1450				1046	402
4300	100	1444				1052	395
4350	99	1435				1054	379
4400	99	1441				1084	390
4450	98	1438				1083	385
4500	97	1449				1090	385
4550	96	1458				1094	385
4600	96	1452				1070	378
4650	95	1466				1092	376
4700	96	1468				1170	382
4750	95	1477				1189	380
4800	95	1486				1200	375
4850	95	1490				1200	375
4900	96	1490				1203	381
4950	97	1493				1187	388
5000	98	1495				1190	393
5050	99	1510				1210	402
5100	102	1504				1205	409
5150	106	1535				1209	423
5200	110	1538				1200	440
5250	114	1527				1194	472
5300	122	1544				1195	488
5350	131	1534				1185	505
5400	152	1538				1178	563
5450	186	1600				1200	
5500	204	1601				1205	
5550	202	1587				1201	
5600	256	1604				1225	
5650	231	1568				1228	
5700	164	1515				1197	605
5750	143	1504				1202	615
5800	146	1490				1188	643
5850	157	1515				1226	636
5900	190	1553				1264	765
5950	318	1590				1312	825
6000	376	1620				1342	840
6050	430	1613				1360	
6100	305	1575				1329	
6150	213	1510				1263	
6200	160	1502				1223	
6250	142	1493				1220	
6300	134	1521				1270	
6350	130	1535				1285	
6400	126	1537				1212	
6450	122	1550				1215	
6500	119	1537				1212	
6550	115	1530				1186	833
6600	112	1548				1200	844
6650	109	1570				1185	854
6700	107	1575				1203	853
6750	105	1559				1187	850
6800	104	1580				1340	885
6850	102	1593				1203	875
6900	101	1600				1195	854
6950	101	1620				1178	848
7000	100	1600				1155	812
7050	100	1595				1161	795
7100	99	1600				1175	792
7150	98	1621				1178	800
7200	98	1604				1172	791
7250	98	1610				1168	790
7280		1622				1183	799
# Line 83-4417A							
# Shot	**Water**	**Wyandot**	**Wyandot-1**	**Reflection A**	**Reflection B**	**Reflection C**	**Reflection D**
# Point	**Depth**						
101	80	1219			1124	670	335
150	80	1210			1123	672	335
200	79	1208			1120	670	345
250	79	1204			1120	668	352
300	79	1202			1118	661	350
350	78	1203			1123	670	350

400	78	1200			1115	670	336
450	77	1200			1115	669	338
500	77	1202			1115	668	338
550	76	1202			1120	672	337
600	76	1203			1118	665	333
650	75	1305			1122	669	330
700	74	1204			1123	662	330
750	73	1203			1115	659	332
800	72	1202			1111	655	321
850	72	1198			1108	638	328
900	72	1192			1105	628	328
950	73	1192			1105	629	353
1000	73	1189			1095	618	341
1050	73	1182			1090	606	348
1100	74	1178			1085	605	354
1150	76	1173			1088	629	362
1200	77	1180			1093	640	370
1250	78	1180			1098	650	375
1300	79	1178			1092	653	380
1350	80	1176			1085	630	385
1400	82	1183			1095	628	405
1450	82	1182			1098	635	416
1500	82	1200			1126	648	422
1550	82	1210			1140	670	420
1600	82	1203			1136	670	410
1650	82	1198			1138	662	417
1700	82	1202			1142	664	435
1750	82	1198			1140	670	442
1800	80	1207			1132	650	433
# Line 83-4417AA							
# Shot	**Water**	**Wyandot**	**Wyandot-1**	**Reflection A**	**Reflection B**	**Reflection C**	**Reflection D**
# Point	**Depth**						
1941	79	1198			1142	667	422
1991	78	1200			1145	678	422
2041	77	1210			1165	685	426
2091	76	1210			1152	675	420
2141	75	1222			1155	645	428
2191	75	1222			1168	705	448
# Line 83-4417BC							
# Shot	**Water**	**Wyandot**	**Wyandot-1**	**Reflection A**	**Reflection B**	**Reflection C**	**Reflection D**
# Point	**Depth**						
4463	76	1245			1159	692	448
4513	76	1230			1144	635	425
4563	76	1236			1156	615	415
4613	76	1262			1190	629	414
4663	76	1270			1203	637	415
4713	76	1290			1220	632	405
4763	76	1317			1258	633	408
4813	76	1330			1265	636	398
4863	76	1340			1278	622	400
4913	75	1311			1284	646	417
4963	75	1337			1290	679	475
5013	75	1349			1306	695	488
5063	75	1355			1325	700	495
5113	75	1359			1332	710	500
5163	75	1363			SP 5160=1360	718	514
5213	75	1370				725	510
# Line 83-4417AB							
# Shot	**Water**	**Wyandot**	**Wyandot-1**	**Reflection A**	**Reflection B**	**Reflection C**	**Reflection D**
# Point	**Depth**						
2994	71	1368				722	513
3044	72	1375				720	510
3094	72	1378				722	513
3144	72	1397				726	535
3194	71	1417				790	545
3244	71	1437				730	555
3294	71	1430				765	583
3344	71	1450				792	613
3394	70	1420				705	561
3444	70	1459				714	570
3494	70	1472				760	605

3544	70	1480				795	603
3594	70	1478				771	570
3644	67	1468				755	557
3694	67	1452				770	563
3744	67	1473				803	585
3794	68	1495					600
3844	68	1460					600
3894	68	1465					622
3944	68	1485					603
3994	67	1521					610
4044	66						
4094	66						
4144	66						
4194	66						
4244	65						
4294	65						
4344	65						
4394	65						
4444	66						
# Line 83-4433BD							
# Shot	**Water**	**Wyandot**	**Wyandot-1**	**Reflection A**	**Reflection B**	**Reflection C**	**Reflection D**
# Point	**Depth**						
2650	64						
2700	65						
2750	65						
2800	66						
2850	66						
2900	66						
2950	66						
3000	67						
3050	65						
3100	64	1332				628	365
3150	63	1332				616	355
3200	63	1333				582	358
3250	65	1323				554	352
3300	66	1327				544	340
3350	68	1330			SP 3350=1330	553	345
3400	68	1323			1285	556	340
3450	68	1315			1268	545	343
3500	68	1310			1268	555	345
3550	68	1328			1274	545	349
3600	67	1320			1266	545	355
3650	66	1308			1256	545	342
3700	65	1305			1242	550	344
3750	65	1260			1185	542	345
3800	66	1258			1195	555	342
3850	68	1278			1208	584	356
3900	70	1247			1180	552	344
3950	70	1240			1170	553	351
4000	70	1240			1162	560	355
4050	70	1222			1144	543	348
4100	70	1178			1103	530	345
4150	70	1160			1089	530	340
4200	71	1148			1073	520	345
4250	71	1139		SP 4270=1130	1048	513	345
4300	71	1130		1105	1018	500	348
4350	70	1122		1090	995	503	349
4400	70	1120		1085	988	498	350
4450	70	1117		1080	970	485	355
4500	70	1114		1079	965	482	355
4550	70	1119		1075	948	478	355
4600	70	1113		1065	935	488	364
4650	70	1115		1063	925	482	360
4700	70	1112		1047	905	492	355
4750	70	1122		1048	886	511	353
4800	70	1122		1051	879	500	345
4850	71	1121		1044	880	503	361
4900	72	1131		1045	905	520	360
# Project 8624-S006-005E,6E Line 226-70/1							
# Shot	**Water**	**Wyandot**	**Wyandot-1**	**Reflection A**	**Reflection B**	**Reflection C**	**Reflection D**
# Point	**Depth**						
2380							

2400							
2450							
2500							
2550		625	545				297
2600		685	593				312
2650		724	620				335
2700		745	625		SP 2730=620		322
2750		710	605		590		305
2800		683	590		567		300
2850		722	618		595		313
2900		770	663		641		308
2950		812	710		662		307
3000		850	745		700		304
3050		885	778		710		308
3100		909	815		740	SP 3120=320	320
3150		937	855		768	340	333
3200		973	895		778	358	320
3250		1000	943		800	365	328
3300		1040	1000		825	370	337
3350		1084	1050		834	383	355
3400		1115	SP 3390=1100		848	390	361
3450		1142			883	403	365
3500		1153			905	428	355
3550		1155			938	473	365
3600		1185			1005	532	374
3650		1211			1078	568	372
3700		1237			1153	635	368
3750		1303			1245	740	405
3800		1390			1348	900	458
3850		1460			1425		565
3900		1565			SP 3870=1488		732
3950		1790					
# Line 2800-70/4							
# Shot	**Water**	**Wyandot**	**Wyandot-1**	**Reflection A**	**Reflection B**	**Reflection C**	**Reflection D**
# Point	**Depth**						
4456							
4500							
4550							
4600							
4650							
4700							
4750							
4800							
4850							
4900							
4950		680	650				345
5000		690	648				340
5050		682	645				329
5100		678	633				323
5150		675	631				305
5200		643	615				284
5250		658	620				290
5300		670	628				302
5350		668	625				309
5400		670	633				314
5450		673	632				325
5500		670	625				345
5550		675	628				368
5600		690	630				372
5650		703	640				395
5700		708	645				403
5750		704	636				368
5800		720	645				375
5850		720	645		SP 5860=640		373
5900		720	630		610		360
5950		711	615		590		643
6000		715	620		595		639
6020		710	612		588		634
# Line 3700-70/3A							
# Shot	**Water**	**Wyandot**	**Wyandot-1**	**Reflection A**	**Reflection B**	**Reflection C**	**Reflection D**
# Point	**Depth**						
3975		1418					

4000		1384					
4050		1330					
4100		1333					
4150		1324					
4200		1295			SP 4200=1295		
4250		1295			1265		
4300		1297			1258		
4350		1268			1225		
4400		1289			1212		
4450		1292			1205		
4500		1349			1259		
4550		1332			1335		
4600		1500			1427		
4650		1525			1453		
4700		1490			1430		
4750		1422			1323		
4800		1295			1226		
4850							
4900							
4950					1148		
5000		1242			1165	725	525
5050		1243			1163	715	510
5100		1238			1158	705	502
5150		1252			1160	692	490
5200		1263					480
5250		1235			1175		465
5300		1230			1180	675	453
5350		1231			1185	672	450
5400		1230			1188	665	445
5450		1240			1195	668	453
5500		1256			1209	665	452
# Line 3700-70/3B							
# Shot	**Water**	**Wyandot**	**Wyandot-1**	**Reflection A**	**Reflection B**	**Reflection C**	**Reflection D**
# Point	**Depth**						
5550		1263			1220	672	445
5600		1278			1219	671	455
5650		1325			1268		448
5700		1290			1225	673	443
5750		1326			1245	680	439
5800		1293			1235	675	425
5850		1278			1225	685	423
5900		1278			1223	668	421
5950		1290			1222	695	418
6000		1290			1213	680	395

Appendix G. Canyon Picks

Canyon location (shotpoint) measurements were made at the centre (or maximum depth) of the canyon, and at the points of maximum curvature and maximum extent on each side of the canyon. Where the absolute extent of the canyon could not be determined precisely, only the centre and maximum curvature of the canyon were recorded.

# Data file containing canyon location (shotpoint) measurements				
# West of Sable Island, Scotian Shelf				
# Measurements by Stephan Bigg, March 2002				
# Project 8624-P028-049E Line 3503-82P				
Outer Edge - left	Max Curve - left	Centre	Max Curve - right	Outer Edge - right
	240	270	290	
	910	1015	1060	
# Line 3505-82P				
Outer Edge - left	Max Curve - left	Centre	Max Curve - right	Outer Edge - right
1965	2020	2130	2230	2305
	2895	2936	2952	
# Line 3528-82P				
Outer Edge - left	Max Curve - left	Centre	Max Curve - right	Outer Edge - right
	485		290	
	590		760	
# Line 3528-82A				
Outer Edge - left	Max Curve - left	Centre	Max Curve - right	Outer Edge - right
	1945	2020	2100	
2155	2220	2355	2425	2500
# Line 3528-82B				
Outer Edge - left	Max Curve - left	Centre	Max Curve - right	Outer Edge - right
	3225	3260	3285	
	3300	3355	3385	
	3405	3440	3465	
# Line 3530-82P				
Outer Edge - left	Max Curve - left	Centre	Max Curve - right	Outer Edge - right
2580	2640	2720	2785	2800
	2900			
# Project 8620-S014-006E Line 83-598AA				
Outer Edge - left	Max Curve - left	Centre	Max Curve - right	Outer Edge - right
	2150	1970		
# Line 83-854C				
Outer Edge - left	Max Curve - left	Centre	Max Curve - right	Outer Edge - right
	1390		1770	
	1790		2015	
# Line 83-4369AB				
Outer Edge - left	Max Curve - left	Centre	Max Curve - right	Outer Edge - right
			6515	6475
5931	5917	5870	5805	5775
# Line 83-4369BC				
Outer Edge - left	Max Curve - left	Centre	Max Curve - right	Outer Edge - right
6740	6720	6680		
# Line 83-4385AA				
Outer Edge - left	Max Curve - left	Centre	Max Curve - right	Outer Edge - right
2440	2395	2315	2220	2185
3385	3340	3245	3080	
	3080	3023	2935	2895
# Line 83-4385BG				
Outer Edge - left	Max Curve - left	Centre	Max Curve - right	Outer Edge - right
6535	6505	6455	6400	6368
# Line 83-4401BD				
Outer Edge - left	Max Curve - left	Centre	Max Curve - right	Outer Edge - right
		2440	2500	2540
	3238	3260	3270	
3650	3678	3723	3790	3815
4335	4425	4475	4515	4530
6320	6350	6385	6420	6465
6740	6760	6795	6845	6870
# Line 83-4417A				
Outer Edge - left	Max Curve - left	Centre	Max Curve - right	Outer Edge - right

1680	1712	1755	1810	1830
# Line 83-4417AA				
Outer Edge - left	Max Curve - left	Centre	Max Curve - right	Outer Edge - right
2101	2135	2195		
# Line 83-4417BC				
Outer Edge - left	Max Curve - left	Centre	Max Curve - right	Outer Edge - right
			4483	4513
	4590	4610	4630	
# Line 83-4417AB				
Outer Edge - left	Max Curve - left	Centre	Max Curve - right	Outer Edge - right
	3175	3195	3215	
3234	3265	3334	3390	3415
3724	3834	3890	3985	4024
4074	4120	4190	4264	4284
4314	4464	5355	5430	
# Line 83-4433BD				
Outer Edge - left	Max Curve - left	Centre	Max Curve - right	Outer Edge - right
2815	2860	2950	3010	
2980	3025	3125	3230	3260
3515	3530	3555	3590	3615
3685	3705	3720	3740	3755
3770	3800	3850	3895	3904
3910	3990	4045	4070	4090
4830	4890	4920		
# Project 8624-S006-005E,6E Line 214-70/1				
Outer Edge - left	Max Curve - left	Centre	Max Curve - right	Outer Edge - right
3410	3440			
# Line 226-70/1				
Outer Edge - left	Max Curve - left	Centre	Max Curve - right	Outer Edge - right
3727	3815			
# Line 3500-70/2,3				
Outer Edge - left	Max Curve - left	Centre	Max Curve - right	Outer Edge - right
	4790	4835	4880	
	5140	5180	5225	
	5540	5575	5605	
# Line 3700-70/3A				
Outer Edge - left	Max Curve - left	Centre	Max Curve - right	Outer Edge - right
4750	4805	4895	4980	5010
5130	5150	5190	5230	5260
	5250	5280	5295	
# Line 3700-70/3B				
Outer Edge - left	Max Curve - left	Centre	Max Curve - right	Outer Edge - right
5630	5640	5655	5675	5700
5735	5755	5775	5790	5805

Appendix H. Fault Picks

Fault location measurements were made at the shotpoint where the reflection is truncated on the foot wall fault block ($SP_{foot\ wall}$), and where the reflection is truncated on the hanging wall fault block ($SP_{hanging\ wall}$). The offsets of the reflections were measured as approximate TWT (ms). Where the offset is indistinguishable, only one shotpoint value is recorded.

# Data file containing fault location (shotpoint) measurements			
# West of Sable Island, Scotian Shelf			
# Offset measured as approximate TWT (ms)			
# Measurements by Stephan Bigg, March 2002			
# Project 8624-P028-049E			
# Line 3506-82P			
# Reflection	**$SP_{foot\ wall}$**	**$SP_{hanging\ wall}$**	**offset**
B	103	100	20
W	100	94	51
# Line 3520-82B			
# Reflection	**$SP_{foot\ wall}$**	**$SP_{hanging\ wall}$**	**offset**
D	3628	N/A	N/A
W-1	3635	3639	22
W	3636	3640	22
# Line 3522-82P			
# Reflection	**$SP_{foot\ wall}$**	**$SP_{hanging\ wall}$**	**offset**
W	1045	N/A	N/A
# This fault was not visible on the line, however monoclinal folding visible deeper in the section and the			
# presence of faults on each adjacent line (3520-82B and 3524-82P) suggest that faulting may be present,			
# although below seismic resolution.			
# The location of the fault was thus extrapolated from the underlying flexure.			
# Line 3524-82P			
# Reflection	**$SP_{foot\ wall}$**	**$SP_{hanging\ wall}$**	**offset**
B	1133	N/A	N/A
W-1	1134	N/A	N/A
W	1142	N/A	N/A
B	1140	N/A	N/A
W-1	1145	N/A	N/A
W	1148	N/A	N/A
B	1156	N/A	N/A
W-1	1165	N/A	N/A
W	1170	N/A	N/A
# Line 3526-82A			
# Reflection	**$SP_{foot\ wall}$**	**$SP_{hanging\ wall}$**	**offset**
W	1575	N/A	N/A
# This line was not available from the CNSOPB.			
# The location of the fault was thus extrapolated from the adjacent line 3526-82P, on which the fault was visible			
# below the study interval, but extended beyond the extent of the line (and onto line 3526-82A) into the shallow			
# part of the section (and into the study interval).			
# Line 3528-82P			
# Reflection	**$SP_{foot\ wall}$**	**$SP_{hanging\ wall}$**	**offset**
W-1	2295	2300	20
W	2296	2300	15
# Line 3528-82A			
# Reflection	**$SP_{foot\ wall}$**	**$SP_{hanging\ wall}$**	**offset**
B	1923	1921	53
W	1923	1921	63
# Project 8620-S014-006E			
# Line 83-790C			
# Reflection	**$SP_{foot\ wall}$**	**$SP_{hanging\ wall}$**	**offset**
B	394	395	25
A	398	400	29
W	398	400	38
B	519	522	41

W	520	523	55
B	665	670	50
W	665	670	53
W	724	726	20
W	870	873	19
# Line 83-838C			
# Reflection	**$SP_{foot\ wall}$**	**$SP_{hanging\ wall}$**	**offset**
B	1013	1017	46
W	1016	1019	44
B	1189	1192	13
W	1192	1195	14
W	1383	1385	30
W	1544	1550	37
W	1705	1710	51
D	1761	1763	56
C	1770	1773	43
W	1796	1800	62
W	1840	1843	13
# Line 83-854C			
# Reflection	**$SP_{foot\ wall}$**	**$SP_{hanging\ wall}$**	**offset**
W	1368	1370	22
W	1965	1968	79
W	2024	2027	20
W	2070	2074	41
W	2140	2158	69
# Line 83-4417BC			
# Reflection	**$SP_{foot\ wall}$**	**$SP_{hanging\ wall}$**	**offset**
B	4910	4906	17
W	4912	4906	33
# Line 83-4417AB			
# Reflection	**$SP_{foot\ wall}$**	**$SP_{hanging\ wall}$**	**offset**
W	3293	3280	42
W	4054	4045	102
# Line 83-4433BD			
# Reflection	**$SP_{foot\ wall}$**	**$SP_{hanging\ wall}$**	**offset**
B	3724	3720	38
W	3722	3720	25
# Project 8624-S006-005E,6E			
# Line 202-70/2			
# Reflection	**$SP_{foot\ wall}$**	**$SP_{hanging\ wall}$**	**offset**
W	2762	N/A	N/A
# Line 214-70/1			
# Reflection	**$SP_{foot\ wall}$**	**$SP_{hanging\ wall}$**	**offset**
W	2763	N/A	N/A

# Line 226-70/1			
# Reflection	**$SP_{foot\ wall}$**	**$SP_{hanging\ wall}$**	**offset**
B	2792	2787	20
W-1	2792	2787	17
W	2791	2786	21
#Note:			
#'$SP_{foot\ wall}$' refers to the shotpoint location where the reflection is truncated on the foot wall fault block.			
#'$SP_{hanging\ wall}$' refers to the shotpoint location where the reflection is truncated on the hanging wall fault block.			
#Where the offset is indistinguishable, only one shotpoint value is recorded.			

Wyandot (R_w) Time-Structure Map

Stephan Bigg
Dalhousie University
April, 2002

coastline (after Wessel and Smith, 1998)
erosional edge of Mesozoic/Cenzoic (after Sanford et al., 1991)
erosional edge of Wyandot (after Wade, 1991)
erosional edge of Banquereau (after after Sanford et al., 1991)
bathymetry (courtesy of the Atlantic Geoscience Centre, 1991)
well locations (courtesy of the CNSOPB)
exploration licences (courtesy of the CNSOPB)

UTM Zone 20
1:500,000
km
0 50

64°W 62°W 60°W
44°N
43°N

HALIFAX

erosional 'trough'

500 ms
600 ms
700 ms
800 ms
900 ms
1000 ms
1100 ms
1200 ms
1300 ms
1400 ms
1500 ms

SAMBRO I-29
NASKAPI N-30
CHIBWA E-07
CREE E-35
DEMASCOTA G-32
ALMA K-85
ONEIDA O-25
MOHEIDA P-15
MORICAN I-100

64°W 62°W 60°W

MAPSHEET 1
Wyandot

Wyandot (R_w) to Wyandot-1 (R_{w-1}) Isochron Map

Stephan Bigg
Dalhousie University
April, 2002

- coastline (after Wessel and Smith, 1998)
- erosional edge of Mesozoic/Cenzoic (after Sanford et al., 1991)
- erosional edge of Wyandot (after Wade, 1991)
- erosional edge of Banquereau (after after Sanford et al., 1991)
- bathymetry (courtesy of the Atlantic Geoscience Centre, 1991)
- well locations (courtesy of the CNSOPB)
- exploration licences (courtesy of the CNSOPB)

UTM Zone 20
1:500,000

km
0 50

64°W 62°W 60°W
44°N 43°N

HALIFAX

limit of interpretation (line 3516-82A)

0 ms 50 ms 100 ms

SAMBRO I-29
NASKAPI N-30
OJIBWA E-07
MOHEIDA P-15
MOHICAN I-100
ONEIDA O-25
CREE E-35
DEMASCOTA G-32
ALMA K-85

MAPSHEET 2
Wyandot to Wyandot-1

Seismic Package 1 (R_w or R_{W-1} to R_B) Isochron Map

Stephan Bigg
Dalhousie University
April, 2002

coastline (after Wessel and Smith, 1998)
erosional edge of Mesozoic/Cenzoic (after Sanford et al., 1991)
erosional edge of Wyandot (after Wade, 1991)
erosional edge of Banquereau (after after Sanford et al., 1991)
bathymetry (courtesy of the Atlantic Geoscience Centre, 1991)
well locations (courtesy of the CNSOPB)
exploration licences (courtesy of the CNSOPB)

UTM Zone 20
1:500,000

km
0 50

64°W 62°W 60°W
44°N
43°N

HALIFAX

0 ms
200 ms
250 ms
300 ms
300 ms
300 ms

QUIBWA E-07
CREE E-35
DEMASCOTA G-32
ALMA K-85
SAMBRO I-29
NASKAPI N-30
ONEIDA O-25
MOHEIDA P-15
MOHICAN I-100

MAPSHEET 3
Seismic
Package 1

Seismic Package 2 (R_B to R_C) Isochron Map

Stephan Bigg
Dalhousie University
April, 2002

- coastline (after Wessel and Smith, 1998)
- erosional edge of Mesozoic/Cenzoic (after Sanford et al., 1991)
- erosional edge of Wyandot (after Wade, 1991)
- erosional edge of Banquereau (after after Sanford et al., 1991)
- bathymetry (courtesy of the Atlantic Geoscience Centre, 1991)
- well locations (courtesy of the CNSOPB)
- exploration licences (courtesy of the CNSOPB)

UTM Zone 20
1:500,000

km
0 50

64°W 62°W 60°W
44°N
43°N

HALIFAX

0 ms
100 ms
200 ms
300 ms
400 ms
500 ms
600 ms
700 ms

QUIBWA E-07
SAMBRO I-29
MASKAPI N-30
ONEIDA O-25
MOHEIDA P-15
MOHICAN I-100
TOBEE E-35
DEMASCOTA G-32
ALMAK B-85

MAPSHEET 4
Seismic
Package 2

Seismic Package 3 (R_c to R_D) Isochron Map

Stephan Bigg
Dalhousie University
April, 2002

coastline (after Wessel and Smith, 1998)
erosional edge of Mesozoic/Cenzoic (after Sanford et al., 1991)
erosional edge of Wyandot (after Wade, 1991)
erosional edge of Banquereau (after after Sanford et al., 1991)
bathymetry (courtesy of the Atlantic Geoscience Centre, 1991)
well locations (courtesy of the CNSOPB)
exploration licences (courtesy of the CNSOPB)

UTM Zone 20
1:500,000

km
0 50

64°W 62°W 60°W
44°N
43°N

HALIFAX
OJIBWA E-07
SAMBRO I-29
NASKAPI N-30
CREE E-35
DEMASCOTA G-32
ALMA K-85
CREIDA O-25
MOHEIDA P-15
MOHICAN I-100

0 ms
50 ms
100 ms
200 ms
300 ms
400 ms
600 ms
700 ms
800 ms
900 ms
1000 ms

MAPSHEET 5
Seismic
Package 3

Canyon Location Map

Stephan Bigg
Dalhousie University
April, 2002

- coastline (after Wessel and Smith, 1998)
- erosional edge of Mesozoic/Cenzoic (after Sanford et al., 1991)
- erosional edge of Wyandot (after Wade, 1991)
- erosional edge of Banquereau (after after Sanford et al., 1991)
- bathymetry (courtesy of the Atlantic Geoscience Centre, 1991)
- well locations (courtesy of the CNSOPB)
- exploration licences (courtesy of the CNSOPB)
- interpreted trace of maximum curvature of canyon
- centre of canyon (maximum depth)
- edge of canyon (correlative)

UTM Zone 20
1:500,000
km
0 50

64°W
62°W
60°W
44°N
43°N
HALIFAX
OJIBWA E-07
CREE E-35
DEMASCOTA G-32
ALMA K-85
SAMBRO I-29
NASKAPI N-30
ONEIDA O-25
MOHEIDA P-15
MOHICAN I-100

MAPSHEET 6
Canyons

Fault Location Map

Stephan Bigg
Dalhousie University
April, 2002

- coastline (after Wessel and Smith, 1998)
- erosional edge of Mesozoic/Cenzoic (after Sanford et al., 1991)
- erosional edge of Wyandot (after Wade, 1991)
- erosional edge of Banquereau (after after Sanford et al., 1991)
- bathymetry (courtesy of the Atlantic Geoscience Centre, 1991)
- well locations (courtesy of the CNSOPB)
- exploration licences (courtesy of the CNSOPB)
- normal fault (tick on downthrown side)
- termination of Wyandot Reflection by foot wall
- termination of Wyandot Reflection by hanging wall

UTM Zone 20
1:500,000
km
0 50

64°W 62°W 60°W
44°N
43°N

HALIFAX
OJIBWA E-07
SAMBRO I-29
NASKAPI N-30
CREE E-35
DEMASCOTA G-32
ALMA K-85
ONEIDA O-25
MOHEIDA P-15
MOHICAN I-100

MAPSHEET 7
Faults